Centre for Interdisciplinary Research on Micro-Nano Methods

ACTIVITY REPORT

April 2023 - March 2024

Takuji Takahashi
Professor & Director
Centre for Interdisciplinary Research on Micro-Nano Methods
IIS University of Tokyo

ACTIVITY REPORT

CONTENT

Centre for Interdisciplinary Research on Micro-Nano Methods (CIRMM)

1-1. What is CIRMM

The CIRMM was established in 2000 to facilitate international collaboration on micromechatronics research, which is the study of micro miniature systems composed of mechanical, electrical, optical and bio/chemical devices. The prospect is to obtain high-performance multi-functional devices using heterogeneous integrated process over scale and materials. The first phase of CIRMM (April 2000 – March 2010) finished successfully. The second phase started for a 6-year mandate in April 2010 and come to an end in March 2016. The third phase has started in April 2016 for another 5 years. The name of the center becomes Centre for Interdisciplinary Research on Micronano Methods. Professors conducting biomedical MEMS research in CIRMM created a new center, named "Center for International Research on Integrative Biomedical Systems (CIBiS)" jointly with other professors working on bioengineering on April 1, 2015. Those two centers share the same technological base, i.e. MEMS, and will work together to continue the international activities of CIRMM.

The international activities of CIRMM date back to 1995 with the creation of Laboratory for Integrated Micro-Mechatronic Systems (LIMMS); the joint research laboratory between Institute of Industrial Science(IIS) in the University of Tokyo and Institut des sciences de l'ingènierie et des systèmes (INSIS) in Centre National de la Recherche Scientifique (CNRS). After 9 years of operation, in 2004, the LIMMS became the first Unité Mixte Internationale de Recherche (UMI 2820) of CNRS situated in Asia. International research networks on nano and micro systems (NAMIS) were organized in 2005. Using the network, LIMMS obtained an EU FP-7 project (EUJO-Limms) in 2011 to extend its activities to other European countries, namely Germany, Finland, Switzerland, and Netherlands. On July 16, 2014, SMMiL-E* laboratory, mirror site of LIMMS was founded at Centre Oscar Lambret in Lille, in North France. Bio-MEMS technology of CIRMM is applied to cancer research in SMMiL-E. IIS/UTokyo Bureau for European Collaboration (IBEC) is open in July, 2015 in Lille for both supporting the SMMiL-E project and strengthening EU relation.

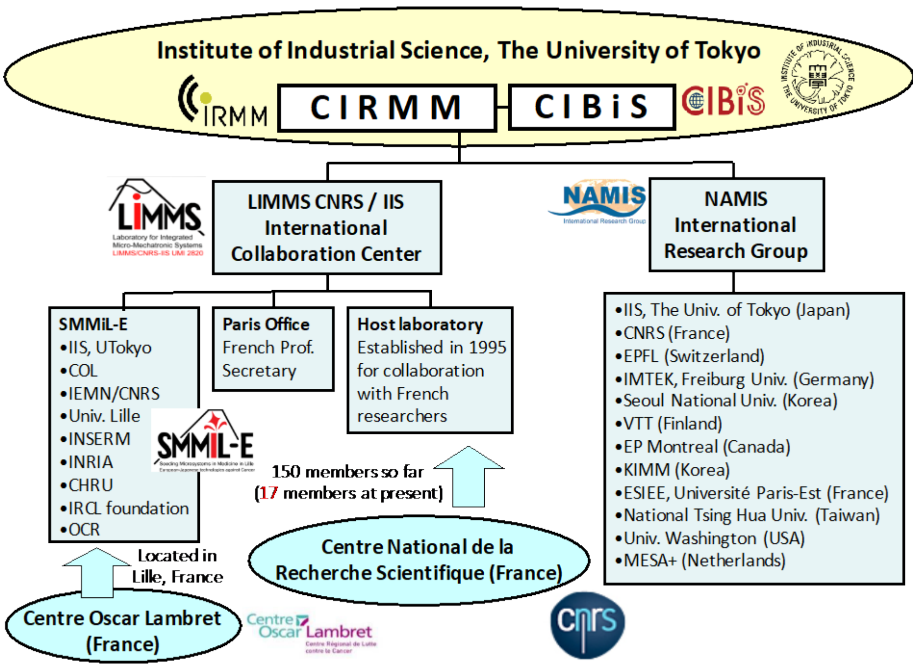

CIRMM Organization

SMMiL-E stands for Seeding Microsystems in Medicine in Lille - European Japanese Technologies against Cancer; this program aims at technology transfer of state-of-the-art bioMEMS research performed in IIS/The University of Tokyo and LIMMS/CNRS-IIS towards the research against cancer conducted in Lille, France in the SIRIC ONCO-Lille program. The fusion of the BioMEMS technology and Cancer research plans to take place in a hosting platform located on the Oscar Lambret Centre site, within the hospital-university campus, in order to be in close contact with medical teams. This platform provides an experimental environment in which IIS researchers can perform joint work in France. In other word, SMMiL-E is a “mirror” structure of LIMMS to welcome researchers from Japan and to organize French/Japanese teams performing tight joint research. The program also includes IEMN/CNRS and Lille-1 University. Currently, there are experimental/office space in IRCL (Institute of Cancer Research in Lille). Laboratory for SMMiL-E will be first installed in IRCL from 2016 and then moved to a new building built by 2020 with the support from the State, Local Government, CNRS, COL, Lille University and INSERM.

In April 2016, CIRMM was renewed under a new name “Centre for Interdisciplinary Research on Micro-Nano Methods”, and welcomed two new professors. The Centre named three axes of its activity, namely, “True-Nano Physics: exploitation of effects and phenomena based on nano to mesoscopic regime”, “Cyber Physical Systems Implementation”, and “Nano-Fabrication”. As the name implies, it puts emphasis on creating new methods, in terms of detection, processing, or implementation of époque making devices. The following schematic depicts the scope of our new centre of research. In April 2021, in addition, CIRMM was renewed as an internal center of IIS, while the main mission of CIRMM has been retained. In 2022, two new associate porfessors joined in CIRMM.

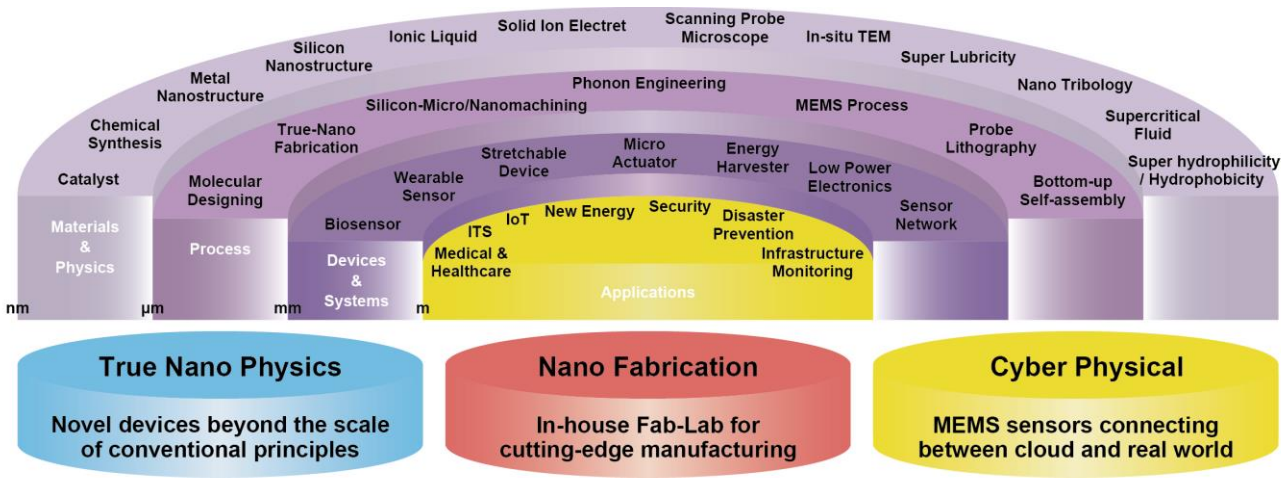

1-2. History of CIRMM

1999	CIRMM is proposed to Ministry of Education in Japan
	Preliminary discussion with CNRS/Science Pour l'Ingenieur(SPI) and positive response
Mar. 2000	Approval of the (Japanese/French) Diet
Apr. 2000	CIRMM is founded for 10-year term
Sep. 2000	CIRMM /CNRS in Paris opens in rue Capitaine Scott, LIP6/UPMC
Nov. 2000	Inauguration ceremony of CIRMM/CNRS Paris is held in CNRS/Headquarter in Paris
Oct. 2001	EPFL in Switzerland agrees to cooperate research activities with CIRMM
Mar. 2002	Twente University in the Netherlands agrees to cooperate research activities with CIRMM
Jul. 2002	Neuchatel University in Switzerland agrees to cooperate research activities with CIRMM
May 2003	KIMM in Korea agrees to cooperate research activities with CIRMM
Jul. 2003	University of Karlsruhe in Germany agrees to cooperate research activities with CIRMM
Aug. 2004	VTT Electronics and VTT Information Technology, Technical Research Center of Finland agreed to cooperate research activity with CIRMM
Apr. 2005	Seoul National University agrees to cooperate research activity with CIRMM
Nov. 2005	CIRMM contributes to establish NAMIS with CNRS, EPFL, IMTEK, SNU and VTT
Nov. 2006	National Tsing Hua University agrees to cooperate research activities with CIRMM
Jul. 2008	Initiation of Beans project founded by METI/NEDO Life-Beans Center and 3D-Beans Center are accommodated in IIS. Bio Nano Process collaboration Center was established.
Mar. 2009	CIRMM Evaluation Committee in Paris, France
Sep. 2009	CIRMM and VTT extended its Agreement of Joint Research
Apr. 2010	CIRMM is renewed for another 6 years / The official name became Center for International Research on Micronano Mechatronics
Oct. 2010	Academic Exchange Agreement signed with College of EECS in Seoul University
Dec. 2011	EU Project: EUJO-LIMMS (EUrope-Japan Opening of LIMMS) started for 4 years
Apr. 2012	Core-to-Core Program of the Japan Society for the Promotion of Science was launched by JSPS for 5 years
May 2012	EUJO-LIMMS Kick-off Meeting at IIS
Dec. 2012	JST Japanese-Taiwanese Cooperative Programme on 'Bioelectronics' started for 4 years with National Tsing Hua University: Neuron-on-CMOS-MEMS

	EUJO-LIMMS Info Day at EPFL
May 2013	LIMMS Workshop at Paris
Jun. 2013	Director General of Research & Technolgy Directorate at the European Commission, Mr. Robert Jan Smits, visited LIMMS
Sep. 2013	Workshop on Japan-Taiwan collaboration Research on Bio electronic at National TsingHuaUniversity in Hshinchu, Taiwan
Oct. 2013	EUJO LIMMS Info.Day at IMTEK in Freiburg, Germany
Dec. 2013	Workshop on Bio MEMS against Cancer at Centre Oscar Lambret in Lille, France
Jun. 2014	Inauguration Ceremony of SMMiL-E in Lille, France
	EUJO-LIMMS Workshop at VTT in Helsinki, Finland
Jul. 2014	Inauguration Symposium of CIBiS at IIS
Jan. 2015	20-year Aniversary of LIMMS at IIS
	Eujo-LIMMS Workshop at IIS
Apr. 2016	Foundation of new CIRMM (Centre for Interdisciplinary Research on Micro-Nano Methods)
Jun. 2016	Innovation show case at JST with the CNRS, LIMMS, CIBiS and the French embassy
Oct. 2016	Participation to Forum-X at the Ecole Polytechnique, Paris France
Dec. 2016	Joint Workshop of CIRMM/LIMMS/CIBiS on “International research leading to innovation and new technology bridging academics and societal demands”, at IIS
Feb. 2017	FEMO-ST Workshop “International Seminar LIMMS and FEMTO-ST and Partners”, Besancon France
Mar. 2019	LIMMS-Next PV Joint Energy Workshop at IIS
Nov. 2019	2019 NAMIS Marathon Workshop, Hsinchu, Taiwan
Nov. 2020	2020 NAMIS Marathon Workshop, Hybrid (Online and Hsinchu, Taiwan)
Apr. 2021	Renewal of CIRMM as Internal Center of IIS
Dec. 2021	2021 NAMIS Marathon Workshop, Hybrid (Online and Hsinchu, Taiwan)
Oct. 2022	NAMIS Core Members Online Meeting
Dec. 2022	2022 NAMIS Marathon Workshop, Hsinchu, Taiwan
Nov. 2023	New NAMIS Workshop, Lausanne, Switzerland
Dec. 2023	2023 NAMIS Marathon Workshop, Hsinchu, Taiwan
Feb. 2024	SNU-IIS Joint Workshop at IIS

1-3. History of NAMIS

Nov. 2005	CIRMM contributes to establish NAMIS with CNRS, EPFL, IMTEK, SNU and VTT
May 2006	The 1st NAMIS Workshop in IEF, Orsay and IEMN, Lille, France
Nov. 2006	The 2nd NAMIS Workshop in EPFL, Laudanne, Switzerland
Jun. 2007	The 3rd NAMIS Workshop in VTT, Oulu, Finland
Oct. 2007	International MEMS school for NAMIS students at IIS
Nov. 2007	The 4th NAMIS Workshop in Seoul, Korea
Apr. 2008	The 5th NAMIS Workshop in Freiburg, Germany
Sep. 2008	NAMIS International Autumn School 2008 at IIS, Tokyo The 6th NAMIS Workshop in Shonan Village, Japan University of Paris South and Tohoku University joined NAMIS as associated partners
Jun. 2009	The 7th NAMIS Workshop in Montreal, Canada.
Sep. 2009	NAMIS International Autumn School 2009 at Toulouse, France
Jun. 2010	The 7th NAMIS Workshop in Hsinchu Taiwan. University of Washington, Seattle, USA joined the network.
Oct. 2010	NAMIS International Autumn School 2010 at IIS, UTokyo, Japan
Jun. 2011	The 9th NAMIS Workshop in Paris, France
Sep. 2011	NAMIS International Autumn School 2011 at Neuchâtel – Arc-et-Senans - Besançon
May 2012	The 10th NAMIS Workshop at Sendai
Sep. 2012	NAMIS International Autumn School 2012 at IIS, UTokyo, Japan
Jul. 2013	The 11th NAMIS Workshop in Seattle
Sep. 2013	NAMIS International Autumn School 2013 in Seoul, Korea
Jun. 2014	The 12th NAMIS Workshop in Vietnum
Sep. 2014	NAMIS International Autumn School 2014 at National TsingHua University in Hshinchu, Taiwan
Jun. 2015	NAMIS International Autumn School 2015 in Montréal, Canada
Sep. 2015	The 13th NAMIS Workshop in Wroclaw University of Technology, Poland
Jul. 2016	The 14th NAMIS Workshop in University of Twente, The Netherlands
Sep. 2016	NAMIS International Autumn School 2016 in IIS, UTokyo, Japan
Jun. 2017	The 15th NAMIS Workshop in Daejeon, Korea
Oct. 2017	NAMIS International Autumn School 2017 in Freiburg, Germany

Jun. 2018	The 16th NAMIS Workshop in VTT-Oulu, Finland
Sep. 2018	NAMIS International Autumn School 2018 in University of Washington, Seattle, USA
Nov. 2019	2019 NAMIS Marathon Workshop, Hsinchu, Taiwan
Jan. 2020	Seoul National Univ.(SNU) / IIS, The Univ. of Tokyo Joint Workshop on Innovative Micro/Nano systems, Seoul, Korea
Nov. 2020	2020 NAMIS Marathon Workshop, Hybrid (Online and Hsinchu, Taiwan)
Dec. 2021	2021 NAMIS Marathon Workshop, Hybrid (Online and Hsinchu, Taiwan)
Oct. 2022	NAMIS Core Members Online Meeting
Dec. 2022	2022 NAMIS Marathon Workshop, Hsinchu, Taiwan
Nov. 2023	New NAMIS Workshop, Lausanne, Switzerland
Dec. 2023	2023 NAMIS Marathon Workshop, Hsinchu, Taiwan

1-4. Research Areas

- Micro/nano 3D fabrication technologies based on silicon process, precision, mechanical machining, printing, bonding, bio coating, soft lithography and self-assembly.
- Basic components such as micro actuators, micro fluidics, mirrors/gratings and nano structures.
- Fundamantals and application of various Microscopy
- Integration and packaging technologies; evaluation methods
- Applications especially in bio/medical systems, optics, wireless communication, IoT (internet of things) and nano technologies.
- Technology transfer to industry

1-5. Missions of Each Organization in CIRMM

❑ CIRMM for global networking activities in Micro- and Nano-systems

- Stimulate exchanges by workshops, meetings, visits
- Establish joint research projects between Japanese university network and foreign Universities/Laboratories.

❑ LIMMS (Laboratory for Integrated Micromechatronic Systems)

- Accept CNRS related French researchers in IIS
- Perform state-of-the art research on MEMS and applications.

- EUJO-LIMMS (2011-2015): Extention to 4 European partners
- SMMiL-E (2014-): Bio MEMS installation in Cancer Hospital in France

❑ NAMIS (International Research Group on Nano and Microsystems)

- Stimulate research exchanges of twelve organizations:
  CNRS (France), EPFL (Switzerland), SNU (Korea), VTT (Finland), IMTEK (Germany), IIS (Japan), EPM (Canada), KIMM (Korea), UPE (France), NTHU (Taiwan), UW (USA), MESA+ (the Netherlands)

❑ IBEC (IIS/UTokyo Bureau for European Collaboration)

- Management of research projects in SMMIL-E and the support for IIS researchers visiting Lille.Technology transfer to clinical applications
- Networking with EU committees and with EU researchers
- Partial support of LIMMS administration in terms of CNRS related operation

1-6. CIRMM Offices and Oversea Laboratory

<u>Tokyo Office</u>

Address: 4-6-1 Komaba, Meguro-ku, Tokyo, 153-8505, Japan
The University of Tokyo, Institute of Industrial Science
Phone +81-3-5452-6248 at Prof. Fujita / Fax +81-3-3402-5078 (IIS main)

<u>IIS/UTokyo Bureau for European Collaboration (IBEC)</u>

Address: CNRS Délégation Nord Pas de Calais et Picardie, 2 rue des Canonniers CS60009, 59046 LILLE CEDEX, France
Phone: + 33 3 20 12 28 16

<u>SMMiL-E Laboratory</u>

Address: IRCL, Place de Verdun, 59000 Lille, France
(IRCL: Institut pour la Recherche sur le Cancer de Lille)

1-7. CIRMM Network

CIRMM's micromechatronics (MEMS) research network in Europe, Asia, US/Canada and in Japan.

Centre de la National Recherche Scientifique (CNRS) France

http://www.cnrs.fr/

Ecole Polytechnique Federal de Lausanne (EPFL) Switzerland

http://www.epfl.ch/

University Paris Est (UPE) France

http://www.univ-paris-est.fr/fr/

VTT Technical Research Centre of Finland Ltd. Finland

http://www.hydromod.de/loleif/Participants/VTT/vtt.html

Department of Microsystem Engineering, University of Freiburg (IMTEK) Germany

http://www.imtek.mml/material

Inter-University Semiconductor Research Center (ISRC) South Korea

http://isrc.snu.ac.kr/

Seoul National University (SNU) South Korea

http://www.useoul.edu/

Korea Institute of Machinery and Materials (KIMM) South Korea

http://www.kimm.re.kr/main.php

Polytechnique of Montreal Canada

http://www.umontreal.ca/

National Tsing Hua University (NTHU) Republic of China (Taiwan)

http://www.nthu.edu.tw/english/index.php

University of Washington (UW) USA

http://www.washington.edu/

MESA+, Twente University the Netherlands

http:// http://www.utwente.nl/mesaplus/

Centre Oscar Lambret (COL) France

http://www. centreoscarlambret.fr/

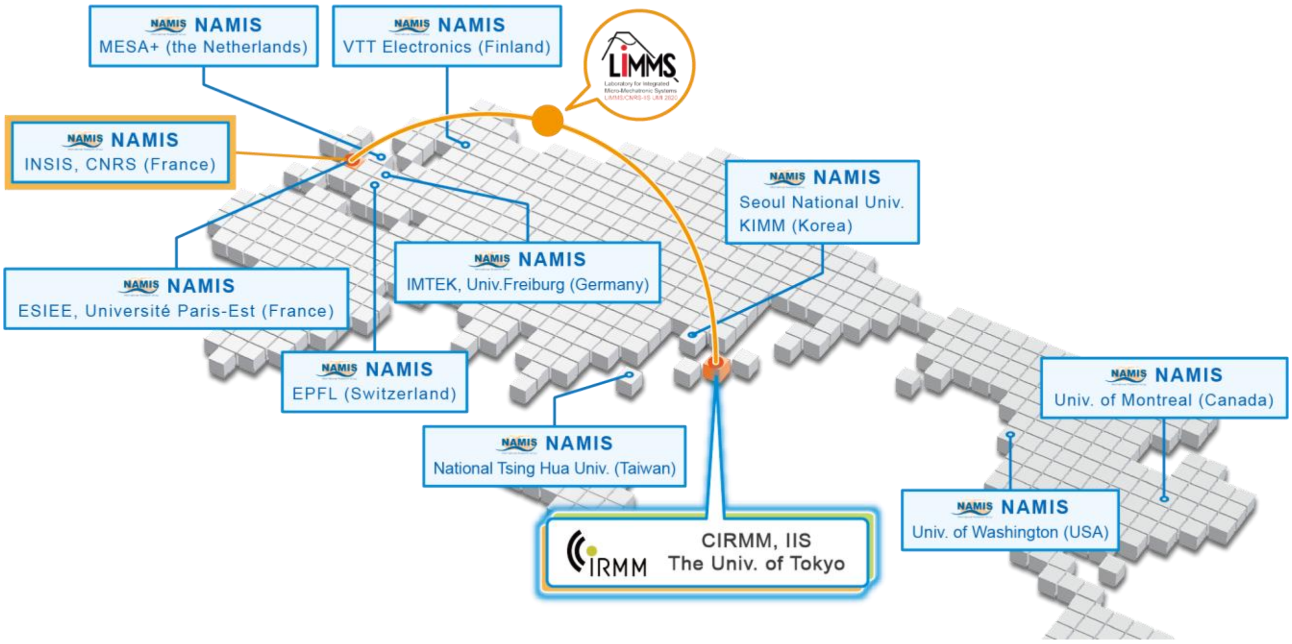

CIRMM International Network

Other Related Organizations

Korea Institute of Industrial Technology	South Korea
http://english.itep.re.kr/	
Research Center for Advanced Science and Technology, The University of Tokyo	Japan
http://www.rcast.u-tokyo.ac.jp/ja/	
VLSI Design and Education Center (VDEC), The University of Tokyo	Japan
http://www.vdec.u-tokyo.ac.jp/English/index.html	
Nanofabrication Platform, The Nanotechnology Platform Japan Program	Japan

1-8. Members

Name	Position	Research Field
TAKAHASHI, Takuji	Director and Professor	Nano-probing Technologies
TOSHIYOSHI, Hiroshi	Deputy Director and Professor	MEMS and NEMS
KAWAKATSU, Hideki	Professor	Coupling to the Nano Regime
KIM, Beomjoon	Professor	Micro Components & Systems
TAKAMIYA, Makoto	Professor	Integrated Power Management Circuits
MIZOGUCHI, Teruyasu	Professor	Understanding Role of Atom and Electron in Material
NOMURA, Masahiro	Professor	Nanoscale Heat Transfer and Thermoelectrics
TIXIER-MITA, Agnes	Associate Professor	Bio CMOS-MEMS Platforms
TOCHIGI, Eita	Associate Professor	Nanoscale Strength of Materials
MATSUHISA, Naoji	Associate Professor	Interactive Electronic Devices

-Takahashi Laboratory Members:
SHIMADA, Yuuji (Technical Support Specialist)
LI, Shenwei (Graduate Student)
WEN, Sihan (Graduate Student)
TAKEMOTO, Kaita (Graduate Student)
YOGI, Naomi (Assistant)

-Toshiyoshi Laboratory Members:
ATAKA, Manabu (Research Associate)
TAKAHASHI, Takuya (Technical Support Specialist)
HASHIGUCHI, Gen (Research Fellow)
SASAKI, Naruo (Research Fellow)

ONO, Shimpei (Research Fellow)
YOKOKAWA, Ryuji (Research Fellow)
KAKUSHIMA, Kuniyuki (Research Fellow)
SEKIYA, Hidehiko (Research Fellow)
ISHIDA, Tadashi (Research Fellow)
KUMEMUEA, Momoko (Research Fellow)
YAMANE, Daisuke (Research Fellow)
NAGAI, Moeto (Research Fellow)
MITA, Makoto (Research Fellow)
HONMA, Hiroaki (Research Fellow)
HIGO, Akio (Associate Research Fellow)
CHIU Wan-Ting (Associate Research Fellow)
YAMADA, Shunsuke (Associate Research Fellow)
MENON, Vivek Anand (Project Researcher)
IHIDA, Satoshi (Private Sector Collaborative Researcher)
ISAMOTO, Keiji (Private Sector Collaborative Researcher)
YI, Xiao (Private Sector Collaborative Researcher)
MITSUYA, Hiroyuki (Private Sector Collaborative Researcher)
ODA, Yutaro (Private Sector Collaborative Researcher)
GUERREIRO, Sara Rodriques Palma (Graduate Student)
SUGAHARA, Junpei (Graduate Student)
HU, Xingzhuo (Graduate Student)
FAURE, Gabriel (Graduate Student)
CHIKAMATSU, Kosuke (Graduate Student)
SHOJI, Takeshi (Graduate Student)
HAYAMA, Yuri (Graduate Student)
DIA, Yero Harouna (JSPS Internship Student)
KOIZUMI, Hiroko (Assistant)

-Kawakatsu Laboratory Members:
KOBAYASHI, Dai (Research Associate)
TOMOFUJI Kouji (Graduate Student)
ZHOU Zheyuan (Graduate Student)
ZHU Zhenyan (Graduate Student)
LI Yifan (Graduate Student)
LI Baitao (Graduate Student)
Ken Nakayama (Graduate Student)
Wei Zihao (Research Student)
Shen Fengyu (Research Student)

-Kim Laboratory Members:

PARK, JongHo (Assistant Professor)
SALLES, Vincent (Visiting Research Fellow)
HWANG, Gilgueng (Visiting Research Fellow)
DEMG, Haitao (Project Researcher)
TAKEUCHI, Kai (Private Sector Collaborative Researcher)
KOMA, Yosuke (Private Sector Collaborative Researcher)
TSURUMA,Yuko (Private Sector Collaborative Researcher)
SUGIMOTO, Koji (Private Sector Collaborative Researcher)
KAI, Yuya (Private Sector Collaborative Researcher)
FUJII, Katsuhito (Private Sector Collaborative Researcher)
JING, Heyi (Graduate student)
SHOBAYASHI, Kotaro (Graduate student)
QIN, Boyu (Graduate student)
ZHANG, Jingzong (Graduate student)
DEBUN, Kotaro (Graduate student)
XU, Chensong (Graduate student)
XIE, Tingyu (Graduate student)
HANAMOTO,Wataru (Graduate student)
INAGAKI, Taishi (Graduate student)
DONG, Li (Internship Student)
AOYAGI, Hoshimi (Technical Staff)
KINOSHITA, Rie (Technical assistant)
OKUDAIRA, Kazuko (Assistant)
KOIZUMI, Hiroko (Assistant)

-Takamiya Laboratory Members:

HATA, Katsuhiro (Research Associate)
SAI, Toru (Research Fellow)
INUMA, Toshiaki (Project Academic Specialist)
ZHANG, Dibo (Project Academic Specialist)
WANG, Ruizhi (Graduate Student)
ZHOU, Haoxi (Graduate Student)
YANO, Hiroki (Graduate Student)
SUKITA,Yohei (Graduate Student)
AMANO, Ayako (Assistant)

-Mizoguchi Laboratory Members:

SHIBATA, Kiyou (Assistant Professor)

FUKUDA, Atsushi (Technical staff)
LEE, Sangjun (Postdoctoral researcher)
NAKANO, Takumi (Company Research Fellow)
SUGIURA, Tasuku (Company Research Fellow)
KAWAGUCHI, Naoto (Graduate student)
CHEN, Poyen (Graduate student)
TAKAHARA, Izumi (Graduate student)
NAKAGAWA, Riuki (Graduate student)
OKUBO, Ren (Graduate student)

-Nomura Laboratory Members:
ANUFRIEV, Roman (Project Associate Professor)
SAWANO, Kentaro (Visiting Professor)
VOLZ, Sebastian (Visiting Research Fellow)
JALABERT, Laurent (Visiting Research Fellow)
ORDONEZ-MIRANDA, Jose (Visiting Research Fellow)
KOSEVICH, Yury (Visiting Research Fellow)
KIM, Byunggi (Project Research Associate)
YANAGISAWA, Ryoto (Project Research Associate)
WU, Yunhui (Project Research Associate)
HUANG, Xin (Project Research Associate)
IKZIBANE Hafsa (Project Researcher)
PIRRO, Matteo (Project Researcher)
DIEGO, Michele (UTokyo Postdoctoral Research Fellow)
KOIKE, Souta (Graduate student)
SHI, Hongyuan (Graduate student)
WANG, Weitao (Graduate student)
LIN, Wen-Chiao (Graduate student)
ITO, Soutarou (Graduate student)
WU, Xin (Visiting Associate Research Fellow)
YANG, Lei （Visiting Associate Research Fellow)
BIN, Chengwen (Visiting Associate Research Fellow)
CORAL, Maelie (Visiting Associate Research Fellow)
BARBIER–CHEBBAH, Felix (Internship Student)
VO VAN QUI, Henri (Internship Student)
MARHIC, Julia (Internship Student)
GASSMANN, Philipp (Internship Student)
OTSUKA, Miho (Private Sector Collaborative Researcher)
NAKAOKA, Toshihiro (Research Fellow)

XIONG, Shiyun (Research Fellow)
PARK, Keunhan (Research Fellow)
MAIRE, Jeremie (Research Fellow)
GUO, Yangyu (Associate Research Fellow)
ZHANG, Zhongwei (Associate Research Fellow)
YOSHIDA, Yoshifumi (Associate Research Fellow)
OKOCHI, Erina (Assistant)

-Tixier-Mita Laboratory Members:
FAURE, Pierre-Marie (Visiting Associate Research Fellow)
DUFOUR Alex (Internship Student)
FLAMANT Juliette (Internship Student)
FOSCHIA Théo (Internship Student)
MENIER Thomas (Internship Student)
KOIZUMI, Hiroko (Assistant)

-Tochigi Laboratory Members:
SATO, Takaaki (Project Researcher)
NAKAMURA, Toshiki (Graduate student)
NODA, Masato (Graduate student)
IMAMIYA, Mana (Technical Assistant)
OGITA, Sakiko (Assistant)

-Matsuhisa Laboratory Members:
LIU, Yijun (Graduate student)
ZHU, Yicheng (Graduate student)
GONG, Huimin (Graduate student)
SHIMURA, Tokihiko (Internship student)
TOMINAGA, Taizo (Internship Student)
WANG, Liren (Internship Student)
LIU, Siyuan (Graduate student)
MITOMO, Hinata (Graduate student)
ZHOU, Yuanyuan (Graduate student)
BHATE, Vishva (Internship student)
PAPIANO, Irene (Internship student)
CHANG, Ting-Wei (Internship student)
O'NEILL, Stephen JK (Internship student)
SEKI, Akiko (Assistant)
TAKEKOSHI, Mai (Assistant)

Affiliated members:

HIRAKAWA, Kazuhiko (Professor)

The University of Tokyo, Institute of Industrial Science
Research Area: Quantum Semiconductor Electronics

SAKAI, Yasuyuki (Professor)

The University of Tokyo, Institute of Industrial Science
Research Area: Organs and Biosystems Engineering

MITA, Yoshio (Associate Professor)

The University of Tokyo, School of Engineering
Research Area: Intelligent Electron Devices by MEMS Technology

SOMEYA, Takao (Professor)

The University of Tokyo, School of Engineering
Research Area: Flexible Electronics

SUGIYAMA, Masakazu (Professor)

The University of Tokyo, Research Center for Advanced Science and Technology
Research Area: Novel Micro-nano Fabrication Processes for Next-generation MEMS, Crystal Growth of III-V Semiconductors for High-efficiency Solar Cells

HIBARA, Akihide (Professor)

Tohoku University, Institute of Multidisciplinary Research for Advanced Materials
Research Area: Nano/Micro Chemical Measurements

HANE, Kazuhiro (Professor)

Tohoku University, Department of Nanomechanics
Research Area: Optical MEMS, especially Optical Micro-sensors and Integrated Optical Systems for Telecom

HASHIGUCHI, Gen (Professor)

Shizuoka University, Research Institute of Electronics
Research Area: Micromachining, Electret-based Energy Harvester

KONISHI, Satoshi (Professor)

Ritsumeikan University
Research Area: Microelectromechanical Systems (MEMS), Microrobotics, Biomedical Engineering

NOJI, Hiroyuki (Professor)

The University of Tokyo, School of Engineering
Research Area: Single Molecular Biophysics

Activity Highlight

April 2023- March 2024

April 18th to July 25th
U-Ideathon 2023

An International Ideathon "U-Ideathon2023" was organized in IIS with CIRMM and NAMIS partners as the core members. The ideathon was carried out on-line with participation from Ochanomizu Women's University, Nara Women's University, National TsingHua University (Taiwan), National Singapore University (Singapore), La Trobe University (Australia) and IIS/UTokyo as the host organizer. On the final day, the event was Hybrid, and we welcomed participants from abroad. We acknowledge the support from local organizers who helped out with technical issues and animated the discussions. We are grateful to Prof. H. Fujita for financial support of the closing meeting.

Fig. From U-Ideathon2023, (a) a stage for the hybrid meeting, (b) Paul and Brian from La Trobe, and (c) closing event.

July 20th, 2023
PRESM2023 Young Researcher Award

Prof. Naoji Matsuhisa won PRESM2023 Young Researcher Award for his presentation at international conference on Precision Engineering and Sustainable Manufacturing (PRESM2023).

September 20th, 2023
PMI Future 50

Prof. Naoji Matsuhisa was listed as one of the innovators in Project management institute (PMI) Future 50 for his development of future wearable devices.

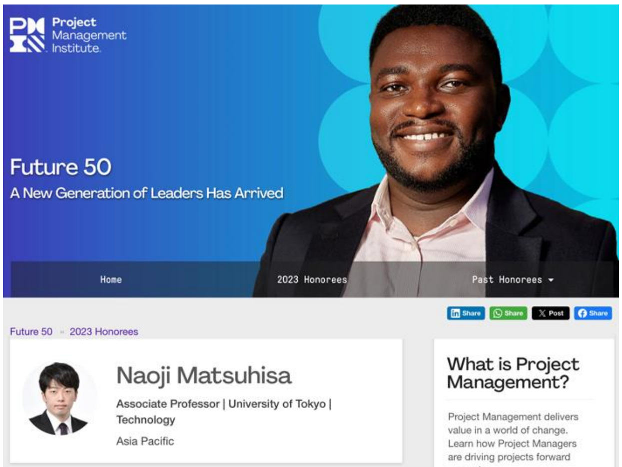

October 24th-25th
Ideathon UTokyo-TsingHua University

We welcomed Professor Yonggang Meng of the State Key Laboratory of Tribology in Advanced Equipment (SKLT), TsingHua University (China) and students for a scientific meeting and a joint Ideathon with UTokyo students and IIS staff.

November 17th
Meeting with Professor Emeritus Hannes Bleuler of EPFL (Switzerland)

Professor H. Kawakatsu met with Professor Hannes Bleuler who is member of IIS, EPFL, and the IIS international evaluation committee to discuss ideas to strengthen ties between IIS and EPFL.

November 20th
New NAMIS Workshop

As a resumption of practical international activities of NAMIS after COVID-19 pandemic, New NAMIS Workshop was held at EPFL in Switzerland, and 5 and 7 professors from CIRMM and EPFL, respectively, participated in one day workshop including a visit to laboratories in EPFL.


November 30, 2023
Prof. H. Toshiyoshi, Prof. G. Hashiguchi (Shizuoka University), and Mr. H. Mitsuya (Saginomiya Seisakusho, Inc.) receive an award from the Promotion Foundation for Electrical Science and Engineering.

This award is presented to their innovative industrial application of MEMS energy harvester.

From left: Prof. G. Hashiguchi, Mr. H. Mitsuya, and Prof. H. Toshiyoshi

December 1st-5th, 2023
NAMIS Marathon Workshop 2023

NAMIS Marathon Workshop was held in Taiwan from the 1st to the 5th of December 2023.
More than ten researchers and students participated in the event from CIRMM and LIMMS. All the participants run the marathon and then gave oral presentations the following day. We are all very grateful to Professor Andrew Yeh, his staff and students for organizing such a stimulating event.

Fig. (a) Outside the scientific meeting building, and (b) visit to Taiwan Semiconductor Research Institute.

February 2nd, 2024
Joint workshop on Innovative Micro/Nano Systems between Seoul National University and IIS, UTokyo.

Joint workshop with Seoul National University was held in convention hall of Institute of Industrial Science, the University of Tokyo on February 2nd., 2024.
11 professors and 10 young researchers, graduate students from Department of Electrical and computer Engineering, Mechanical Engineering, as well as Material Science, Seoul National University attended this joint workshop. For one day full program, there were 9 professors' research presentations from IIS and all 11 professors' presentation from SNU as well as 17 poster presentations from both parts. Through this fruitful onsite joint workshop, new findings of the works related with the micro/nano systems for bio/medical applications as well as energy harvesting and future sensor networks were discussed. This Joint workshop was supported by "Super-global network on Seoul National Univ. (SNU)/ IIS, The Univ. of Tokyo" by Strategic Partnership Program, partially by CRIMM and CREMEB at IIS, as well as by SNU BK21 program (Education and Research program for future ICT Pioneers & SNU Mechanical engineering 10-10 project).

February 22nd, 2024
CIRMM symposium for sharing research achievements of Doctoral/Master students

Doctoral and master students in CIRMM gave presentations about their research achievements for their thesis. In addition, there were presentations about three collaboration projects initiated by students in CIRMM. More than 30 people, including professors and students, discussed various research conducted in CIRMM.


March 24, 2024
Prof. H. Honma (Kobe University), Mr. Y. Mizuno (graduate student), and Prof. H. Toshiyoshi receive a paper award from JSAP Integrated MEMS Symposium 2024.

This award is presented for their paper on MEMS vibrational energy harvester reported at the 15th Integrated MEMS Symposium held in Kumamoto Castle Hall, Nov. 6-9, 2023.

From left: Prof. S. Hata (Nagoya Univ.) presenting the certificate to Prof. H. Honma.

Research Activities
April 2023 - March 2024

TAKAHASHI Laboratory

Current Research Activities 2022-2023

Takahashi Laboratory

1. Research Topics

1.1 Electrostatic Force Microscopy with Dual Bias Modulation Methods

Dual bias modulation electrostatic force microscopy (DEFM) enables us to examine a capacitance including a depletion capacitance at high spatial resolution under various modulation frequencies. We used this DEFM to observe a cross section around an n-type GaN/GaN junction fabricated by surface-activated bonding, and the effect of thermal annealing on interfacial properties was investigated based on the DEFM signals which correspond to the $\partial C/\partial z$ signals.

Figure (a) shows a topographic image taken on a cross-section around the bonding interface in the sample after annealing (1 min. at 800 °C in N_2 gas), although the bonding interface was not clearly identified. From the image on the same area taken by Kelvin probe force microscopy (KFM) shown in Figure (b), on the other hand, the interface was supposed from a boundary of regions with different surface potentials. In the DEFM image, in addition, the signals were enhanced around the interface compared with those on the bulk, being attributable to an enhancement of carrier transfer via nitrogen vacancy states along the interface induced by the annealing process. We can also investigate dependence of the $\partial C/\partial z$ signal on the modulation frequency in the DEFM method.

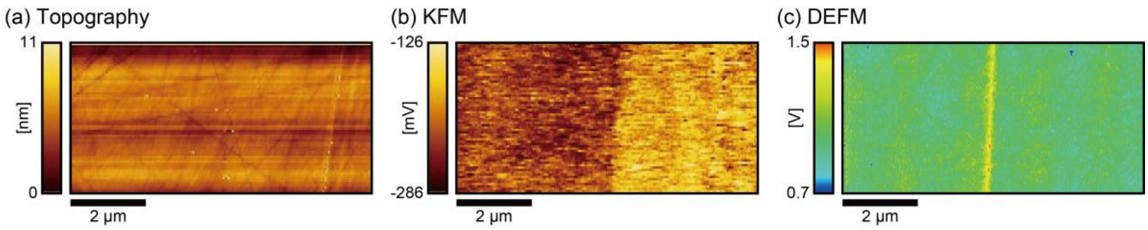

1.2 Quantitative Capacitance Measurements on Semiconductor by Electrostatic Force Microscopy

An electrostatic force between a tip and a semiconductor is strongly related with electrical properties, such as surface potential, capacitance, and charge density, of a semiconductor, and local characterization of the semiconductor is possible through the electrostatic force detected by AFM. However, quantitative estimation of the tip-sample capacitance from AFM is difficult when the capacitance includes a surface depletion capacitance of the semiconductor because a straightforward formulation considering the dependence of the surface depletion on the external bias voltages is not well established. In this study, we have formulated the frequency shift induced by the electrostatic force, detected in frequency modulation electrostatic force microscopy (FM-EFM), and we also have performed quantitative capacitance-voltage (C-V) measurements on n- and p-type Si substrates by FM-EFM.

First, we theoretically derived a conversion formula from a frequency shift of cantilever resonance in EFM into a capacitance value based on the parallel plate capacitor model, by which a pair of an EFM tip and a semiconductor sample is expected to be equivalently represented. Then the capacitance measurements were experimentally conducted on the n- and p-type Si substrates using FM-EFM with a dual bias modulation method. Figure shows a capacitance–voltage curve acquired on the n-type Si, indicating that the obtained capacitance values were consistent with the expected ones and that the carrier densities evaluated from the depletion capacitances were also in good agreement with those evaluated by the conventional Hall effect measurements. Similar consistency was also obtained on the p-type substrate. These results support the validity of our quantitative analytical method.

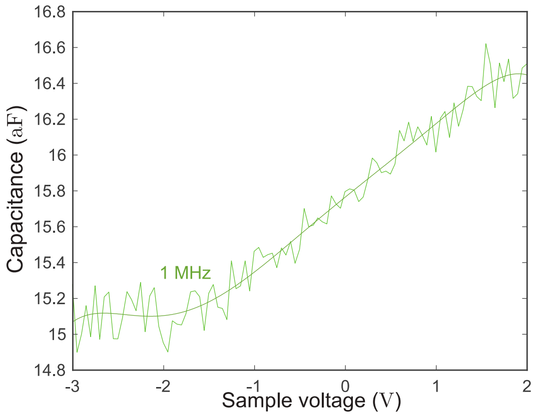

1.3 Time-resolved Electrostatic Force Microscopy

Time-resolved measurements in electrostatic force microscopy (EFM) allows us to investigate charging and discharging properties of near-surface states in samples. By combining the intermittent bias application method which has been developed for improving a spatial resolution in electrostatic force detection in AFM and the pump-probe method which is widely used for time-resolved measurements, time-resolved EFM (Tr-EFM) has been constructed. In EFM measurements, however, the electrostatic force depends on an external d.c. bias as well as a contact potential difference (CPD) between a sample and tip. In order to nullify an influence of CPD, we also added a function of Kelvin probe force microscopy as shown in Figures (a)-(d) below and realized real time control of base bias level in Tr-EFM measurements. Figures (e) and (f) shows waveforms of electrostatic force induced by a pulsed bias modulation taken on SiO_2/Si sample with and without FGA-gas treatment. As shown in them, electrostatic forces before and after the modulation were nearly null, indicating the base-bias-level control worked well. In addition, different responses were obtained: an overshoot was observed on the as-fabricated sample, being attributable to the response of charges accumulated at dense interface states between SiO_2 and Si.

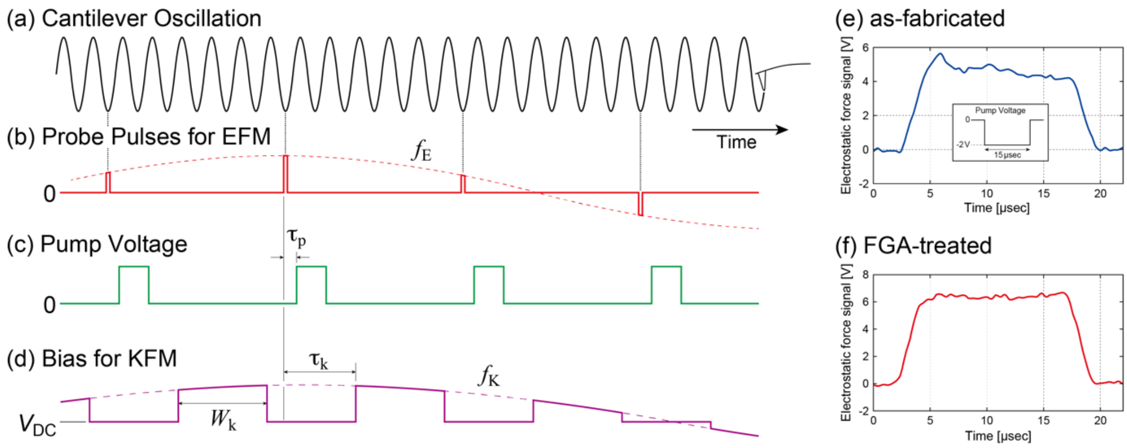

1.4 Time-resolved Photo-assisted Kelvin Probe Microscopy on Solar Cells

Photo-assisted Kelvin probe force microscopy (P-KFM) allows us to investigate photovoltaic properties especially in solar cells, and if a temporal change in photovoltage can be observed by P-KFM, photocarrier dynamics will be analyzed in further detail. Using a similar system to Tr-EFM, where the electrical pump signal was replaced with an optical pump and the intermittent probe pulses were used for KFM, time-resolved P-KFM has been realized.

Figure shows temporal change of photovoltage distribution observed by P-KFM on a $Cu(In,Ga)Se_2$ solar cell just after the onset of the optical pump with different photon energies. Similarly, photovoltage decay process could be analyzed. From these measurements, we can investigate how photovoltage rising and decay processes differ between grain interiors and their boundaries.

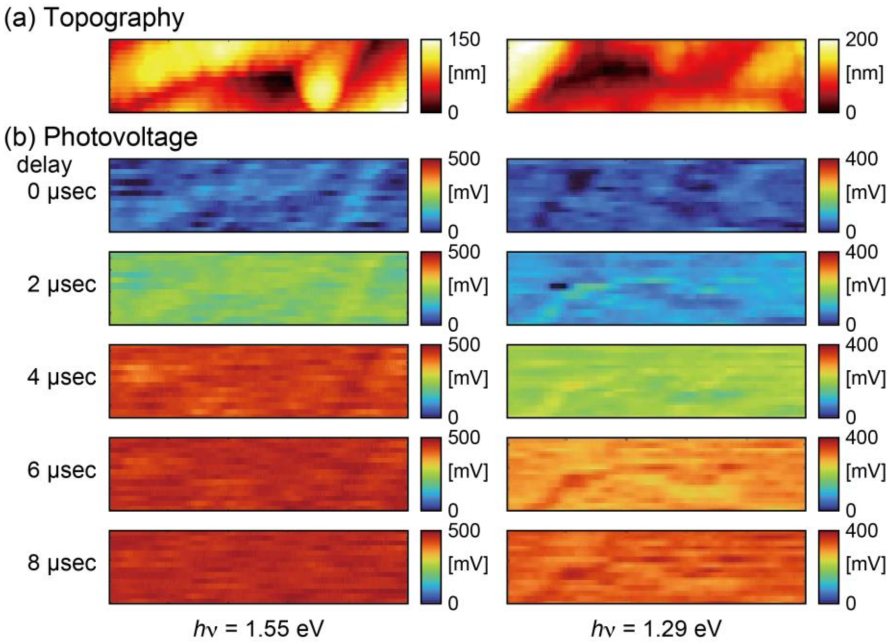

2. Research Achievements

2.1 Number of original journal papers: 1

2.2 International conference: 5

2.3 Domestic conference: 5

2.4 Number of patents: 0

3. List of awards

- none

4. Research Grants

4.1 Total number of research grants: 1

4.2 Number of collaboration research with industries: 1

4.3 List of major research grants (serving as Principal Investigator)

- Grant-in-Aid for Scientific Research "Dynamics of photo-generated carriers in multinary compound semiconductor solar cells investigated by photo-assisted nanoprobes" from JSPS

5. Education

5.1 Number of Ph.D. students (including current students): 0

5.2 Number of master students (including current students): 3

5.3 Number of other students: None

6. Publication list

Journal Papers

1. Jo Sato, Ryota Ishibashi, and T. Takahashi, "Time-resolved Electrostatic Force Microscopy under Base-bias-level Control", *Measurement Science and Technology*, **35**, 035005 (2024).

Conference Presentations

1. Ryota Fukuzawa and Takuji Takahashi, "Quantitative Capacitance and Carrier Density Measurements on Semiconductor by Electrostatic Force Microscopy", *24th International Conference on Non-contract Atomic Force Microscopy*, OR-08-008, Singapore, Sep. (2023).
2. Takuji Takahashi, "Photo-assisted Scanning Probe Microscopy on Solar Cells", *Annual LIMMS Workshop*, Lille, France, Oct. (2023). [Invited]
3. Sihan Wen, Kazuki Sawai, Jianbo Liang, Naoteru Shigekawa, and Takuji Takahashi, "Cross-sectional Investigation by Kelvin Probe Force Microscopy around a GaN/GaN Interface Fabricated by Surface-activated Bonding", *31st International Colloquium on Scanning Probe Microscopy (ICSPM31)*, Tokyo, Japan, Dec. (2023).
4. Takuji Takahashi, "Photo-assisted SPMs on Solar Cells", *New NAMIS Workshop*, Lausanne, Switzerland, Nov. (2023). [Invited]
5. Sihan Wen, Kazuki Sawai, Jianbo Liang, Naoteru Shigekawa, and Takuji Takahashi, "Cross-sectional Investigation around an Interface of Directly Bonded GaN/GaN Substrates Using Electrostatic Force Microscopy", *Seoul National University (SNU) / Institute of Industrial Science, the University of Tokyo (IIS, UTokyo) Joint Workshop*, Tokyo, Japan, Feb. (2024).
6. Takuji Takahashi, "Nanoprobing Technology", *Seoul National University (SNU) / Institute of Industrial Science, the University of Tokyo (IIS, UTokyo) Joint Workshop*, Tokyo, Japan, Feb. (2024). [Invited]

IOP Publishing | Measurement Science and Technology
Meas. Sci. Technol. **35** (2024) 035005 (7pp) https://doi.org/10.1088/1361-6501/ad10e0

Time-resolved electrostatic force microscopy under base-bias-level control

Jo Sato[1], **Ryota Ishibashi**[1] **and Takuji Takahashi**[1,2,*]

[1] Institute of Industrial Science, The University of Tokyo, 4-6-1 Komaba, Meguro, Tokyo 153-8505, Japan
[2] Institute for Nano Quantum Information Electronics, The University of Tokyo, 4-6-1 Komaba, Meguro, Tokyo 153-8505, Japan

E-mail: takuji@iis.u-tokyo.ac.jp

Received 22 August 2023, revised 27 November 2023
Accepted for publication 29 November 2023
Published 7 December 2023

Abstract

We propose a base-bias-level control method, in which the contact potential difference is always compensated in a similar way to Kelvin probe force microscopy, applicable to time-resolved electrostatic force microscopy using the pump–probe method. We experimentally acquired temporal waveforms of the electrostatic force signal on two SiO_2/*n*-type Si samples, one of which was as-grown and the other was treated by forming gas annealing. Consequently, the effectiveness of the proposed method was confirmed.

Keywords: electrostatic force microscopy, Kelvin probe force microscopy, pump–probe method, time-resolved measurement, intermittent bias

1. Introduction

Atomic force microscopy (AFM) [1] enables us to investigate a local surface structure with atomic resolution [2, 3], and various applications of AFM have been developed to evaluate the local electrical properties of a sample. By using a conductive AFM tip, an electrostatic force can be detected, and electrostatic force microscopy (EFM) [4] and Kelvin probe force microscopy (KFM) [5] have been developed to analyze the distributions of charge, capacitance, surface potential, and so on. In most EFM and KFM, an alternating current (AC) voltage together with a direct current (DC) voltage are applied between the sample and the tip to generate the electrostatic force, and a lock-in amplifier is used to extract a certain frequency component of the electrostatic force from the entire force signal detected as a cantilever deflection signal. Since the bandwidth of the lock-in amplifier is narrow, the response time for electrostatic force detection in the normal operation mode of EFM and KFM is limited to the order of msec at most [6–9]. Thus, it is highly desired to achieve superior time resolution in both EFM and KFM, and some methods have been innovated [10, 11]. For example, a method was proposed where the cantilever deflection signal was directly recorded in real time and then the frequency and phase shifts in the time domain were computationally demodulated to investigate the time constants for their response in the sub-µs range[12–14]. Another demodulation method was proposed, where pulse trains synchronized with the tip motion were applied [15, 16], and the charge dynamics under pulsed laser excitation or electrical voltage application were investigated with a time resolution around µs. Furthermore, the pump–probe method [17–21] is another promising way to realize time-resolved measurements in EFM and KFM. The advantage of the pump–probe method is that fast signal detection and/or large data storage systems are not always required.

On the other hand, when a tapping mode is used for EFM and/or KFM, a relatively large change in the sample–tip distance due to the cantilever oscillation causes a degradation in accuracy and spatial resolution for the electrostatic force detection [22] because the electrostatic force is a long-range force. The authors of this paper previously proposed an intermittent bias application method for KFM [23, 24], where an electrical pulse train having a sinusoidal envelope was used

[*] Author to whom any correspondence should be addressed.

QUANTITATIVE CAPACITANCE AND CARRIER DENSITY MEASUREMENTS ON SEMICONDUCTOR BY ELECTROSTATIC FORCE MICROSCOPY

Ryota Fukuzawa[1,2] and Takuji Takahashi[2,3]

[1]*Dept. of Electrical Engineering and Information Systems, The University of Tokyo, 113-8656 Japan,*
[2]*Institute of Industrial Science/ 3Institute for Nano Quantum Information Electronics,*
The University of Tokyo, 153-8505 Japan
Email: fukuzawa@ntech.t.u-tokyo.ac.jp

An electrostatic force between a tip and a semiconductor is strongly related with electrical properties, such as surface potential, capacitance, and charge density, of a semiconductor, and frequency modulation electrostatic force microscopy (FM-EFM) with direct current (DC) and/or alternating current (AC) bias application enables local characterization of the semiconductor through the electrostatic force detection between a tip-apex and a sample. Although a frequency shift of the cantilever resonance induced by the electrostatic force is measured in a typical FM-EFM, quantitative estimation of the tip-sample capacitance from the measured frequency shift is difficult when the capacitance includes a surface depletion capacitance of the semiconductor because a straightforward formulation considering the dependence of the surface depletion on the external bias voltages is not well established. On the other hand, S. Hudlet et al. indicated that the electrostatic force F^ele between the tip and the semiconductor sample could be expressed to be proportional to square of charge using virtual work method [1]. Based on it, in this study, we have formulated the frequency shift induced by the electrostatic force under linear approximation of the charge response with the changes in tip-sample distance and voltage, and we also have performed quantitative capacitance-voltage (C-V) measurements on p- and n-type Si substrates by FM-EFM.
For variable AC frequency measurements in FM-EFM, we applied dual AC voltages and DC voltage $V_{dc}+V_1 \sin\omega t+V_2\sin(\omega+\omega_d)t$ between the tip and the sample, and the capacitance was calculated from the ω_d ($\ll \omega$) component of the frequency shift $\Delta f^{\mathrm{ele}}_{\omega_\mathrm{d}}(\omega)$ using Eq. (1) brought from our formulation [2], where $\omega_0/2\pi$ and k are a resonant frequency (~300 kHz) and a spring constant (~ 40 N) of the cantilever in free oscillation, and ϵ0 and S are the dielectric constant of vacuum and equivalent area of the tip-sample capacitor, respectively. The value of S was evaluated from F^{ele}-z characteristic at the voltage condition for accumulation, where the surface depletion capacitance could be neglected, and it is considered that the tip-sample capacitance is dominated by the series capacitance of the air gap and oxide film capacitances. Figure 1 shows C-V characteristic on the p-type Si substrate evaluated by applying Eq. (1) to the $\Delta f^{\mathrm{ele}}_{\omega_\mathrm{d}}(\omega)$ values measured at 1 MHz and around 300 kHz. We found that the capacitance gradually decreased in the direction toward negative DC bias voltage where the surface was more depleted, and values of capacitance around atto-farad are considered reasonable for the tip-sample capacitance.
Furthermore, we evaluated the charrier density from maximum depletion layer width which was estimated from the C-V characteristic obtained by FM-EFM. The evaluated carrier density was 2.0×10^{17} cm^{-3}, which agrees well with a value of 2.4×10^{17} cm^{-3} obtained by conventional hall effect measurements. Similar consistency was also obtained on the n-type substrate. These results support the validity of our quantitative analytical method.

$$C(\omega)=\left(\frac{4\pi k\epsilon_0^2 S^2}{\omega_0 V_1 V_2}\right)^{1/3}\left[\frac{\Delta f^{\mathrm{ele}}_{\omega_\mathrm{d}}(\omega)}{\left(\Delta f^{\mathrm{ele}}_{\omega_\mathrm{d}}(\omega_0)\right)^{1/3}}\right]^{1/2} \quad (1)$$

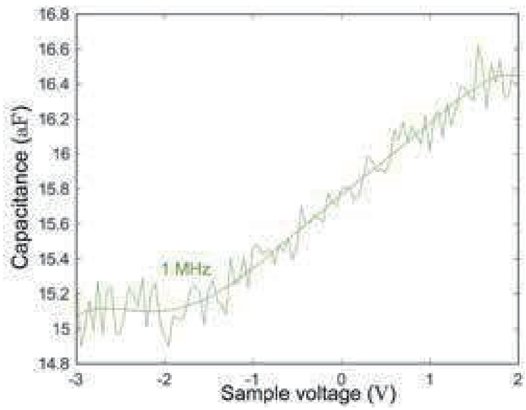

Fig. 1 Capacitance-voltage characteristics on a p-Si substrate using Eq (1) under AC voltage modulation at **1 MHz**.

References
[1] S. Hudlet, et al., J. Appl. Phys., **77**, 3308 (1995).
[2] R. Fukuzawa et al., Jpn. J. Appl. Phys., **61** SL1005 (2022).

S7-3

Cross-sectional Investigation by Kelvin Probe Force Microscopy around a GaN/GaN Interface Fabricated by Surface-activated Bonding

Sihan Wen[1], Kazuki Sawai[3], Jianbo Liang[3], Naoteru Shigekawa[3], and Takuji Takahashi[1, 2]
[1]IIS / [2]NanoQuine, The Univ. of Tokyo, 4-6-1 Komaba, Meguro, Tokyo 153-8505, Japan
[3] Grad. Sch. Eng., Osaka Metropolitan Univ., 3-3-138 Sugimoto, Sumiyoshi, Osaka 558-8585, Japan

The surface-activated bonding (SAB) method can bond two semiconductor substrates regardless of lattice matching or crystallographic axis orientation. Since a GaN material has spontaneous electrical polarization in it, an electric field and potential distribution around a bonded interface depend on the orientation of the substrates, and such a potential distribution might affect the electrical conduction across the interface. Kelvin force probe microscopy (KFM) is very effective to investigate the surface potential distribution with high spatial resolution, and therefore, cross sections around the GaN/GaN interface fabricated by the SAB method were analyzed by KFM in this study.

Two pieces of substrate cut from a freestanding n-type GaN (0001) substrate ($n \sim 10^{18}$ cm^{-3}) were bonded by the SAB method so that the Ga surfaces were contacted with each other. We prepared two samples: one was as-bonded and the other was thermally annealed. For KFM observation, the sample was polished to expose a cross section with a non-polar m-plane. Figure 1 shows the topographic and surface potential images on both samples, where the potential was defined as that for electrons. From Fig. 1(a-2), we found the linear region with higher potential, and we consider that this region corresponds to the junction interface indicated by the arrows in Fig. 1(a-1). We attribute this potential increase to the negatively charged interface states, and such an increase could be also deduced from the results of I-V-T measurement on a similar sample [1]. Note that some other stripes shown in the topographic images (Figs. 1(a-1) and (b-1)) are considered the scratches due to the polishing process. On the annealed sample, on the other hand, such an increase was not observed which is owing to the thermal passivation of the interface states, although some differences in the surface potential between two sides of the interface was observed, probably due to a slight difference of the surface orientation.

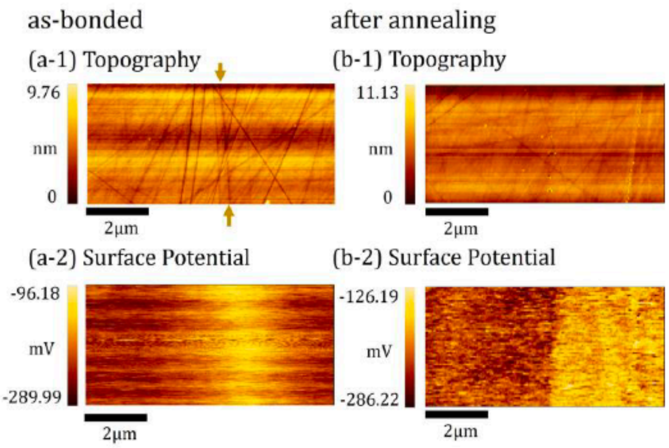

Fig. 1 Cross-sectional images taken by KFM around the GaN/GaN interface bonded by the SAB method.

References:

[1] K. Sawai, J. Liang, Y. Shimizu, Y. Ohno, Y. Nagai, and N. Shigekawa, *Jpn. J. Appl. Phys*, **62**, SN1013 (2023).

TOSHIYOSHI Laboratory

Current Research Activities 2023-2024

Toshiyoshi Laboratory

1. Research Topics

1.1 Simultaneous Process for Electret Forming and Anodic Bonding

Reducing material and manufacturing costs is essential for the widespread adoption of MEMS vibrational energy harvesters in practical IoT sensor applications. We have recently developed a simultaneous process to perform electret formation and wafer bonding so that MEMS vibrational energy harvesters would be made without the use of expensive bonded SOI (silicon on insulator) wafers.

Figure 1 illustrates the fundamental structure of the newly designed MEMS energy harvester. The top substrate is made of silicon that has been processed to shape the form of an electret-type vibrational energy harvester with hundreds of tiny electrodes that are designed to produce electrostatically induced current when forced to vibrate at the resonant frequency. The bottom part is a recessed glass substrate processed by sandblast. The two wafers are put together by anodic bonding caused by the voltage applied across the wafer interface. At the same time, the electrodes in the upper silicon substrate are also electrically charged to form an electret skin using additional voltage applied between the electrode pairs. **Figure 2** schematically shows the way to apply such voltages to form the electret and to bond wafers simultaneously. This silicon-on-glass process is beneficial in not only suppressing the parasitic capacitance but also increasing its output power compared with those made by the conventional SOI-based process.

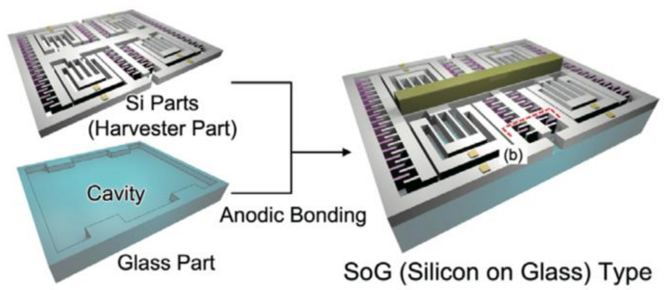

Figure 1. Double-deck MEMS vibrational energy harvester [J8].

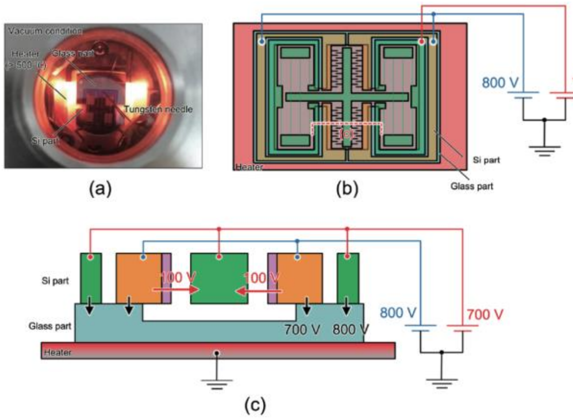

Figure 2. Simultaneous process for electret forming and anodic bonding [J8]

1.2 Electret MEMS Vibration Energy Harvester with Reconfigurable Frequency Response

We report a MEMS electret-type vibrational energy harvester with a wide bandwidth between 25 Hz and 60 Hz (span 35Hz) for a small sinusoidal acceleration of a few mG (G = 9.8 m/s^2). We have developed a method to tailor the nonlinear characteristics by adjusting the mutual position of the opposing electrodes. Both soft and hard spring effects are realized, thereby further extending the frequency bandwidth between 25 Hz and 95 Hz so that power could be effectively retrieved from extremely small vibrations of 10 mG. This reconfigurable nature of the developed harvester device is suitable for autonomous distributed sensors that gain power from the environmental vibrations.

The frequency response of electrostatic micro actuator depends on the added virtually spring constant caused by the electrostatic force caused by the applied bias voltage. When the electrodes are designed to mutually attract by electrostatic force, the overall mechanical performance will resemble a soft-spring effect, which has a frequency response peak tilted toward the lower frequency side. Considering this effect in the laterally movable electrodes shown in **Figure 3**, we have developed a mechanism to tune the frequency response by the initial offset position of the movable electrode.

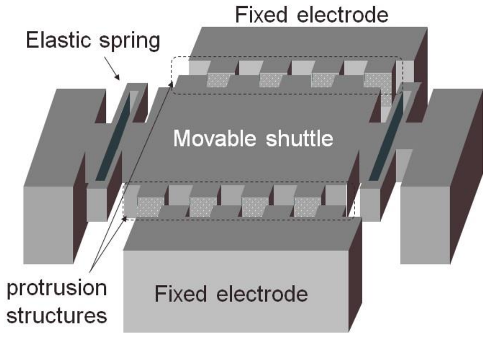

Figure 3. Analytical model for frequency response-tunable energy harvester using staggered electrodes [J7]. Depending upon the initial offset between the electrodes, the overall potential curve (electrostatic and elastic) is altered to produce a virtually flat bottom around the origin, thereby enabling post-process tuning of the frequency response.

Due to the energy-harvesting capability in a small acceleration range in a wide frequency span, the harvester developed in this work could be used in a battery-free network sensor to keep monitoring the time-degradation of social infrastructures such as bridges, highways, and railroads. A field test for such applications is under investigation, along with the development of the commercial-use MEMS energy harvesters.

1.3 MEMS Wavelength Tunable Laser Diode for Chip Scale Atomic Clock

At MEMS 2024 Conference, we reported a suspension design for a tunable vertical cavity surface-emitting laser (VCSEL) electrostatic MEMS mirror that separates the reflector from the electrostatic actuator to reduce the influence of secondary mechanical resonance modes. Compared to a monolithic actuating membrane design, a hundredfold reduction in the mechanical displacement of the mirror in the secondary resonance mode relative to the fundamental mode has been achieved. This enhancement of the main mode over higher-order modes is expected to improve interferometric stability when higher-frequency feedback may otherwise cause undesired fluctuation, especially during low frequency operation.

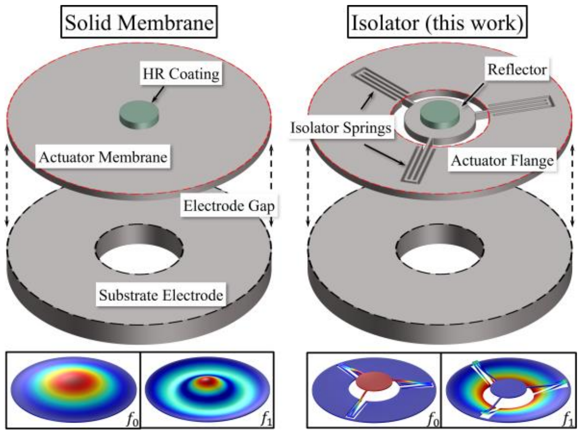

Figure 4. Schematic design of MEMS reflector with solid actuator (left) and isolator suspension (right). The first and second resonant modes (bottom) show significantly lower reflector displacement at the secondary resonant frequency f1 for the isolator design.

Separating the actuator and reflector regions of a MEMS mirror for VCSEL wavelength tuning enables selective filtering of the mechanical energy that is ultimately transmitted to the reflector and translated into mirror motion. By tuning the properties of the connecting suspension, the mirror can be designed to largely reject intermittent and high-frequency fluctuations that can cause instability in the resulting VCSEL output wavelength. This kind of isolator design was shown to be capable of reducing the influence of higher-order resonance mode, and interferometric analysis confirmed that this resulted in increased wavelength stability at lower MEMS drive frequencies.

2. Research Achievements (April 2023 – March 2024)

2.1 Number of original journal papers: 12

2.2 International conference: 11 (including 3 invited presentation)

2.3 Domestic conference: 15 (including 2 invited presentations)

2.4 Number of patents: 3

3. List of awards

1. H. Mitsuya, G. Hashiguchi, and H. Toshiyoshi, "Industrialization of high-efficiency MEMS vibrational energy harvester," The 71th Award, The Promotion Foundation for Electrical Science and Engineering, Nov. 30, 2023
2. H. Honma, Y. Mizuno, and H. Toshiyoshi, "Influence of phase-monitoring electrodes on power generation of MEMS vibrational energy harvester," The 15th Integrated MEMS Symposium Award, JSAP Study Group on Integrated MEMS, March 24, 2024.

4. Research Grants

4.1 Total number of research grants: 3

4.2 Number of collaboration research with industries: 4

4.3 List of major research grants (serving as Principal Investigator)

- JST CREST Number JPMJCR19Q2, "Perpetual Electronics" (one year extension)
- JSPS Grant in Aid 21H01271, "Electret Degradation Mechanism"
- MIC 0155-0189, "Miniaturization of Atomic Clock"

5. Education

5.1 Number of Ph.D. students (including current students): 2

5.2 Number of master students (including current students): 4

6. Publication list

Journal Paper (selected, *attached)

J1. Riku Ito, Ten Sekiguchi, Vivek Menon, Ryo Ichige, Yuya Tanaka, Hiroshi Toshiyoshi, and Takaaki Suzuki, "Near-zero Poisson's ratio and large-area metamaterial made of UV-PDMS using 3D backside exposure," Trans. IEEJ SM., vol. 144, no. 1, 2024, pp. 17-22.

J2. Takaaki Sato, Vivek Anand Menon, Hiroshi Toshiyoshi, and Eita Tochigi, "Microfabricated double-tilt apparatus for transmission electron microscope imaging of atomic force microscope probe," Review of Scientific Instruments, vol., 95, 023705 (2024).

J3. *Shunsuke Yamada and Hiroshi Toshiyoshi, "Battery-less luminance sensor biomimicking human sensory nervous system," Applied Physics Letters, vol. 123, 2023, p. 264101.

J4. *Shunsuke Yamada and Hiroshi Toshiyoshi, "A biodegradable ionic gel for stretchable ionics," Sensors and Actuators: A. Physical, vol. 361, 2023, p. 114574.

J5. Masahide Goto, Yuki Honda, Masakazu Nanba, Yoshinori Iguchi, Takuya Saraya, Masaharu Kobayashi, Eiji Higurashi, Hiroshi Toshiyoshi, and Toshiro Hiramoto, "Pixel-Parallel 3-Layer Stacked CMOS Image Sensors Using Double-Sided Hybrid Bonding of SOI Wafers," IEEE Transaction on Electron Devices. (published online)

J6. Ten Sekiguchi, Hidetaka Ueno, Vivek Anand Menon, Ryo Ichige, Yuya Tanaka, Hiroshi Toshiyoshi, and Takaaki Suzuki, "UV-curable PDMS Photolithography and Its Application for Flexible Mechanical Metamaterials," Sensors and Materials, vol. 35, no. 6(2), 2023, pp. 1995-2011.

J7. *Gen Hashiguchi and Hiroshi Toshiyoshi, "Electret MEMS Vibration Energy Harvester with Reconfigurable Frequency Response," Sensors and Materials, vol. 35, no. 6(2), 2023, pp. 1957-

1983.

J8. *Hiroaki Honma, Sho Ikeno, and Hiroshi Toshiyoshi, "MEMS Electrostatic Energy Harvester Developed by Simultaneous Process for Anodic Bonding and Electret Charging," Sensors and Materials, vol. 35, no. 6(2), 2023, pp. pp. 1941-1955.

International Conference (selected)

C1. *Vivek Anand Menon, Yi Xiao, Mohammed Saad Khan, Changdae Keun, Keiji Isamoto, Nobuhiko Nishiyama, and Hiroshi Toshiyoshi, "ACTUATOR/REFLECTOR DECOUPLING FOR REDUCED EXCITATION OF SECONDARY MECHANICAL RESONANCE MODES IN MEMS-TUNABLE VCSELS," in Proc. The 37th IEEE International Conference on Micro Electro Mechanical Systems (MEMS 2024), Jan. 21-25, 2024, Austin, Texas, pp. 1075-1078.

C2. Hiroyuki Mitsuya, Katsufumi Hashimoto, Kai-Chun Chang, Hisayuki Ashizawa, Hiroaki Honma, Gen Hashiguchi, Hiroshi Toshiyoshi, and Tomoki Shiotani, "Low-Power Frequency Monitoring System for Bridge using MEMS Vibrational-Energy Harvesting Sensor," Innovative Non-Destructive Testing for Civil Engineers (INDTCE) and 4th International Workshop on Self-Healing & Intelligent Materials (SHIM), Oct. 30 - Nov. 2, 2023, Hilton Hawaiian Village, Honolulu, Hawaii, US. (invited)

C3. Hiroyuki Mitsuya, Hisayuki Ashizawa, Takuma Ishiguro, Gen Hashiguchi, Kenji Shiraishi, and Hiroshi Toshiyoshi, "Highly reliable electret for heat resistive vibrational energy harvester," in Proc. 19th International Symposium on Electret (ISE19), Sept. 18-22, 2023, Bildungshaus Sankt Magdalena Educational Center, Linz, Austria. (invited)

C4. Yuto Akai, Hiroaki Honma, and Hiroshi Toshiyoshi, "FREQUENCY TRACKING OF VIBRATIONAL ENERGY HARVESTER USING PHASE-LOCKED LOOP (PLL)," in Proc. 22nd International Conference on Solid-State Sensors, Actuators and Microsystems (Transducers 2023), June 25-29, 2023, Kyoto International Conference Center, Kyoto, Japan, pp. 284-287. (oral)

C5. Hiroaki Honma, Yukiya Tohyama, and Hiroshi Toshiyoshi, "A MEMS VIBRATIONAL ENERGY HARVESTER CAPABLE OF RESTLESS CHARGING CAPACITOR FROM RANDOM VIBRATIONS," in Proc. 22nd International Conference on Solid-State Sensors, Actuators and Microsystems (Transducers 2023), June 25-29, 2023, Kyoto International Conference Center, Kyoto, Japan, pp. 1252-1255. (poster)

C6. Sara GUERREIRO, Markus BAINSCHAB, Adrien PIOT, Rodrigo TUMOLIN ROCHA, Hiroshi TOSHIYOSHI, Alain BOSSEBOEUF, Takashi SASAKI, Anton LAGOSH, and Moridi MOHSSEN, "Optical and Environmental Characterization Bench for 2D Micromirrors," in Proc. Design, Test, Integration & Packaging of MEMS/MOEMS (DTIP 2023), Valletta, Malta, May 28-31, 2023. (oral)

C7. Hiroaki Honma, Yuto Mizuno (Akai), and Hiroshi Toshiyoshi, "Characterization of Resonance Sensor Integrated in MEMS Vibrational Energy Harvester," in Proc. Design, Test, Integration & Packaging of MEMS/MOEMS (DTIP 2023), Valletta, Malta, May 28-31, 2023. (oral)

C8. Hiroaki Honma, Yukiya Tohyama, and Hiroshi Toshiyoshi, "Bandwidth Extension for MEMS Vibrational Energy Harvester using High-Voltage Electret," in Proc. Design, Test, Integration & Packaging of MEMS/MOEMS (DTIP 2023), Valletta, Malta, May 28-31, 2023. (oral)

C9. H. Toshiyoshi, "Design and Test for MEMS Vibrational Energy Harvesters," 35th International Conference on Microelectronic Test Structures (ICMTS), March 27, 2023, The University of Tokyo, Tokyo, Japan. (Tutorial)

ACTUATOR/REFLECTOR DECOUPLING FOR REDUCED EXCITATION OF SECONDARY MECHANICAL RESONANCE MODES IN MEMS-TUNABLE VCSELS

Vivek A. Menon[1], Yi Xiao[2], Mohammed S. Khan[2], Keiji Isamoto[2], Nobuhiko Nishiyama[3], and Hiroshi Toshiyoshi[1]

[1]The University of Tokyo, JAPAN

[2]santec OIS corporation, JAPAN and

[3]Tokyo Institute of Technology, JAPAN

ABSTRACT

This report describes a suspension design for a tunable vertical cavity surface-emitting laser (VCSEL) electrostatic MEMS mirror that separates the reflector from the electrostatic actuator to reduce the influence of secondary mechanical resonance modes. Compared to a monolithic actuating membrane design, a hundredfold reduction in the mechanical displacement of the mirror in the secondary resonance mode relative to the fundamental mode has been achieved. This enhancement of the main mode over higher-order modes is expected to improve interferometric stability when higher-frequency feedback may otherwise cause undesired fluctuation, especially during low frequency operation.

KEYWORDS

Vertical Cavity Surface Emitting Laser, Resonance, Interferometry.

INTRODUCTION

Vertical cavity surface emitting lasers (VCSELs) can be combined with MEMS mirrors to form variable optical cavities that enable tuning the output laser wavelength [1,2]. A schematic of one such MEMS-VCSEL can be seen in Figure 1. A half-VCSEL chip with multilayer distributed Bragg reflector (DBR) and quantum well (QW) regions serves as the initial light emitter [3]. The chip is oriented above a MEMS chip with a highly reflective (HR) coating on a suspended mirror which forms a lasing cavity with the half-VCSEL DBR. The reflector on the MEMS chip can be actuated downward electrostatically by applying a voltage between it and the silicon substrate below. In this way, the length of the lasing cavity can be dynamically changed, enabling tuning of the wavelength of the laser output.

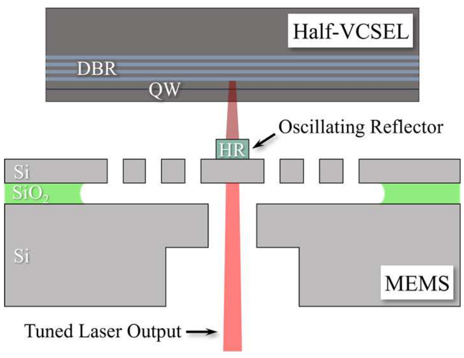

Figure 1: MEMS-VCSEL structure. Electrostatic actuation of the reflector changes the laser cavity length and thereby the output wavelength.

MEMS-VCSELs are suitable for various applications that require dynamically alterable laser sources in compact packages. One such application of interest is the development of chip-scale atomic clocks (CSACs). As outlined in Figure 2, a micro gas cell, when excited with a laser of a particular wavelength, can be used to generate an effective frequency standard [4,5].

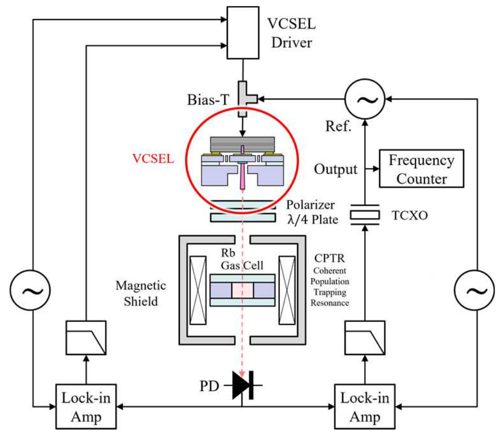

Figure 2: Block diagram of MEMS-VCSEL as a laser source for a Rb-based chip-scale atomic clock [5].

For this and other MEMS-VCSEL use cases, the wavelength of the output laser must be sufficiently stable for the desired application. Atomic frequency standards generally require a single laser wavelength, with VCSEL tunability being applied to initially achieve and subsequently maintain the necessary laser cavity length. As such the wavelength stability of the MEMS-VCSEL, and therefore the mechanical stability of the MEMS, is paramount when operated at low MEMS drive frequencies.

The stability of a tunable MEMS-VCSEL can be characterized by performing an interferometric analysis of the output laser. Figure 3 depicts a schematic illustration of such an analysis. The upper signal represents that produced by a stable MEMS actuator whose motion can be described by a single resonance mode. The spacing of the interference fringes transition smoothly across the travel of the MEMS stroke, representing the tunable range of the device. However, if the MEMS experiences fluctuations caused by the mechanical excitation of secondary modes as well, the output wavelength will fluctuate irregularly, manifesting as interruptions in the interferometer signal as shown in the lower panel.

In this paper, we describe a novel MEMS structure designed to inhibit the excitation of secondary resonance modes during operation to prevent this kind of instability.

Sensors & Actuators: A. Physical 361 (2023) 114574

Contents lists available at ScienceDirect

Sensors and Actuators: A. Physical

journal homepage: www.journals.elsevier.com/sensors-and-actuators-a-physical

A biodegradable ionic gel for stretchable ionics

Shunsuke Yamada [a,*,1], Hiroshi Toshiyoshi [b]

[a] Department of Robotics, Division of Mechanical Engineering, Tohoku University, 6-6-01 Aoba, Aramakiaza, Aobaku, Sendaishi, Miyagi, 980-8579, Japan
[b] Institute of Industrial Science (IIS), The University of Tokyo, 4-6-1 Komaba, Meguro-ku, Tokyo 153-8505, Japan

ARTICLE INFO

Keywords:
Biodegradability
Ionic gel
Electrolyte
PEGDA
Electrical double layer

ABSTRACT

Gel electrolytes are a promising material in the field of electronics, energy, and wearable devices due to their preferrable physical and electrochemical characteristics such as non-volatility, relatively large potential window, and high ionic conductivity. Ionic gels, however, possess toxicity that would potentially pollute environment and hinder application for environmental sensing. Decomposability and moderate toxicity are therefore required for disposable use. In this work, we develop a biodegradable ionic gel (BDiG) using a poly(ethylene glycol) diacrylate (PEGDA) combined with a biodegradable ionic liquid, 1-Butyl-3-methyl-Imidazolium bis(trifluoromethanesulfonyl)imide ([BMIM][TFSI]). The developed BDiG exhibits mechanical flexibility of fracture strain upwards of 300% and Young's modulus of 14 kPa. Electrical characteristics of the BDiG were a potential window of 4.8 V, ionic conductivity of 3.1 mS cm^{-1}, and electrical double layer capacitance of 34 μF cm^{-2} when 90% weight ratio of ionic liquid was used. A tactile sensor is demonstrated as a proof of concept of ionic skin, whose electrical conductivity increases linearly with the pressure.

1. Introduction

Biodegradability is inherent to organisms and basement of sustainability in nature. Body of animals, leaves, and woods decompose into carbon and nitrogen composites due to the biochemical reactions of bacteria and microbes in soils. The decomposed matters are essential for vegetation and origins of the carbon and nitrogen cycles. To realize IoT (internet of things) in sustainable society, biodegradable electronics is crucially important. Conventional silicon semiconductor devices have pursued high performance by the scaling effect. On the other hand, organic electronics have achieved unprecedent properties such as mechanical stretchability [1–6], self-healing [7–11], and biodegradability [12–18]. Ionic conductors have been studied as a material for stretchable or flexible electronics[19–25]. The electrical carriers of ionic conductors are the ions which bridge the gap between the different signal carriers, i.e., ions in biological cells and electrons in electronics [26]. Furthermore, those materials possess stretchability of a few hundreds of percent in strain and low Young's moduli of hundreds of kPa, thereby having high affinity to curved surface such as human body [22–24,27]. Ionic liquid (IL) and its gel form (ionic gel, IG) are newly adapted as electrolyte because of their electrochemical characteristics including high ionic conductivity, electrical double layer, and large potential window [28–31]. IL consists of cations and anions, and its characteristics depend on various combination of different ions molecules [32] that are commercially available [33]. The ILs and IGs are, therefore, widely used as sensing materials for flexible electronics, including tactile [34], strain sensors [35], and display devices [36]. Some ILs, however, show toxicity and low biodegradability, which hinders application to environmental sensing.

Here, we present a biodegradable ionic gel (BDiG) as a solution to the issue. We used biodegradable ionic liquid 1-Butyl-3-methyl-Imidazolium bis(trifluoromethanesulfonyl)imide ([BMIM][TFSI]) mixed with a photoinitiator 2-Hydroxy-4'-(2-hydroxyethoxy)−2-methylpropiophenone (Irgacure 2959) into a polymer poly(ethylene)glycol diacrylate (PEGDA) to form an ionic gel [19–25]. The biodegradability of the IL used is confirmed to be 90% in 28 days with bacterium *S. paucimobilis* [37]. The photoinitiator is widely used for polymerization of biodegradable hydrogels [38–40]. The PEGDA-based hydrogels have been tested to decompose more than 70% in 70 days under in vitro test [37–39]. Those materials are suitable for biodegradable ionic gels.

The electrical carriers of ionic conductors are the ions which bridge the gap between the different signal carriers, i.e., ions in biological cells and electrons in electronics [26]. Furthermore, those materials possess stretchability of a few hundreds of percent in strain and low Young's

* Corresponding author.
E-mail address: santa@tohoku.ac.jp (S. Yamada).
[1] http://orcid.org/0000-0002-9084-2070

https://doi.org/10.1016/j.sna.2023.114574
Received 19 March 2023; Received in revised form 21 July 2023; Accepted 25 July 2023
Available online 29 July 2023

Applied Physics Letters ARTICLE pubs.aip.org/aip/apl

Battery-less luminance sensor biomimicking human sensory nervous system

Cite as: Appl. Phys. Lett. **123**, 264101 (2023); doi: 10.1063/5.0181949
Submitted: 18 October 2023 · Accepted: 11 December 2023 ·
Published Online: 26 December 2023

View Online Export Citation CrossMark

S. Yamada[1,a] and H. Toshiyoshi[2]

AFFILIATIONS

[1]Department of Robotics, Division of Mechanical Engineering, Tohoku University, Miyagi 980-8579, Japan
[2]Institute of Industrial Science, The University of Tokyo, Tokyo 153-8505, Japan

[a)]Author to whom correspondence should be addressed: santa@tohoku.ac.jp

ABSTRACT

With the evolution of materials science and microfabrication processes, energy harvesters have become sophisticated, achieving power outputs in the range of several milliwatts, and have become a promising alternative to conventional batteries. Although their output power is insufficient to continuously operate a wireless sensor module, energy harvesters can operate small integrated circuits, including timers, watches, and ring oscillators. In this study, we emulated the human sensory nervous system to develop a battery-less sensor with a built-in analog-to-digital converter. The human sensory nervous system comprises a sophisticated sensing mechanism that digitalizes external stimuli by pulse-density modulation. To mimic this behavior, we integrated a ring oscillator with photovoltaics, allowing it to function as a luminance sensor with an event-driven operation. The oscillation frequency of the ring oscillator changes with respect to the operating voltage; hence, the output voltage of the photovoltaic modulates the frequency by more than two orders of magnitude. The sensor exhibits oscillation frequencies of 10 kHz and 7.7 MHz corresponding to luminance levels of 25–25 000 lx. Its response times are 40 μs and 15 ms when the light source is turned on and off, respectively. Battery-less sensors expand the opportunities for the application of energy harvesters in biomedical, wearable, and environmental sensing.

Receptors beneath the human epidermis detect external stimuli, including mechanical pressure, heat, and light, with high sensitivity and resolution. When such stimuli are applied to receptors, they generate serial pulses to convert the stimuli into electrical signals (Fig. 1), similar to analog/digital converters. E-skin, an artificial skin that imitates the function of human skin, has evolved in recent decades, and researchers have developed functional temperature,[1–3] tactile,[4,5] and luminance sensors.[6–8] E-skins comprise organic and thin inorganic materials that render them flexible and stretchable for conformable attachment to curved surfaces. However, E-skins imitate the softness of human skin, and their sensing principles are the same as those of conventional electronics. Kim *et al.* reported a flexible, organic, artificial afferent nerve comprising pressure sensors, an organic ring oscillator (RO), and a synaptic transistor to detect pressure (1–80 kPa) and stimulate the efferent nerve.[9] Wang *et al.* integrated emerging sensors with memristors to develop a neuromorphic sensing system.[10] The RO modulates its oscillation frequency (f_{osc}) with respect to the operating voltage, and its power consumption is lower than that of energy harvesters. Furthermore, integrated with memristors, the RO achieved spike-timing-dependent plasticity imitating in neuromorphic computing.[11–13] We developed a battery-less sensor comprising lead zirconate titanate (PZT) and RO.[14] The output voltage of the PZT operated the RO, which digitalized the voltage via pulse-density modulation. The system includes a built-in analog–digital converter with battery-less event-driven operations using PZT. These battery-less and event-driven operations are beneficial for implants whose batteries cannot be easily changed,[15] and an artificial vision system can be an application of this system. Furthermore, we previously demonstrated normally off sensor modules that get activated by the output of energy harvesters.[16] A trigger is an analog signal, owing to which the module suffers from noise, leading to an incorrect action. The proposed battery-less sensor generates AC signals and, with bandpass filters, the normally off sensor module operates when an event, which needs to be detected, takes place. Major changes in frequency further enable the development of biomimicking sensors with high sensitivity.

Herein, we imitated the human sensory nervous system to develop a battery-less sensor for illumination detection using RO and

Sensors and Materials, Vol. 35, No. 6 (2023) 1957–1983
MYU Tokyo

S & M 3301

Electret MEMS Vibration Energy Harvester with Reconfigurable Frequency Response

Gen Hashiguchi[1*] and Hiroshi Toshiyoshi[2]

[1]Department of Mechanical Engineering, Shizuoka University,
3-5-1 Johoku, Naka-ku, Hamamatsu, Shizuoka 432-8011, Japan
[2]Institute of Industrial Science, The University of Tokyo,
4-6-1 Komaba, Meguro-ku, Tokyo 153-8505, Japan

(Received March 1, 2023; accepted April 25, 2023)

Keywords: MEMS, vibrational energy harvester, electret, wide bandwidth, reconfigurable frequency response

We demonstrate a microelectromechanical systems (MEMS) electret-type vibrational energy harvester with a wide bandwidth between 25 and 60 Hz (span of 35 Hz) for a small sinusoidal acceleration of less than 10 mG (G = 9.8 m/s^2). We have developed a method of tailoring the nonlinear characteristics by adjusting the mutual position of the opposing electrodes. Both soft- and hard-spring effects are realized, thereby further extending the frequency bandwidth between 25 and 95 Hz so that power can be effectively retrieved from extremely small vibrations of 10 mG. This reconfigurable nature of the developed harvester device is suitable for autonomous distributed sensors that obtain power from environmental vibrations.

1. Introduction

Miniaturized vibrational energy harvesters have been developed as inexhaustible power sources for distributed sensor nodes. Studies have been performed to develop various harvesters using microelectromechanical systems (MEMS) technology.[1–11] Of particular interest is to realize a vibrational energy harvester with a wide frequency response in a low frequency range in order to enhance the efficiency of energy retrieval from environmental vibrations. For instance, our field work of the acceleration waveforms and its spectra measured on an actual viaduct of a highway[12] showed a distinguished vibration at 45 Hz and the power spectrum spreading between 10 and 200 Hz. Retrievable power is theoretically proportional to the integral of the power spectrum and the conversion efficiency over the frequency range. Therefore, a wide frequency response and a high conversion efficiency are required for vibrational energy harvesters.

Studies have been performed to develop vibrational power generation mechanisms in a wide frequency range. For instance, Liu *et al.* examined a piezoelectric cantilever-type vibrational energy harvester whose displacement was intentionally restricted by a mechanical stopper;[13]

*Corresponding author: e-mail: hashiguchi.gen@shizuoka.ac.jp
https://doi.org/10.18494/SAM4367

ISSN 0914-4935 © MYU K.K.
https://myukk.org/

Sensors and Materials, Vol. 35, No. 6 (2023) 1941–1955 1941
MYU Tokyo

S & M 3300

MEMS Electrostatic Energy Harvester Developed by Simultaneous Process for Anodic Bonding and Electret Charging

Hiroaki Honma,* Sho Ikeno, and Hiroshi Toshiyoshi

Institute of Industrial Science, The University of Tokyo, 4-6-1 Komaba, Meguro-ku, Tokyo 153-8505, Japan

(Received March 24, 2023; accepted June 15, 2023)

Keywords: IoT, MEMS, vibrational energy harvester, electret, anodic bonding

In this paper, we present a new structure and a process for electrostatic energy harvesters fabricated using a silicon-on-glass wafer. Conventional electret-based MEMS energy harvesters are produced using a silicon-on-insulator (SOI) wafer, which is inevitably accompanied by parasitic capacitances across the buried oxide layer. The new harvester, on the other hand, can be formed by individually developing silicon and glass parts and subsequently putting them together by anodic bonding, thereby virtually eliminating parasitic capacitance. Special caution is taken not to cause the destruction of the electret layer during high-temperature anodic bonding. The device has been successfully fabricated and experimentally confirmed to function as an energy harvester. This silicon-on-glass structure is beneficial in not only suppressing the parasitic capacitance but also increasing its output power compared with those made by the conventional SOI-based process.

1. Introduction

The operating power for wireless sensor nodes is usually provided through batteries for ease of installation.[1] However, batteries require periodical replacement when depleted, leading to extra maintenance and labor cost.[2] As their alternative, power sources called energy harvesters that generate energy from the surrounding environment have attracted attention as an enabling technology to realize, for example, a sensor network for infrastructure monitoring.[3] There are various types of ambient energy source, among which environmental vibration is popular. The power density of vibrations is not as high as that of sunshine, but it ubiquitously exists regardless of the weather conditions[4] and the time of day. Most environmental vibrations are seen in the acceleration range of 1 G (G = 9.8 m/s^2) or smaller,[5,6] and they can be converted into electrical power using a carefully designed MEMS-based energy conversion mechanism such as the piezoelectric effect,[7–11] electromagnetic induction,[12–16] and electrostatic induction.[17–32] Amongst them, electrostatic energy harvesters using the permanent electrical charge or so-called electret can effectively convert small mechanical vibrations into electrical power, owing

*Corresponding author: e-mail: honma-hh@mech.kobe-u.ac.jp
https://doi.org/10.18494/SAM4402

ISSN 0914-4935 © MYU K.K.
https://myukk.org/

KAWAKATSU Laboratory

Current Research Activities 2022-2023

Kawakatsu Laboratory

1. Research Topics

1.1 Colour Atomic Force Microscopy with Chemical Contrast

In this project, the AFM cantilever is oscillated at 2 MHz, and the tip-sample distance is modulated at 1kHz. By employing such modulation techniques, the potential landscape is detected as the frequency shift of the cantilever. Three effective Morse parameters are calculated per pixel to best curve fit the measured values. The work was published in 2017 on APL and was selected as the editor's pick. In 2020, discussions on the control scheme as well as results on imaging of solder was published in JJAP.

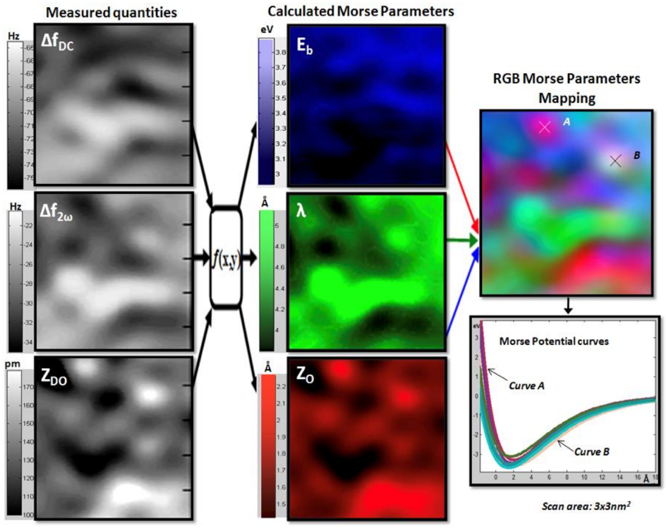

Figure 1. Effective Morse Parameters represented in RGB obtained from modulation of the tip sample distance. The sample was quenched Si(111). Cantilever Oscillation 2MHz.

1.2 Towards a TRUE-COLOUR AFM

Adamanitine-3-thiol (ATT) molecules are a new candidate for functionalizing AFM tip apexes due to their size, stability and their chemical bonding to the AFM tip. The molecules are synthesized by Professor T. Kitagawa of Mie University. Functionalised tips were evaluated for different values of base tip radius ***R***, inter molecular spacing ***a*** and tip height. The use of Bromo Adamantine-3-thiol (BATT) was evaluated as a molecule for AFM tip functionalization. The tips were evaluated in terms of maximum attractive force (smaller the better), comparison to an ideal floating Br atom that serves as an AFM tip, and the effect of functionalization on the effective-Morse parameters which are currently used to generate a colour expression of the sample. Studies showed that there exists a range of tip radius ***R*** and molecular spacing ***a*** that gives a marked improvement to the naked base tip. The results showed that the method is effective in lessening background forces and avoiding multiple-tip effects. As for the evaluation of BATT, where ***a***=8.7 å, it is not a bad choice, but a larger value of ***a*** above 10 å would be preferable.

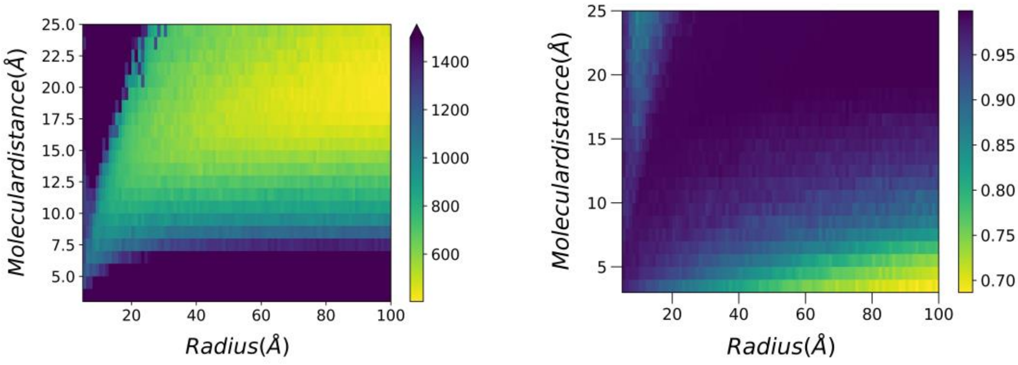

(a) (b)

Figure 2 (a) Average maximum attractive force of 100 functionalised tips with different values of ***R*** and ***a***. End atom Br, colour bar in pm. (b) Average **SSIM** (structural similarity index measure) for different values of ***R*** and ***a***. Reference image is an image obtained(calculation) with a single floating Br atom.

1.3 Conductive Polymer Dehydrant (Joint research with Tohoku University)

Conductive polymers have been known to show absorption of humidity in air. This project is a collaboration with Professor Hikaru Kobayashi of Tohoku University. We focused on various design for removing humidity from air, as well as improving conductance of the functional polymers and its deterioration due to current, heat and exposure to light.

1.4 Measurement of uterus peristalsis.

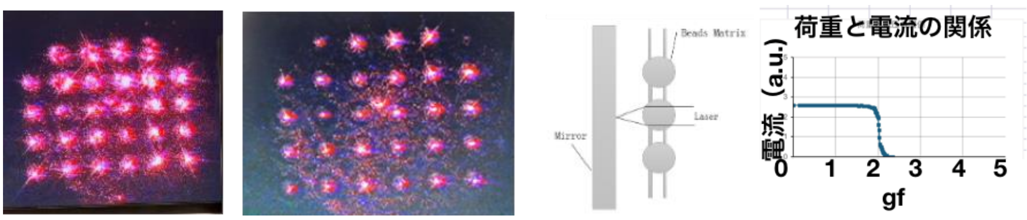

(a) (b) (c) (d)

Figure 3 Examples of methods to detect peristalsis. (a)(b) cats-eye returning beam modulated by mirror displacement, (c) cats-eye schematic, and (d) relation of ionic current to exerted force on the elastic micro channel.

Implantation of the fertilized egg in the uterus is an important process to accomplish pregnancy. It has been suggested that excessive peristalsis of the uterus can lead to implantation difficulties, but the lack of safe and high-sensitivity clinical methods to detect or visualize peristalsis has prevented profound studies on the relation and mechanism of implantation failure. We are currently comparing three different methods, which are (i) optical, (ii) flexible micro fluidic network probe, and (iii) fluid flow mapping. Prototypes are made in collaboration with doctors and embryologists for future clinical studies.

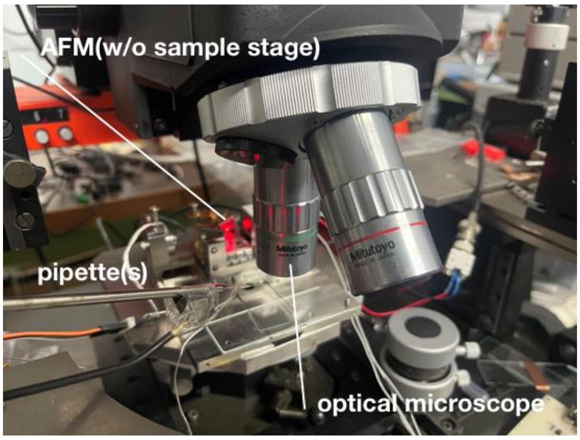

Figure 4. AFM based fertilization process force measurement apparatus. The optical microscope is equipped with two pipette probers, an AFM cantilever, and an optical microscope (Prober courtesy of Prof. Toshiyoshi of CIRMM).

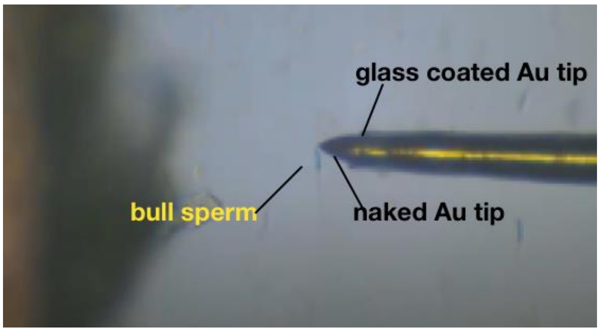

Figure 5. Fabrication process of a glass coated gold tip was established. The picture shows a bull sperm caught with the protruding naked gold tip. DEP solution in collaboration with Professor S.H. Kim.

1.5 Dielectrophoresis of bull sperm with a glass coated gold tip

A glass coated gold tip was implemented to enable simple manipulation of the bull sperm under the optical microscope. By using dielectrophoresis (DEP) , bull sperm could be caught and released with application of a few volts to the gold tip. CIRMM initiative budget was used for inter-lab student collaborations.

1.6 Acoustic detection of zygote activities

Following last year’s trial to detect zygote activity with a microphone, a more sensitive acoustic detection is in preparation using a 2x2 photo coupler, homodyne detection scheme and a graphite flake microphone diaphragm. CIRMM initiative budget was used for inter-lab student collaborations.

1.7 Activities at Fablab “Camp Komaba 4” (CK4)

We are running a student / staff MakerSpace or FabLab, open to all students and staff of IIS. The number of users rapidly increased from 2024. Students are working on a daily bases at CK4. We have received numerous technical questions covering a wide spectrum of research. CK4 carried out international ideathon with participation from The Women’s University of Ochanomizu, Women’s University of Nara, National Tsinghua University, National Singapore University, La Trobe University, and Tsinghua University. Credits have been granted to the first two universities.

2. Research Achievements

2.1 Number of original journal papers: 0

2.2 International conference: 4 (including 1 invited presentation)

2.3 Domestic conference: 4

2.4 Number of patents: 0

3. List of awards

4. Research Grants

4.1 Total number of research grants: 3

4.2 Number of collaboration research with industry: 3 (not excluding non-Grant based collaborations)

5. Education

5.1 Number of Ph.D. students :0

5.2 Number of master students: 7

5.3 Number of other students: 2

6. Publication list

Conference Presentations

1) Study on a method to grow self-assembled-monolayer covered tips for quantitative Atomic Force Microscopy, Koji Tomofuji, Toshikazu Kitagawa, Naruo Sasaki, Dai Kobayashi, and Hideki Kawakatsu, in abstracts of Nanospec FY2023 (2024).

2) Study on a method to grow self-assembled-monolayer covered tips for quantitative Atomic Force Microscopy, Koji Tomofuji, Toshikazu Kitagawa, Naruo Sasaki, Dai Kobayashi, Hideki Kawakatsu, in abstracts of ISSPWS 2023 (2023)

3) Study on a method to grow self-assembled-monolayer covered tips for quantitative Atomic Force Microscopy (Tentative), Koji Tomofuji, Toshikazu Kitagawa, Naruo Sasaki, Dai Kobayashi, Hideki Kawakatsu, in Abstracts of NAMIS Marathon Workshop 2023

4) Force Sensing for Colour Atomic Force Microscopy and Assisted Reproductive Technology (Tentative), Hideki Kawakatsu, in Abstracts of NAMIS Marathon Workshop

(in Japanese) Presentations on application of PEDOT/PSS to humidity control, with H. Kobayashi(4 papers).

KIM Laboratory

Current Research Activities (2023 April-2024 March)

B.J. KIM Laboratory

1. Research Topics

Our research goals are to build smart nanosystems and integrate nanoscale components in micro sensors, in particular for environment, bio-sensing, through both bottom-up and top-down approaches. We focus on interdisciplinary research about local "bottom-up" surface modification using functional self-assembled monolayers and "top-down" approaches for micro/nano patterning technologies. Based on these studies on nano/micro components systems for the fabrication of novel nano devices, we investigate to develop various micro sensors for biological applications, health care as well as environmental monitoring.

In the transdermal drug delivery methods, **the microneedle-mediated drug delivery system (DDS)** has been developed to replace the hypodermic injection-mediated DDS, to provide painless self-administration of biological drug with patient friendly manner. Dissoluble microneedles are attracting much attentions as it has several advantages such as no needle-related risks. We have developed new fabrication method for biodegradable microneedles patches, which is different with the conventional fabrication ones, such as stepwise casting method. We anticipate that shadow mask assisted drawing lithography as well as 3D printing based novel mass fabrication methods, will be suitable to improve the fabrication throughput of dissoluble microneedle for new generation of drug delivery system.

On the other hands, we observed the permeability of several commercially-available microneedle patches for cosmetic purposes to human skin and investigated methods of evaluating permeability to the stratum corneum, and its' degree of pain.

1.1 Dissoluble Microneedle patch for transdermal drug delivery systems

The transdermal drug delivery has experienced several-generation revolutions: From the transdermal delivery of small, lipophilic, low-dose drug to the delivery system using chemical enhancer, non-cavitational ultrasound and iontophoresis. With the development of the micro-scale engineering, microneedles show the potential to be the next generation delivery system. The microneedle mediated drug delivery system has been developed to provide painless self-administration of biological drug with patient friendly manner. Especially, dissolving microneedles, which deliver the target drugs as the drug-loaded microneedle dissolves into the skin, have been spotlighted recently. We investigate a novel fabrication method to achieve the user-friendliest, low-cost, and safest way for dissoluble microneedle patches with vaccine delivery and several medical treatments.

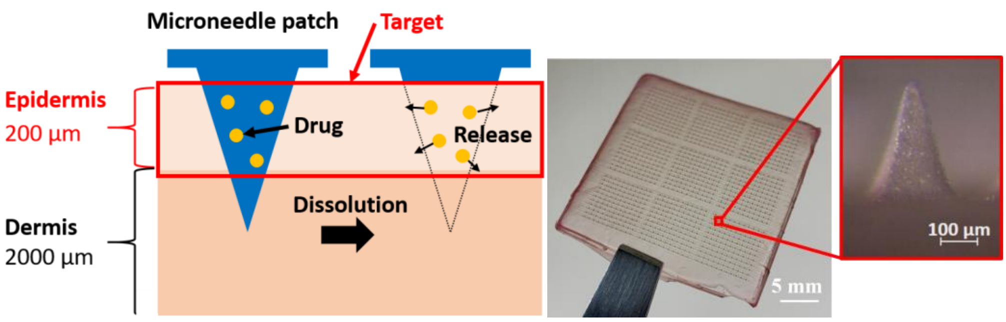

Fig. 1: *COVID-19 Vaccine delivery MNP(Microneedles patch) using vaccinia virus vector.*

1.2 Porous Microneedle for Self-testing diagnostic Bio-sensing

The porous microneedles are expected to have great potential for diagnostic application due to their ability to penetrate human skin painlessly and extract interstitial fluid (ISF) by capillary action. However, the prior approach about porous microneedles had not directly integrated sensor system as an application due to the small amount of sample porous microneedle can absorb. Here, we fabricated porous microneedle on a paper substrate to develop a novel platform for direct integration of sensors.

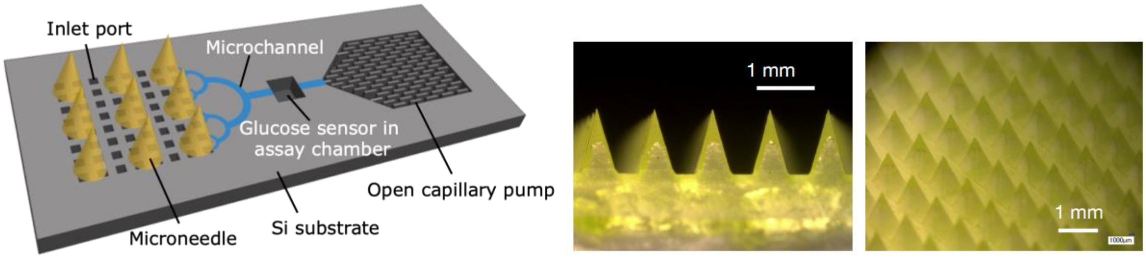

Fig.2: *Schematic of minimally invasive glucose monitoring system (left) integrated with an array of PDMS porous microneedles (right) in a microfluidic chip.*

ISF is a promising bio-sample since it contains a wide range of common biomarkers to blood such as glucose. In order to utilize ISF for continuous healthcare monitoring, ISF sampling is a key technology. However, the conventional ISF sampling technologies such as microdialysis have several drawbacks including highly invasive operation and limited measurement methodologies. Among the MNs, porous MNs have advantages such as applicability to fluidic systems and to biocompatible materials. Although the porous MNs were applied to ISF sampling, continuous ISF sampling has not been realized. For this, a new type of porous MN should be developed to address the challenges of mechanical and fluidic requirements for successful insertion into the skin and ISF extraction continuously. Furthermore, the microfluidic chip should also be realized to interface the porous MNs and realize a continuous flow of ISF, which is ideally at a flow rate of 0.08 μL/min.

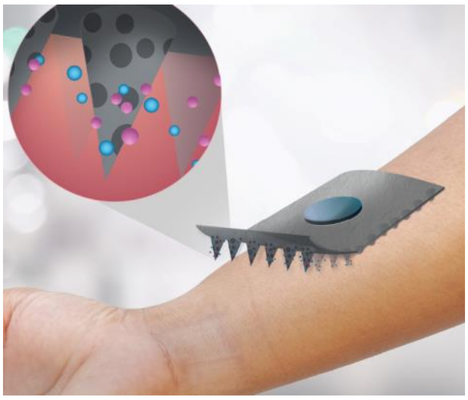

Fig.3*: Porous microneedle-on-paper device with a simple colorimetric sensor can painlessly measure glucose levels from interstitial fluid in the skin.*

One of the core targets is employing the micro-electro-mechanical systems (MEMS) fabrication technologies to the bio-degradable materials, then realizing specific structures, such as free-standing membrane, ultra-thin transparent film, etc. Therefore, our aim is to employ micro-nano technology to accurately control and deeply investigate the bio-degradable materials at micro/nano level, and develop novel materials for multiple application fields, such as biomedical field and energy harvesting.

As the power sources of wireless sensors, batteries are mainly utilized until now. These days, devices of energy harvesting become more focused. **Energy harvesting** is a methodology of scavenging power from ambient energy sources such as solar, thermal and vibration without the need for batteries.

In 2012, a novel energy harvesting approach was proposed and named TENG (**Triboelectric Nano Generator**), which is based on the combination of electrification effect and electrostatic induction. Due to remarkable properties, such as high-performance and the use of environmentally friendly materials, TENG has raised increasing interest. Several techniques have been developed to enhance the power density, including structural optimization, operation mechanism, surface texturing and hybrid TENG.

Herein, we propose a very simple and cost-efficient approach to fabricate high-performance TENG based on paper and graphite pencil. Moreover, we propose a novel device, which can utilize ambient vibration with wideband and low frequencies. Due to high stiffness of piezo electric energy harvesters, resonant frequency of the piezo electric energy harvesters tends to be much higher than ambient vibrational frequency. To solve these problems, the proposed energy-harvesting device is to utilize a stochastic resonance.

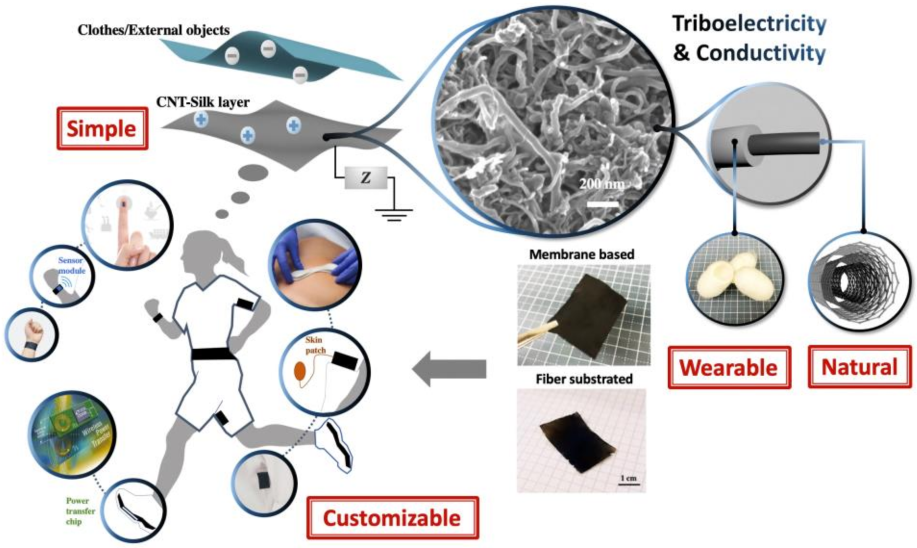

***Fig. 4**: Wearable TENG device of the electro-sprayed silk fibroin fiber mixed with carbon nanotubes.*

This high-output energy harvester shows the attractive potential in the integrated flexible electronics and wearable device.

2. Research Achievements (2023年度中)

2.1 Number of original journal papers: 5 (116 total)

2.2 International conference: 20 (241 total),

2.3 Domestic conference: 14 (223 total)

2.4 Number of patents: 5 (21 total)

3. Research Grants

3.1 Total number of research grants: 10 (2022-2023)

3.2 Number of collaboration research with industries: 8 companies

3.3 List of major research grants (serving as Principal Investigator)

- JSPS Core-to-Core A, JETMeE project, ウイルス医療学寄附研究部門など.

4. Education

4.1 Number of Ph.D. students (including current students): 16 (4)

4.2 Number of master students (including current students): 55 (7)

4.3 Number of other students: 39 (including current students 3)

5. Publication list

Journal Paper (2023-2024) *attached

1*. Jongho Park, Beomjoon Kim: Biotagging method for animal identification using dissolvable microneedle arrays prepared by customisable moulds, ***Scientific Reports***, 13, 22843, Springer Nature, 2023

2*. Chensong Xu, Gwenael Bonfante, Jongho Park, Vincent Salles, Beomjoon Kim: Fabrication of an electrospun polycaprolactone substrate for colorimetric bioassays, ***Biomedical Microdevices***, 25, 32, 2023

3*. 金範埈: 予防医学におけるウェアラブルバイオセンサー:生体分解性マイクロニードルパッチの開発、(特別寄稿論文)、*日本情報経営学会誌*, Vol. 42, No. 4, pp.9-16, July 2023 (Journal of Information and Management, ISSN 1882-2614,

Wearable Biosensor for Predictive/Preventive Medicine: Biodegradable Polymer Microneedles Patch)

4*. Kai Takeuchi, Junsha Wang, Beomjoon Kim, Tadatomo Suga, and Eiji Higurashi: Room temperature bonding of Au assisted by self-assembled monolayer, ***Applied Physics Letters***, 122, 051603, 2023 (https://doi.org/10.1063/5.0128187)

5*. Hai-Tao Deng, Danliang Wen, Jingrui Liu, Xinran Zhang, Yilin Wang, Peng Huang, Beomjoon Kim, Xiaosheng Zhang: Stretchable multifunctional sensor based on porous silver nanowire/silicone rubber conductive film, ***Nano Research***,16, pp.7618-7626, 2023 (https://doi.org/10.1007/s12274-023-5400-0)

International Conference (2023 y, selected)

1. Yusuke Koma, Yuko Tsuruma, Rie Kinoshita, Hoshimi Aoyagi, Shigenori Aoki, Shinya Takyu, Jongho Park, Beomjoon Kim: Development of a highly porous polycaprolactone (PCL) microneedles array patch to improve the absorption of interstitial fluid (ISF), ***12th. IEEE CPMT Symposium Japan 2023*** **(ICSJ 2023)**, Ritsumeikan University Suzaku Campus, Kyoto, Japan, Proceeding of ICSJ 2023, pp. 57-60, November 15-17, 2023 (oral).

2. Yuko Tsuruma, Yusuke Koma, Shigenori Aoki, Shinya Takyu, Hoshimi Aoyagi, Rie Kinoshita, Jongho Park, Beomjoon Kim: Sampling of biological interstitial fluid by porous microneedle array patches, ***12th. IEEE CPMT Symposium Japan 2023*** **(ICSJ 2023)**, Ritsumeikan University Suzaku Campus, Kyoto, Japan, Proceeding of ICSJ 2023, pp.53-56, November 15-17, 2023 (oral) 11/15

3. Dominique Decanini, Abdelmounaim Harouri, Ayako Mizushima, Jongho Park, Beomjoon Kim, Yoshio Mita, and Gilgueng Hwang: Novel fabrication of Arbitrary optical probe array by 4D printing, The 49th. International Conference on ***Micro and Nano Engineering (MNE 2023)***, Berlin, Germany, 25-28 September, 2023 (9/27, Oral presentation)

4. Jongho Park, Beomjoon Kim: Microneedle array patch (MAP), the promising biomedical device for total personal healthcare, ***International conference on PRecision Enigineering and Sustainable Manufacturing (PRESM2023)***, proceedings pp. W3-FI4, July 16- 21, 2023, Bankoku Shinryokan, Okinawa, July19, 2023, (oral, **Outstanding Presentation Award**)

5. Chensong Xu, Bonfante Gwenael, Jongho Park, Vincent Salles, Beomjoon Kim: Fabrication of electrospun polycaprolactone (PCL) substrate for colorimetric bio-assay, ***International Conference on Precision Engineering and Sustainable Manufacturing (PRESM 2023)***, proceedings pp. PP6-007, A093, Bankoku Shinryokan, Okinawa, Japan,16-21. July, 2023 (poster, **Outstanding Presentation Award**)

6. Boyu Qin, Jongho Park, Beomjoon Kim: Fabrication of polylactic acid porous microneedles using microfluidic technology, ***7th International Conference on Microneedles (Microneedles 2023)***, Hyatt At Olive 8, Seattle, WA, USA, Microneedles 2023 Oral presentation Abstract book, p. 7, May 15-May 17, 2023 (Oral)

7. Jingzong Zhang, Kotaro Shobayashi, Boyu Qin, Jongho Park and Beomjoon Kim: Optical microneedle lens array for photodynamic therapy, ***7th International Conference on Microneedles (Microneedles 2023)***, Hyatt At Olive 8, Seattle, WA, USA, Microneedles 2023 Oral presentation Abstract book, p. 36, May 15-May 17, 2023 (Oral)

scientific reports

OPEN

Biotagging method for animal identification using dissolvable microneedle arrays prepared by customisable moulds

Jongho Park & Beomjoon Kim✉

Properly handling animals and understanding their habits are crucial to establish a society where humans and animals coexist. Thus, identifying individual animals, including their possessions, and adequately managing each animal is necessary. Although several conventional identification methods exist, such as the use of ear punch, tattoos, and radio frequency (RF) chips, they require several processes and external apparatus. In this study, we proposed a new biotagging method using a microneedle array for animal identification. Our approach uses dissolvable microneedle arrays as a single patch to deliver dyes directly into the skin layer. Additionally, we developed a new fabrication method for customised female moulds to realise microneedle array patches (MAPs) with patterns of different characters and number. The characteristics and feasibility of the patterned MAPs were confirmed through basic evaluations and animal experiments. Moreover, we confirmed that patterns formed from biotagging using the developed patterned MAPs lasted over one month with clear readability. Finally, we confirmed that our patterned MAPs successfully realised biotagging on rat skin with the designated patterns including characters and number patterns. The proposed method is expected to enable minimally invasive tagging without external equipment or complex processes. In addition, the developed method could be used to embed various tags into the skin of animals and humans in the future.

The Animal Welfare Act (AWA) is a federal law that was enacted in 1966 in the United States. It regulates animal treatment in research, exhibitions, and transportation[1]. The primary objective of AWA is to prevent cruelty and suffering in animals and ensure humane treatment. Under AWA, animal welfare standards are established and applied to research facilities, exhibitors, and transporters. The law requires these facilities to provide animals with adequate housing, food, water, and veterinary care. In addition, a framework for enforcing these standards, including regular inspections of facilities and penalties for those found violating the law, has been established[2].

Other countries have similar laws and regulations to protect animal welfare. For example, in the European Union (EU), animal welfare laws are implemented through the "European Convention for the Protection of Animals Kept for Farming Purposes" and the "Directive on the Protection of Animals Used for Scientific Purposes"[3,4]. In the United Kingdom, the Animal Welfare Act of 2006 provides a framework for protecting animal welfare and sets standards for animal housing, care, and treatment[5]. In other countries, such as Japan and South Korea, animal welfare acts focus on animal health and regulation of animal-related industries, such as livestock production and laboratory animal use[6,7]. Thus, it is well understood that animal management and its system are highly relevant in treating animals properly under the related laws and regulations described above.

Animal tagging, a useful method for identifying individual animals, plays an important role in animal identification and management. Animal tagging involves attaching a tag, device, or marker to an animal for identification or tracking purposes[8]. The purpose of animal tagging can vary, but it is commonly used for monitoring animal populations, tracking the movements of animals, and for research purposes[9]. Such animals include wildlife, industrial animals (such as livestock), and experimental animals. Thus, animal tagging has several advantages, such as providing a permanent identifier for the animal, allowing for easy tracking and monitoring, improving management, and conserving wildlife populations.

Various types of animal tags exist, including physical tags attached to or implanted inside the animal's body and physical markings such as ear punching, tattooing, and toe clipping. Among them, physical tags are

Institute of Industrial Science, The University of Tokyo, 4-6-1 Komaba, Meguro-Ku, Tokyo 153-8505, Japan. ✉email: bjoonkim@iis.u-tokyo.ac.jp

Biomedical Microdevices (2023) 25:32
https://doi.org/10.1007/s10544-023-00673-z

RESEARCH

Fabrication of an electrospun polycaprolactone substrate for colorimetric bioassays

Chensong Xu[1] · Gwenaël Bonfante[2,3] · Jongho Park[2] · Vincent Salles[3] · Beomjoon Kim[2]

Accepted: 10 August 2023

Abstract

Colorimetric assays rely on detecting colour changes to measure the concentration of target molecules. Paper substrates are commonly used for the detection of biomarkers due to their availability, porous structure, and capillarity. However, the morphological and mechanical properties of paper, such as fibre diameter, pore size, and tensile strength, cannot be easily tuned to meet the specific requirements of colorimetric sensors, including liquid capacity and reagent immobilisation. As an alternative to paper materials, biodegradable polymeric membranes made of electrospun polycaprolactone (PCL) fibres can provide various tunable properties related to fibre diameter and pore size.

We aimed to obtain a glucose sensor substrate for colorimetric sensing using electrospinning with PCL. A feeding solution was created by mixing PCL/chloroform and 3,3',5',5'-tetramethylbenzidine (TMB)/ethanol solutions. This solution was electrospun to fabricate a porous membrane composed of microfibres consist of PCL and TMB. The central area of the membrane was made hydrophilic through air plasma treatment, and it was subsequently functionalized with a solution containing glucose oxidase, horseradish peroxidase, and trehalose.

The sensing areas were evaluated by measuring colour changes in glucose solutions of varying concentrations. The oxidation reactions of glucose and TMB in sensor substrates were recorded and analysed to establish the correlation between different glucose concentrations and colour changes. For comparison, conventional paper substrates prepared with same parameters were evaluated alongside the electrospun PCL substrates. As a result, better immobilization of reagents and higher sensitivity of glucose were achieved with PCL substrates, indicating their potential usage as a new sensing substrate for bioassays.

Keywords Glucose colorimetric sensing · Biosensing · Electrospinning · Microfiber sheet · Paper sensor · Polycaprolactone

1 Introduction

Biosensing aims to detect the presence of biomarkers in the patients' body (Promphet et al. 2020; Ray and Steckl 2019; Wang et al. 2021). It is an important tool in nowadays medical routine as an indicator of the patients' body condition. A lot of different biofluids such as saliva, blood, sweat, tears, or interstitial fluid are used and each of them has advantages and drawbacks (Donati et al. 2020; Lee et al. 2020; Vyas et al. 2020; Zhang et al. 2016). They can help monitor the current condition as well as defining risk factors such as cancer, diabetes, etc. Each one has a specific composition in biomarkers but are all proportional (Corrie et al. 2015; Wang et al. 2021). Blood is the most widely used sample but involve invasive technics needing medical professional. Urine, sweat, or tear are linked to body response and not

Chensong Xu and Gwenaël Bonfante contributed equally to this work.

✉ Beomjoon Kim
bjoonkim@iis.u-tokyo.ac.jp

[1] Department of Precision Engineering, School of Engineering, The University of Tokyo, Tokyo 153-8505, Japan

[2] Institute of Industrial Science, The University of Tokyo, Tokyo 153-8505, Japan

[3] LIMMS, CNRS-IIS UMI 2820, The University of Tokyo, Tokyo 153-8505, Japan

Published online: 17 August 2023

■ 特 別 寄 稿 論 文

予防医学におけるウェアラブルバイオセンサー：生体分解性マイクロニードルパッチの開発

Wearable Biosensor for Predictive/Preventive Medicine: Biodegradable Polymer Microneedles Patch

東京大学 生産技術研究所　　金　範埈*

Institute of Industrial Science, The University of Tokyo　Beomjoon KIM

Abstract : *Wearable sensors provide an alternative pathway to clinical diagnostics by exploiting various physical, chemical, and biological sensors to mine physiological information in real time and in a non-invasive or minimally invasive manner with mobile connectivity in autonomously operating. Here, new transdermal drug delivery system by using dissoluble micro needle patch will be introduced. Recently, in the transdermal drug delivery methods, the microneedle-mediated drug delivery system (DDS) has been developed to replace the hypodermic injection-mediated DDS, to provide painless self-administration of biological drug with patient friendly manner. Especially, dissolving microneedles, which deliver the target drugs as the drug-loaded microneedle dissolves into the skin, have been spotlighted recently. We investigate a novel fabrication method to achieve the user-friendliest, low-cost, and safest way for dissoluble microneedle patches with vaccine delivery, several medical treatments, and even glucose sensing as well as antibody detection for SARS-CoV-2 (COVID-19).*

Keywords : *Wearable biosensor, Polymer microneedles, DDS (Drug delivery System), POCT (Point of Care Testing)*

1. 序論

最近 3 年余りの新型コロナウイルス感染症（COVID-19）による世界的パンデミック状況は，グローバル public healthcare だけではなく，社会すべての生産，経済，輸送，医療および様々なシステムにおいて，AI,Digital transformation（DX），IoT,Metaverse などデジタル化技術と併合して，急激な変化や変革を起こし，新たに進んでいる．今までの人類の「治療の医学」が高齢化社会に伴い「予防医学」への進化，さらに遠隔医療やデジタル医療サービス，個人化医療化などの変革を呼び起こしており，それに伴う科学技術的，特に新しい形態の医療機器等の開発が求められている．特に，予防医療における「ヘルスケア・バイオモニタリングのためのバイオセンサー」に関する研究・開発分野もその重要性が高まっている．まずバイオセンサーという研究自体が，環境，化学，電気，生物，医療など幅広いセンシングの分野に関わっているので，それらすべてを包括したものとして紹介するのは非常に大変である．そこで，本報では，患者の医療測定の中で，例え採血によるバイオ測定をする生体バイオセンサー（血糖値，コレステロール値，各種ホルモン値などの計測）に限って議論する．具体的には，生体分解性ポリマ材料のマイクロニードルを用いたセンサーパッチに関するものを紹介する．多孔質のセンサー用マイクロニードル製造技術を開発し，痛みなく，容易に自分の体

＊東京大学　生産技術研究所　教授

Applied Physics Letters ARTICLE scitation.org/journal/apl

Room temperature bonding of Au assisted by self-assembled monolayer

Cite as: Appl. Phys. Lett. **122**, 051603 (2023); doi: 10.1063/5.0128187
Submitted: 27 September 2022 · Accepted: 7 January 2023 ·
Published Online: 3 February 2023

Kai Takeuchi,[1,a)] Junsha Wang,[2] Beomjoon Kim,[3] Tadatomo Suga,[2] and Eiji Higurashi[1]

AFFILIATIONS

[1]Graduate School of Engineering, Tohoku University, Sendai, Miyagi 9808579, Japan
[2]Collaborative Research Center, Meisei University, Tokyo 1918506, Japan
[3]Institute of Industrial Science, the University of Tokyo, Tokyo 1538505, Japan

[a)]Author to whom correspondence should be addressed: kai.takeuchi@tohoku.ac.jp

ABSTRACT

The surface activated bonding (SAB) technique enables room temperature bonding of metals, such as Au, by forming metal bonds between clean and reactive surfaces. However, the re-adsorption on the activated surface deteriorates the bonding quality, which limits the applicability of SAB for actual packaging processes of electronics. In this study, we propose and demonstrate the prolongation of the surface activation effect for room temperature bonding of Au by utilizing a self-assembled monolayer (SAM) protection. While the bonding without SAM fails after exposure of the activated Au surface to ambient air, the room temperature bonding is achieved using SAM protection even after 100 h exposure. The surface analysis reveals that the clean and activated Au surface is protected from re-adsorption by SAM. This technique will provide an approach of time-independent bonding of Au at room temperature.

Au is one of the promising bonding materials for assembly and packaging of integrated semiconductor systems, micro-electro-mechanical systems (MEMS), and power devices. Since Au does not have a native oxide layer, the direct bonding of Au is achieved under mild conditions, such as low process temperature, while native oxides on the surface obstacle the low temperature bonding for other metals, such as Cu.[1] For this reason and its high thermal conductivity, the bonding via Au has been reported for the sealing of optical MEMS devices,[2] thermal interface of power device,[3] packaging of MEMS sensors,[4] bump interconnection of optical device,[5,6] and interconnection of 3D stacked image sensors.[7]

Although Au bonding has advantages over other metal bonding, the bonding process yet requires heating at least 200 °C to diffuse Au atoms across the bonding interface.[8,9] The heating step is considered as risk of damage to the device performance and to the bonding interface due to the mismatch of the coefficient of thermal expansion of substrates. Therefore, it is desirable to bond Au at low temperature, especially at room temperature, for packaging of those applications mentioned above.

For this, surface activated bonding (SAB) is a promising technique to bond metals including Au at room temperature. In the SAB process, the metal surfaces are activated by the ion beam, fast atomic bombardment (FAB), or plasma to remove the native oxides, organic contamination, and adsorbed water.[10–12] The activated Au surface by Ar plasma or FAB can be bonded at the wafer level even in the ambient air.[13–15] Since the Au surface is not oxidized, the removal of organic contamination and water is critical for successful bonding at room temperature. This is also proved by atomic diffusion bonding (ADB), in which freshly deposited Au layers are bonded at room temperature without surface activation.[16–18]

However, the effect of surface activation does not last long. In the case of the SAB for Au using Ar plasma, the bonding right after the surface activation achieves the bulk fracture toughness. Yet, the bond strength drastically decreases with the exposure of the activated Au surface to ambient air, resulting in a bond strength of 0.1 J/m^2 after 60 min exposure.[16] This also applies to ADB, which shows a decrease in the bond strength from 12 to 0.15 J/m^2 when the deposited Au surface is exposed to air for 800 h.[16]

Therefore, in order to achieve a high bond strength, the Au should be bonded immediately after the surface activation. However, the industrial packaging process often requires a certain period of time after surface activation for handling of samples, jig set, alignment, and so on. Hence, the protection of the activated surface is necessary for a feasible bonding process at room temperature.

On the other hand, the low temperature bondings of Cu and Au have also been demonstrated using a self-assembled monolayer (SAM)

Nano Research
2023, 16(5): 7618–7626

ISSN 1998-0124 CN 11-5974/O4
https://doi.org/10.1007/s12274-023-5400-0

Stretchable multifunctional sensor based on porous silver nanowire/silicone rubber conductive film

Hai-Tao Deng[1], Dan-Liang Wen[1], Jing-Rui Liu[1], Xin-Ran Zhang[1], Yi-Lin Wang[1], Peng Huang[1], Beomjoon Kim[2], and Xiao-Sheng Zhang[1] (✉)

[1] *School of Electronic Science and Engineering, University of Electronic Science and Technology of China, Chengdu 611731, China*
[2] *CIRMM, Institute of Industrial Science, The University of Tokyo, Tokyo 153-8505, Japan*

Received: 5 September 2022 / **Revised:** 7 December 2022 / **Accepted:** 8 December 2022

ABSTRACT

As one of the promising human–machine interfaces, wearable sensors play an important role in modern society, which advances the development of wearable fields, especially in the promising applications of electronic skin (e-skin), robotics, prosthetics, and healthcare. In the last decades, wearable sensors tend to be capable of attractive capabilities such as miniaturization, multifunction, and smart integration, and wearable properties such as lightweight, flexibility, stretchability, and conformability for wider applications. In this work, we developed a stretchable multifunctional sensor based on porous silver nanowire/silicone rubber conductive film (P-AgNW/SR). Its unique structural configuration, i.e., an assembly of the P-AgNW/SR with good conductivity, stability, and resistance response, and the insulated silicone rubber layer, provided the feasibility for realizing multiple sensing capabilities. Specifically, porous microstructures of the P-AgNW/SR made the device to be used for pressure sensing, exhibiting outstanding dynamic and static resistive responsive behaviors and having a maximum sensitivity of 9.062 $\%\cdot N^{-1}$ in a continuous compressive force range of ~ 16 N. With the merit of the good piezoresistive property of AgNW/SR networks embedded into the surface of micropores of the P-AgNW/SR, the device was verified to be a temperature sensor for detecting temperature changes in the human body and environment. The temperature sensor had good sensitivity of 0.844 $\%\cdot °C^{-1}$, high linearity of 0.999 in the range of 25–125 °C, and remarkable dynamic stability. Besides, the developed sensor was demonstrated to be a single electrode-triboelectric sensor for active sensing, owing to the unique assembly of the conductive P-AgNW/SR electrode and the silicone rubber friction layer. Based on the coupling effect of the triboelectrification and electrostatic induction, the generated electrical signals could be used to sense the human motions, according to the quantitative correlation between the human motions and the features in amplitude and waveform of the output signals. Thus, the developed stretchable sensor successfully achieved the integration of two types of passive sensing capabilities, i.e., pressure and temperature sensing, and one type of active sensing capability, i.e., triboelectric sensing, demonstrating the feasibility of monitoring multiple variables of the human body and environment.

KEYWORDS

wearable electronics, porous microstructures, multiple sensors, pressure sensing, temperature sensing, triboelectric sensing

1 Introduction

The advances in material science, micro/nanomanufacturing technologies, and wearable and flexible electronics have significantly promoted the development of wearable sensors [1–3]. As one of the promising human–machine interfaces for realizing the interaction between humans and machines, wearable sensors have been demonstrated to transduce the virtual feeling of real-world objects into realistic signals for real-time monitoring and data analysis, exhibiting the attractive application potential in various fields of modern society, such as the applications in electronic skin (e-skin), robotics, biomedicine, prosthetics, and healthcare [4–8].

In the last decades, much effort has been devoted to developing different wearable sensors based on different types of sensing mechanisms. There are many different categorizations for wearable sensors. The typical categorization basis is the measured physical quantity [9] and the sensing mechanism [10]. In detail, according to the measured physical quantity, the wearable sensors can be mainly summarized into pressure sensors [11–13], strain sensors [14, 15], tactile sensors [16, 17], temperature sensors [18, 19], humidity sensors [20, 21], chemical sensors [22, 23], and optical sensors [24, 25]. In terms of the sensing mechanism, wearable sensors are mainly classified as piezoresistive sensors [26, 27], capacitive sensors [28, 29], piezoelectric sensors [30, 31], and triboelectric sensors [32–34]. Nowadays, to meet promising demands such as miniaturization, multifunction, and smart integration of wearable sensors for real applications, they tend to integrate two or more sensing capabilities to provide feedback on the multiple physical variables in the human body (e.g., breath, heartbeat, pulse, temperature, and body motions) or environment (e.g., temperature, humidity, and air condition). Moreover, several attractive wearable features, such as lightweight, flexibility,

Address correspondence to zhangxs@uestc.edu.cn

清华大学出版社 Tsinghua University Press · Springer

TAKAMIYA Laboratory

Current Research Activities 2023-2024

Takamiya Laboratory

1. Research Topics

1.1 Variable Gate Current Range Digital Gate Driver IC Always Providing 6-bit Controllability in Various IGBTs

To eliminate the need to redesign digital gate driver (DGD) ICs for each of a wide variety of power devices, the world's first variable gate current (I_G) range DGD (VIR-DGD) ICs with variable maximum I_G and resolutions are proposed. The innovation of VIR-DGD ICs is that a variable resistor on PCB allows one-bit I_G (I_{1BIT}) to be freely varied, thereby maintaining 6-bit controllability of DGD at all times for a wide variety of power devices. A 6-bit VIR-DGD IC with variable maximum I_G from 0.51 A to 5.1 A and I_{1BIT} from 8.1 mA to 81 mA has been developed. The trade-off problem between loss and noise during turn-on has been successfully solved by an active gate driving using the VIR-DGD IC for two types of IGBTs with twice the rated current.

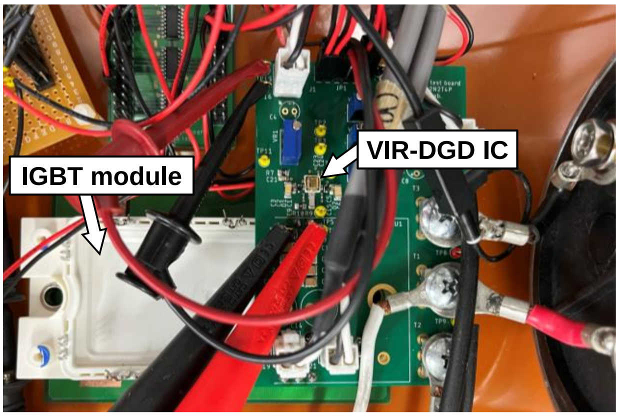

1.2 Fully Integrated Overcurrent Protection Method During SiC MOSFET Conduction

A gate driver IC with fully integrated overcurrent protection functions developed for IGBTs is successfully applied to overcurrent protection for SiC MOSFETs. In the gate driver IC, while the SiC MOSFETs are ON, constant gate charge is periodically discharged and charged, and when gate-to-source voltage dropped by each discharge is less than the reference voltage, it is detected as the overcurrent and the SiC MOSFETs are immediately turned off to protect from the overcurrent. Overcurrent protection can be achieved at low cost, since external components such as high-voltage diodes are not required. While the overcurrent detection threshold is constant and cannot be changed for IGBTs, it is found for the first time in SiC MOSFETs that the overcurrent detection threshold can be varied by changing the gate charge to be discharged. In a single-pulse test of an inductive load at 300 V for an SiC MOSFET with DC rating of 134 A and pulse rating of 240 A, the gate driver IC successfully protected the overcurrent with the protection delay of 226 ns or less, while the overcurrent detection threshold is variable in the range of 104 A to 306 A.

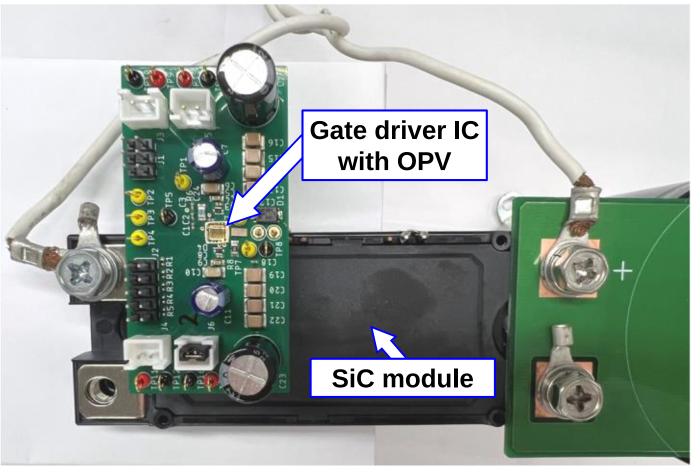

2. Research Achievements

2.1 Number of original journal papers: 11

2.2 International conference: 6 (including 1 invited presentations)

2.3 Domestic conference: 8(including 0 invited presentations)

2.4 Number of patents: 1

3. List of awards

- 1st prize of the ECCE 2022 William Portnoy Award, 2023/9/27, IEEE- IAS Power Electronics Devices and Components Committee (PEDCC) (K. Horii, R. Morikawa, K. Hata, K. Morokuma, Y. Wada, Y. Obiraki, Y. Mukunoki, and M. Takamiya)

4. Research Grants

4.1 Total number of research grants: 4

4.2 Number of collaboration research with industries: 7

4.3 List of major research grants (serving as Principal Investigator)

- Research Grant for “ ALCA-Next” from JST

5. Education

5.1 Number of Ph.D. students (including current students): 1

5.2 Number of master students (including current students):3

5.3 Number of other students: 0

6. Publication list

Journal Papers

1. H. Qiu, X. Zhang, J. Chen, M. Takamiya, and Y. Shi, "A 6.78-MHz Coupling Coefficient Sensorless Wireless Power Transfer System Charging Multiple Receivers With Efficiency Maximization by Adaptive Magnetic Field Distributor IC," IEEE Transactions on Circuits and Systems—I: Regular

Papers, Vol. 71, No. 2, pp. 974 - 983, Feb. 2024.

2. Q. Ma, X. Zhang, A. Zhao, H. Li, Y. Jiang, M. -K. Law, M. Takamiya, R. P. Martins, and P. -I. Mak, " A 10.5 W, 93% Efficient Dual-Path Hybrid (DPH)-Based DC–DC Converter Incorporating a Continuous-Current-Input Switched-Capacitor Stage and Enhanced IL Reduction for 12 V/24 V Inputs," IEEE Transactions on Circuits and Systems—I: Regular Papers, Vol. 70, No. 12, pp. 5482 - 5495, Dec. 2023.
3. D. -H. Yao, T. -N. Liu, M. Takamiya, and P. -H. Chen, "A 6.78-MHz Wireless Power Transfer System With Dual-Output Resonant Current-Mode Regulating Rectifier and Transmission Power Regulation," IEEE Transactions on Circuits and Systems—I: Regular Papers, Vol. 70, No. 12, pp. 4986 - 4998, Dec. 2023.
4. X. Zhang, Q. Ma, A. Zhao, Y. Jiang, M. -K. Law, J. Jiang, M. Takamiya, R. P. Martins, and P. -I. Mak, " A 12/24 V-Input HV-LV-Separated Hybrid SC PoL Converter With 355 mW/mm3 Power Density at 3 A Load Current and 15.2 mm3 Power Passives," IEEE Transactions on Power Electronics, Vol. 38, No. 12, pp. 15109 - 15114, Dec. 2023.
5. T. Mamee, Z. Lou, K. Hata, M. Takamiya, S. Nishizawa, and W. Saito, "Bond Wire Lift-off Detection by Gate Voltage Waveform in IGBT Turn-Off Process Enhanced by Digital Gate Control," Elsevier Power Electronic Devices and Components, Vol. 6, 100052, pp. 1 - 8, Oct. 2023.
6. X. Mu, G. Zhao, A. Zhao, Y. Jiang, M. -K. Law, M. Takamiya, P. -I. Mak, and R. P. Martins, "Floating-Domain Integrated GaN Driver Techniques for DC–DC Converters: A Review," IEEE Transactions on Circuits and Systems—I: Regular Papers, Vol. 70, No. 9, pp. 3790 - 3805, Sept. 2023.
7. T. -W. Wang, T. Inuma, P. -H. Chen, and M. Takamiya, "Search Method of Robust Gate Driving Vectors for Digital Gate Drivers With Low Test Cost Against Load Current and Temperature Variations in IGBTs," IEEE Transactions on Power Electronics, Vol.38, No.9, pp. 10669 - 10679, Sep. 2023.
8. T. Mamee, Z. Lou, K. Hata, M. Takamiya, S. Nishizawa, and W. Saito, "Enhancement of Turn-Off Gate Voltage Waveform Change by Digital Gate Control for Bond Wire Lift-Off Detection in IGBT Module," Elsevier Microelectronics Reliability, Vol. 147, 115067, pp. 1 - 6, Aug. 2023.
9. R. Wang, C. -H. Wu, and M. Takamiya, "Integrated Imager and 3.22 µs/Kernel-Latency All-Digital In-Imager Global-Parallel Binary Convolutional Neural Network Accelerator for Image Processing," IEEE Access, Vol.11, pp. 74364 - 74378, July 2023.
10. K. Horii, H. Yano, K. Hata, R. Wang, K. Mikami, K. Hatori, K. Tanaka, W. Saito, and M. Takamiya, "Large-Current Output Digital Gate Driver for 6500 V, 1000 A IGBT Module to Reduce Switching Loss and Collector Current Overshoot," IEEE Transactions on Power Electronics, Vol.38, No.7, pp. 8075 - 8088, July 2023.
11. H. Yamasaki, K. Hata, and M. Takamiya, "Estimation of Both Junction Temperature and Load Current of IGBTs from Output Voltage of Gate Driver," IEEJ Journal of Industry Applications, Vol.12, No.3, pp. 392 - 400, May 2023.

Conference Presentations

C1. H. Zhou, T. Inuma, D. Zhang, K. Hata, and M. Takamiya, “Variable Gate Current Range Digital Gate Driver IC Always Providing 6-bit Controllability in Various IGBTs” IEEE Applied Power Electronics Conference and Exposition (APEC), Long Beach, USA, pp. 1125-1129, Feb. 2024.

C2. H. Zhang, D. Zhang, K. Hata, K. Wada, K. Akatsu, I. Omura, and M. Takamiya, "Fully Integrated

Overcurrent Protection Method During SiC MOSFET Conduction," IEEE Southern Power Electronics Conference (SPEC), Florianopolis, Brazil, pp. 1-8, Dec. 2023.

C3. H. Qiu, X. Zhang, J. Chen, Y. Shi, and M. Takamiya, "Transmitter IC Enabling Magnetic Field Shaping for High-Efficiency Wireless Charging of Multiple Receivers," IEEE International Conference on ASIC (ASICON), Nanjing, China, pp. 1-4, Oct. 2023.

C4. H. Zhang, D. Zhang, H. Yamasaki, K. Hata, K. Wada, K. Akatsu, I. Omura, and M. Takamiya, "Gate Driver IC with Fully Integrated Overcurrent Protection Function by Measuring Gate-to-Emitter Voltage During IGBT Conduction," IEEE International Symposium on Power Semiconductor Devices and ICs (ISPSD), Hong Kong, pp. 76 – 79, May 2023.

C5. D. Zhang, K. Horii, K. Hata, and M. Takamiya, "Digital Gate Driver IC with Real-Time Gate Current Change by Sensing Drain Current to Cope with Operating Condition Variations of SiC MOSFET," 11th International Conference on Power Electronics – ECCE Asia (ICPE 2023-ECCE Asia), Jeju, Korea, pp. 374-380, May 2023.

C6. D. Zhang, K. Horii, K. Hata, and M. Takamiya, "Digital Gate ICs for Driving and Sensing Power Devices to Achieve Low-Loss, Low-Noise, and Highly Reliable Power Electronic Systems," IEEE Custom Integrated Circuits Conference (CICC), San Antonio, USA, pp. 1-7, April 2023. (Invited)

Large-Current Output Digital Gate Driver for 6500 V, 1000 A IGBT Module to Reduce Switching Loss and Collector Current Overshoot

Kohei Horii, Hiroki Yano, Katsuhiro Hata, *Member, IEEE*, Ruizhi Wang, Kazuto Mikami, Kenji Hatori, Koji Tanaka, Wataru Saito, *Senior Member, IEEE*, and Makoto Takamiya, *Senior Member, IEEE*

***Abstract*—An 8-bit digital gate driver (DGD) using a half-bridge digital-to-analog converter IC and two power MOSFETs is proposed to enable the output voltage swing of ±15 V and the large gate current up to 28 A to reduce the switching loss (E_{LOSS}) and the collector current overshoot ($I_{\mathrm{OVERSHOOT}}$) in a high-voltage, large-current IGBT module (HVIGBT) rated at 6500 V and 1000 A. By using the DGD to drive HVIGBT, the effectiveness of the active gate driving (AGD) is demonstrated for the first time in the world in the high-voltage and large-current range of 3.0–4.5 kV, 1000 A. The values of 1000 A, 4500 V, and ±15 V are the world's highest records in AGD. For the purpose of investigating the optimum gate driving waveforms of AGD for HVIGBT, four different gate drive methods are compared in detail by measurements at 3.6 kV, 1000 A, and the stop-and-go gate driving is selected from a cost–performance perspective. Finally, a design guideline of AGD for HVIGBTs is clarified. The design guideline is to align the two peak heights of the collector current waveforms, thereby minimizing E_{LOSS} and $I_{\mathrm{OVERSHOOT}}$.**

***Index Terms*—Gate driver, IGBT, loss, overshoot.**

I. Introduction

THE needs for power electronics' applications in the high-voltage, large-current area, such as renewable energy and high-voltage dc transmission systems, are rapidly increasing to realize the carbon neutral society. Thus, it is very important to reduce the losses of the high-voltage, large-current power devices. Active gate drivers (AGDs), which control gate waveforms during the switching transient of power devices, and digital gate drivers (DGDs), which digitize AGDs, have attracted attention as technologies that simultaneously reduce both the switching loss (E_{LOSS}) and the switching noise.

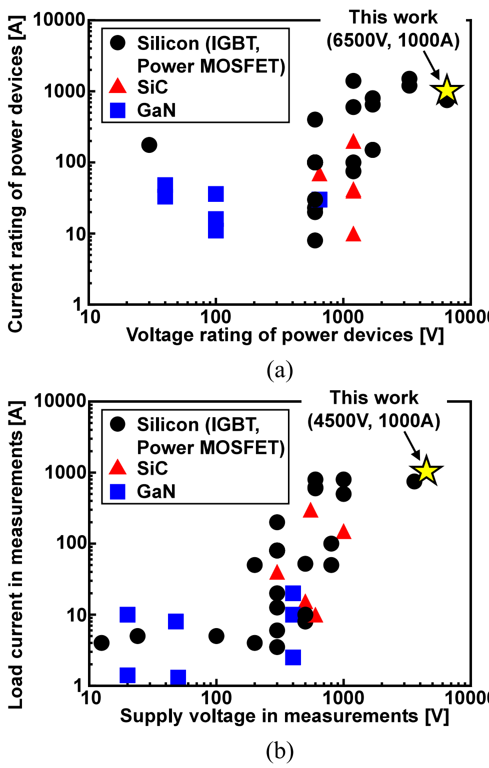

Fig. 1. (a) Voltage and current ratings of power devices and (b) supply voltage and load current of measurements in previous papers on AGDs [1], [2], [3], [4], [5], [6], [7], [8], [9], [10], [11], [12], [13], [14], [15], [16], [17], [18], [19], [20], [21], [22], [23], [24], [25], [26], [27], [28], [29], [30], [31], [32], [33], [34], [35], [36] by type of power devices.

Fig. 1(a) shows the voltage and current ratings of power devices used in previous papers on AGDs by type of power devices [1], [2], [3], [4], [5], [6], [7], [8], [9], [10], [11], [12], [13], [14], [15], [16], [17], [18], [19], [20], [21], [22], [23], [24], [25], [26], [27], [28], [29], [30], [31], [32], [33], [34], [35], [36]. There have been few reports on AGDs of power devices above 3000 V and 1000 A. Fig. 1(b) shows the supply voltage and the load current of measurements in previous papers on AGDs by type of power devices [1], [2], [3], [4], [5], [6], [7], [8], [9], [10], [11], [12], [13], [14], [15], [16], [17], [18],

Manuscript received 7 October 2022; revised 23 January 2023; accepted 13 March 2023. Date of publication 20 March 2023; date of current version 19 May 2023. This work was supported by NEDO under Grant JPNP21009. Recommended for publication by Associate Editor F. Luo. *(Corresponding author: Makoto Takamiya.)*

Kohei Horii, Hiroki Yano, Katsuhiro Hata, Ruizhi Wang, and Makoto Takamiya are with the Institute of Industrial Science, The University of Tokyo, Tokyo 153-8505, Japan (e-mail: horii@iis.u-tokyo.ac.jp; hyano@iis.u-tokyo.ac.jp; khata@iis.u-tokyo.ac.jp; oueichi@iis.u-tokyo.ac.jp; mtaka@iis.u-tokyo.ac.jp).

Kazuto Mikami, Kenji Hatori, and Koji Tanaka are with the Mitsubishi Electric Corporation, Fukuoka 819-0192, Japan (e-mail: mikami.kazuto@dp.mitsubishielectric.co.jp; hatori.kenji@dx.mitsubishielectric.co.jp; tanaka.koji@ds.mitsubishielectric.co.jp).

Wataru Saito is with the Research Institute for Applied Mechanics, Kyushu University, Fukuoka 816-8560, Japan (e-mail: wataru3.saito@riam.kyushu-u.ac.jp).

Color versions of one or more figures in this article are available at https://doi.org/10.1109/TPEL.2023.3259521.

Digital Object Identifier 10.1109/TPEL.2023.3259521

Digital Gate Driver IC with Real-Time Gate Current Change by Sensing Drain Current to Cope with Operating Condition Variations of SiC MOSFET

Dibo Zhang, Kohei Horii, Katsuhiro Hata, and Makoto Takamiya
The University of Tokyo, Tokyo, Japan

Abstract**-- A digital gate driver IC with real-time gate current (I_G) change by sensing drain current (I_D) is applied to SiC MOSFETs, and it is demonstrated that the IC always reduces switching loss and switching noise by always performing appropriate active gate driving even when the operating conditions of SiC MOSFETs, such as load current and junction temperature, change. The IC integrates all of a current-source based digital gate driver which changes I_G in 6 bits, a dI_D/dt sensor to detect I_G switching timing, and a controller into a single chip. In the turn-on measurement of an SiC MOSFET at 600 V and 25 °C, when the load current changes to 20 A, 70 A, and 120 A, compared with the conventional single-step gate drive, the active gate drive using the developed IC reduced the switching loss by 17 %, 12 %, and 11 % under I_D overshoot-aligned condition, respectively.**

Index Terms**-- Gate driver, switching loss, switching noise, SiC.**

I. Introduction

A lot of active gate drivers (AGDs), where the gate driving waveform is controlled during the turn-on/off transients, have been proposed to reduce both the switching loss (E_{LOSS}) and the switching noise of power devices. AGDs can be classified into two types, open-loop control [1-6] and closed-loop control [7-20]. The closed-loop AGDs are required instead of the open-loop AGDs, because the optimal driving waveform changes depending on the operating conditions (e.g. load current (I_L) and junction temperature (T_J)) [21]. Fig. 1 summarizes the design choices in conventional closed-loop AGDs. To make the closed-loop AGDs practical, the following three points are required: (1) single-chip integration instead of PCB implementation for lower cost, (2) real-time control instead of iterative control to reliably handle dynamic change of operating conditions, and (3) programmable AGDs instead of fixed-function AGDs that require individual optimization for different product varieties of power devices. In the closed-loop AGDs, however, no previous paper has realized all of (1) to (3).

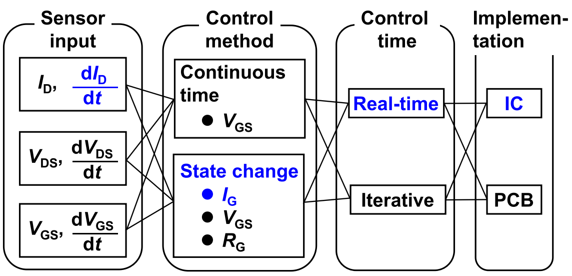

Fig. 1. Design choices in closed-loop AGDs. This work is shown in blue.

To solve the problems, a digital gate driver (DGD) IC with real-time gate current change (RGC) by sensing drain current (I_D) that realizes all of (1) to (3) was proposed in [22]. The design choices in [22] are shown in blue in Fig. 1. The IC [22] integrates all of a current-source based digital gate driver which changes gate current (I_G) in 6 bits, a dI_D/dt sensor to detect I_G switching timing, and a controller into a single chip. In [22], the operation was demonstrated for IGBTs. In contrast, in this paper, the DGD IC with RGC [22] is applied to SiC MOSFETs for the first time. It is shown that the IC always reduces E_{LOSS} and switching noise by always performing appropriate active gate driving even when I_L and T_J of an SiC MOSFET change.

II. Digital Gate Driver IC With Real-Time Gate Current Change

Figs. 2 and 3 show a circuit schematic and a timing chart of the DGD IC with RGC [22], respectively. In the following, turn-on is discussed, whereas the exact same is true for turn-off. The IC includes dI_D/dt detector for the state change, controller for RGC, and a 6-bit current-source type digital gate driver with variable I_G in 64 levels, where $I_G = n_{PMOS} \times 48$ mA and n_{PMOS} is an integer from 0 to 63. At turn-on, an active gate driving is performed in three slots from t_1 to t_3 with different I_G of strong (n_1) -weak (n_2) -strong (n_3), and this driving method is defined as stop-and-go gate drive (SGGD) [23]. n_1 to n_3 are preset by a digital input (Scan In), while t_1 and t_2 are automatically determined by RGC by sensing I_D. An important feature of this IC is the full integration of t_1 and t_2 real-time automatic control functions on a single chip. The real-time control is completed only by the IC and the external FPGAs or MCUs are not required. The real-time control of t_1 and t_2 is done by detecting dI_D/dt by sensing the voltage (V_{SS}) of the parasitic inductance (L_{SS}) between Kelvin source and power source in Fig. 2, because $V_{SS} = -L_{SS}$ (dI_D/dt). Specifically, as shown in Fig. 3, the end timing of t_1 is determined by detecting the negative V_{SS} at the beginning of I_D flow using a comparator with the reference voltage of V_{REFL}, and the end timing of t_2 is determined by

IEEE Access
Multidisciplinary ⋮ Rapid Review ⋮ Open Access Journal

Received 30 June 2023, accepted 12 July 2023, date of publication 18 July 2023, date of current version 25 July 2023.

Digital Object Identifier 10.1109/ACCESS.2023.3296429

RESEARCH ARTICLE

Integrated Imager and 3.22 μs/Kernel-Latency All-Digital In-Imager Global-Parallel Binary Convolutional Neural Network Accelerator for Image Processing

RUIZHI WANG, CHENG-HSUAN WU, AND MAKOTO TAKAMIYA, (Senior Member, IEEE)
Institute of Industrial Science, The University of Tokyo, Tokyo 153-8505, Japan

Corresponding author: Ruizhi Wang (oueichi@iis.u-tokyo.ac.jp)

This work was partly supported by Japan Society for the Promotion of Science (JSPS) KAKENHI Grant Number 19H02188.

ABSTRACT This paper presents an innovative approach to achieve ultralow-latency convolutional neural network (CNN) processing, which is critical for real-time image processing applications such as autonomous driving and virtual reality. Traditional CNN accelerators employing in/near-array-computing (inclusive of in/near-memory-computing and in/near-sensor-computing) architectures have struggled to meet real-time requirements due to latency bottlenecks encountered with conventional column-parallel processing for image processing. To address this challenge, we propose a novel, all-digital in-imager global-parallel binary convolutional neural network (IIGP-BNN) accelerator. This new approach employs a global-parallel processing concept, which enables multiply-and-accumulate operations (MACs) to be executed simultaneously within the imager array in a 2D manner, eliminating the additional latency associated with row-by-row processing and data access from random access memories (RAMs). In this design, convolution and subsampling operations using a 3×3 kernel are completed within just nine steps of global-parallel processing, regardless of image size. This results in a theoretical reduction of over 88.5% of repeated row scans compared to conventional column-parallel processing architectures, thus significantly reducing computing latency. We have designed and prototyped a 30×30 integrated imager and IIGP-BNN accelerator IC using a 0.18 μm CMOS process. This prototype achieved a latency of 3.22 μs/kernel on the first layer convolution at a power supply of 1 V and a clock frequency of 35.7 MHz. This represents a latency reduction of 35.6% compared to the state-of-the-art in/near-imager-computing works. This proposed global-parallel processing concept opens up the potential for processing high-resolution images in 4K and 8K with the same ultralow latency, marking a significant advancement in high-speed image processing.

INDEX TERMS Convolutional neural network, ultralow latency, global-parallel processing, in-imager-computing, image processing.

I. INTRODUCTION

Convolutional Neural Networks (CNNs) have recently advanced considerably within the machine learning (ML) domain, becoming a piece of crucial innovative technology in the majority of image and vision processing tasks [1], [2]. Proposals for CNN accelerators employing in/near-array-computing (inclusive of in/near-memory-computing and in/near-sensor-computing) architectures aim to achieve superior energy or area efficiency due to their effective reduction on the computational data loading [3], [6], especially the in/near-sensor-computing architectures have shown better energy efficiency and communication latency performance than in/near-memory-computing architectures due to the further reduction of data access for raw image and extracted features [7], [8]. Among various sensors, image

The associate editor coordinating the review of this manuscript and approving it for publication was Mario Donato Marino.

Fully Integrated Overcurrent Protection Method During SiC MOSFET Conduction

Haifeng Zhang[1], Dibo Zhang[1], Katsuhiro Hata[1], Keiji Wada[2], Kan Akatsu[3], Ichiro Omura[4], and Makoto Takamiya[1]
[1] The University of Tokyo, Tokyo, Japan
[2] Tokyo Metropolitan University, Tokyo, Japan
[3] Yokohama National University, Kanagawa, Japan
[4] Kyusyu Institute of Technology, Fukuoka, Japan

Abstract*—A gate driver IC with fully integrated overcurrent protection functions developed for IGBTs is successfully applied to overcurrent protection for SiC MOSFETs. In the gate driver IC, while the SiC MOSFETs are ON, constant gate charge is periodically discharged and charged, and when gate-to-source voltage dropped by each discharge is less than the reference voltage, it is detected as the overcurrent and the SiC MOSFETs are immediately turned off to protect from the overcurrent. Overcurrent protection can be achieved at low cost, since external components such as high-voltage diodes are not required. While the overcurrent detection threshold is constant and cannot be changed for IGBTs, it is found for the first time in SiC MOSFETs that the overcurrent detection threshold can be varied by changing the gate charge to be discharged. In a single-pulse test of an inductive load at 300 V for an SiC MOSFET with DC rating of 134 A and pulse rating of 240 A, the gate driver IC successfully protected the overcurrent with the protection delay of 226 ns or less, while the overcurrent detection threshold is variable in the range of 104 A to 306 A.

Keywords— overcurrent, protection, gate driver, IC, gate voltage, SiC

I. INTRODUCTION

Overcurrent detection and protection of power devices are important technologies to realize reliable power electronic systems. The target of this work is to develop an overcurrent protection method for SiC MOSFETs used in large-current, short-pulse current generator circuits with an inductive load [1] that (1) can be fully integrated into a gate driver IC without external components such as high-voltage diodes for low cost, (2) can detect overcurrent while the SiC MOSFETs are ON, and (3) has a variable overcurrent detection threshold (I_{TH}).

Table I shows a summary of conventional detection and protection for overcurrent. Methods for detecting overcurrent by measuring drain current (I_D) [2-5], and drain-to-source voltage (V_{DS}) [3, 6] of SiC MOSFETs have been proposed. I_D measurement requires a current sensor, and V_{DS} measurement for desaturation detection requires a high-voltage diode, which are expensive. All conventional overcurrent detection methods by gate-to-emitter voltage (V_{GE}) measurement in IGBTs [7, 8, 10] and gate-to-source voltage (V_{GS}) measurement in SiC MOSFETs [9, 11] have the disadvantage that overcurrent during ON of IGBTs/SiC MOSFETs cannot be detected, because V_{GE}/V_{GS} is measured during the turn-on transient. No conventional overcurrent protection methods, however, satisfy all three targets.

TABLE I. COMPARISON TABLE OF DETECTION AND PROTECTION FOR OVERCURRENT

Reference	[2-5]	[3, 6]	[10]	[11]	[12]	This work
Method	Current monitor	Desaturation	V_{GE} at Miller plateau	Gate charge	MGDC	MGDC
Measured value	I_D	V_{DS}	V_{GE}	Q_G, V_{GS}	V_{GE}	V_{GS}
Power device	SiC	SiC	IGBT	SiC	IGBT	SiC
Measurement from gate terminal	No	No	Yes	Yes	Yes	Yes
Overcurrent detection during ON	Yes	Yes	No	No	Yes	Yes
Fully integrated protection	No	No	No	No (Only detection)	Yes	Yes
Variable threshold for overcurrent detection	Yes	Yes	Yes	No	No	Yes by VDOS
Detection / protection delay [ns]	22 [2] 100 [3]	250 [3] 400 [6]	500	369	810	< 226

Therefore, in this paper, an overcurrent protection method for SiC MOSFETs that satisfies all three targets is proposed by applying the gate driver IC [12] with a fully integrated overcurrent protection function called "monitoring gate voltage while periodically repeating discharging and charging of constant gate charge (MGDC) [13]" developed for IGBTs to SiC MOSFETs. When the gate driver IC [12] is applied to SiC MOSFETs, a new phenomenon called "V_{GS} drop due to overheating of SiC (VDOS)" is found. Therefore, the variable I_{TH} using the phenomenon is achieved in this paper.

II. PROPOSED FULLY INTEGRATED OVERCURRENT PROTECTION

A. *Gate Driver IC with Fully Integrated Overcurrent Protection*

Fig. 1 shows an operation principle of the gate driver IC [12] with a fully integrated overcurrent protection function by measuring gate-to-source voltage (OPV) while SiC MOSFETs are ON. Two functions, a periodic constant gate charge (Q_C) discharger and recharger, and an overcurrent protection by V_{GS}, are added to the gate driver IC. While the SiC MOSFETs are ON, the periodic Q_C discharger and recharger periodically discharges and recharges Q_C. When V_{GS} dropped by each discharge is less than the reference voltage (V_{REF}), it is detected as the overcurrent

Variable Gate Current Range Digital Gate Driver IC Always Providing 6-bit Controllability in Various IGBTs

Haoxi Zhou, Toshiaki Inuma, Dibo Zhang, Katsuhiro Hata, and Makoto Takamiya
The University of Tokyo, Tokyo, Japan

***Abstract*— To eliminate the need to redesign digital gate driver (DGD) ICs for each of a wide variety of power devices, the world's first variable gate current (I_G) range DGD (VIR-DGD) ICs with variable maximum I_G and resolutions are proposed. The innovation of VIR-DGD ICs is that a variable resistor on PCB allows one-bit I_G (I_{1BIT}) to be freely varied, thereby maintaining 6-bit controllability of DGD at all times for a wide variety of power devices. A 6-bit VIR-DGD IC with variable maximum I_G from 0.51 A to 5.1 A and I_{1BIT} from 8.1 mA to 81 mA has been developed. The trade-off problem between loss and noise during turn-on has been successfully solved by an active gate driving using the VIR-DGD IC for two types of IGBTs with twice the rated current.**

Keywords*— *IGBT, IC, surge current, energy loss, active gate driver

I. Introduction

Digital gate drivers (DGD) ICs, which digitally change the gate current (I_G) multiple times in fine time slots during the switching period of power devices, are attracting attention as a technology that can solve the trade-off problem between loss and noise during power device switching [1-8]. In all conventional DGD ICs [1-8], the I_G range and steps are fixed for each IC. Different power devices require different I_G ranges and steps, which means that DGD ICs must be redesigned for each power device, which has been one of the challenges for the practical application of DGD ICs. For example, in a 6-bit DGD IC, when more than half of the maximum I_G is not needed, one bit of MSB is not used, and the IC operates as a 5-bit DGD, thereby preventing DGD from fully utilizing the original 6-bit I_G controllability. To solve the problem, in this paper, a world's first variable I_G range DGD (VIR-DGD) IC is proposed.

II. Proposed Variable I_G Range Digital Gate Driver IC

Figs. 1 and 2 show a circuit schematic and a timing chart of the proposed VIR-DGD IC, respectively. In the following, turn-on is discussed for simplicity, whereas the exact same is true for turn-off. This 6-bit DGD IC is based on the DGD IC in [6], and differs from [6] in the following two points: (1) the ability to change $V_{GS\,(PMOS)}$ amplitude of the 6-bit pMOSFETs in the output stage with an analog voltage ($CONT_{PMOS}$) via a variable resistor (R_2) on PCB to realize a variable I_G function, and (2) the addition of t_{ON}, t_{OFF} generator (TGEN), which generates the timing signals that define the time slots (t_{ON}) of the DGD using on-chip voltage controlled oscillators. The equation for I_G is shown in Fig. 1. The innovation of the VIR-DGD IC is that it can always achieve 6-bit controllability for a wide variety of power devices, because the 1-bit I_G (I_{1BIT}) is variable. As shown in Fig. 2, I_G can be varied 9 times with 6 bits (= 64 levels) in a t_{ON} time slot. Fig. 3 shows a die photo of VIR-DGD IC fabricated with 180-nm BCD process.

III. Measured Results

Fig. 4 shows the measured n_{PMOS} dependence of I_G at three different I_{1BIT} values of 81 mA (maximum value), 41 mA, and 0.51 mA (minimum value), where n_{PMOS} is a 6-bit control bit of I_G and is an integer from 0 to 63. To measure I_G, a 10 µF capacitor is connected to the output of DGD. As shown in Fig. 1, R_1 on PCB is fixed at 27 kΩ, and by varying the variable resistor R_2 on PCB, $V_{GS(PMOS)}$ amplitude is varied to change I_{1BIT}. Specifically, $V_{GS(PMOS)}$ amplitudes are 5.0 V, 3.0 V, and 1.7 V when I_{1BIT} is 81 mA, 41 mA, and 0.51 mA, respectively. Variable I_G range and I_{1BIT} are demonstrated.

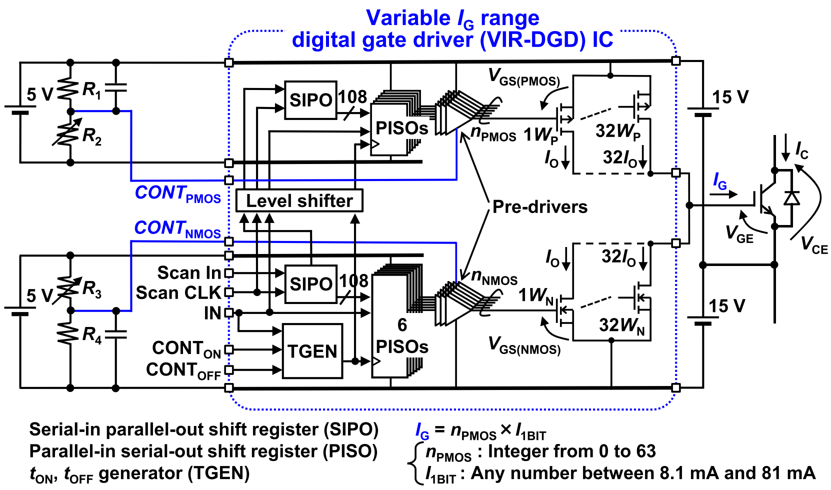

Fig. 1. Circuit schematic of proposed variable I_G range DGD (VIR-DGD) IC.

979-8-3503-1664-3/24/$31.00 ©2024 IEEE

MIZOGUCHI Laboratory

Current Research Activities 2023-2024

Mizoguchi Laboratory

1. Research Topics

1.1 Prediction of the Ground State Electronic Structure from Core-loss Spectra of Organic Molecules by Machine Learning

With the development of technology, various nano-materials with specific properties are needed to deal with multifarious situations. In this case, local atomic and electronic structures play an important role due to their intimate correlation with the properties of nano-materials. Thus, characterizing the local atomic and electronic structures becomes essential for investigating and designing the nano-materials. Among characterization methods for the nano-materials, core-loss spectroscopy, namely, energy loss near-edge spectroscopy (ELNES) and X-ray absorption near-edge structure (XANES), has been widely used since it reflects the atomic and electronic structures of materials in high spatial resolution and sensitivity. For example, the electronic states of catalysis can be probed through ELNES/XANES spectra to investigate the oxidation states of catalysis. Besides, ELNES/XANES spectra are also useful to understand the mechanism and dynamics during chemical reactions. Also, for carbon materials, Suenaga et al. used the carbon K-edge ELNES spectra to discriminate the local electronic and atomic structures for graphene.

However, the molecular structure, chemical bonding, and various molecular properties, such as magnetic and mechanical properties, are mainly governed by the ground state electronic structure of the occupied orbital, which cannot be directly obtained from the core-loss spectra. Furthermore, the connection between the ground-state electronic structure and core-loss spectra is indirect because the spectra are merely corresponding to the excited state. If the way to obtain the ground state electronic structure of both occupied and unoccupied orbitals from the core-loss spectra would be paved, the acceleration of functional nano-materials design will be achieved. Besides, investigating the s- and p-orbital density of states (DOS) has traditionally been a challenging task, with non-resonant inelastic x-ray scattering being the most common method, despite its seldom available and inconvenience. Therefore, finding a correlation between s- and p-orbital DOS and the widely used core-loss spectra would simplify the material characterization process.

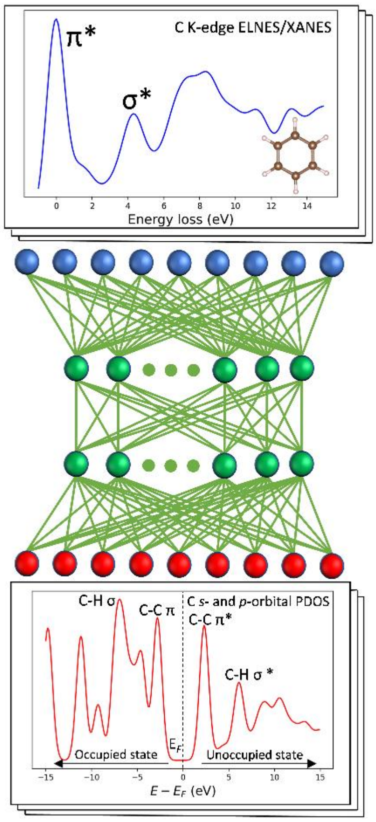

Hence, we introduced the machine learning (ML) method to achieve these targets. ML is a technique that can find out the unclear relationship between variant events. Recently, it has been used in materials science for replacing time-consuming processes to reduce computation costs. Besides, ML enables scientists to discover the obscure relationship between material properties and spectroscopies to explore unknown applications for these spectroscopies. Therefore, in this work, we aimed to use ML to obtain the full ground-state electronic structures, in particular s- and p-orbital partial DOS (PDOS), for organic molecules from carbon K-edge core-loss spectra.

The present study is schematically illustrated as shown in right figure. We used a feedforward neural network (FNN) with two hidden layers as the ML model, and the carbon K-edge ELNES/XANES in the database and the ground-state PDOS of carbon s- and p-orbital were used as the input and output, respectively.

Consequently, the ground state s- and p-orbitals PDOS including occupied and unoccupied states can be predicted from the carbon K-edge ELNES/XANES spectra qualitatively by the ML model by taking advantage of their close correlation. We found that there is a difference in the regularity of the PDOS prediction for the small molecules and the large molecules through the extrapolation analysis and that it is better to exclude the extremely small molecules from the training data to improve the PDOS prediction for larger molecules.

1.2 Possible New Graphite Intercalation Compounds for Superconductors and Charge Density Wave Materials: Systematic Simulations with Various Intercalants Using a van der Waals Density Functional Method

Graphite intercalation compounds (GICs) have been extensively studied because of their unique physical properties. For example, LiC*6*, which can be synthesized by a reversible reaction of graphite and Li ions, is widely used in Li-ion secondary batteries. Moreover, superconductivity has been reported in several GICs with chemical formulae MC_6 (M = Ca , Sr, Ba, and Yb) and MC_8 (M = K, Rb, and Cs). The GICs are typically characterized by their stacking order and compositions. Three types of stacking structures have been reported for the MC_6 composition and the stackings have been reported for the MC_8. Although several studies have suggested the synthesis of CF_x ($2 < x < 5$) as GICs, their treatment in the same category as other GICs is controversial because their bonding is relatively covalent and their structure is different from that of others.

In computational science, various correction methods that include long-range dispersive interaction, particularly van der Waals (vdW) interaction, have been proposed using the first-principles calculation based on density functional theory (DFT) as vdW density functional methods. Consequently, much research on vdW materials has been demonstrated, such as graphite and GIC wherein considering the vdW interaction is essential. Thus, various investigations using first-principles calculation have been performed on the phenomenon that alkali metals (AMs) and alkaline earth metals (AEs) can be inserted into graphite, except Na (among AMs), Be, and Mg (among AEs); various insights have also been provided.

Furthermore, some of the GICs are known to exhibit peculiar electronic properties, such as superconductivity and charge density wave (CDW) state. The mechanism for arising the superconductivity of GICs has been investigated and it has been pointed out that the origin of the superconductivity is electron-phonon coupling, and to achieve it, a partially occupied free-electron-like interlayer band between the C–C layers of GICs is required irrespective to its finite occupancy.

Based on those experimental, theoretical, and functional viewpoints of GICs, in this study, we investigated the formation energies, electronic structure, and superconductivity of GICs with the five reported crystal structures using the vdW density functional method by varying the elements as intercalants. The calculated results are in good agreement with the experimentally reported materials and provide important insights into GIC processing using the Li-based molten alloy and LiCl–KCl molten salts. Furthermore, we also investigated electronic band structures of GICs and estimated possibility of superconductivity and Tc through the simulation. As a result, it was indicated that several GICs with new compositions, which have not been reported to date, are possibly stable and they have the potential to show superconductivity and CDW state.

The following figure shows the heat map of their formation energy obtained the present study. All GICs of M = Li, K, Rb, Cs, Ca, Sr, and Ba, which were experimentally confirmed as stable GICs, have negative formation energies (blue color), indicating their stability in the simulations. We confirmed the same tendency in other stacking orders by their heat maps. The result indicates that our calculations are in good agreement as they were inserted experimentally. Although the negative value of M = F was also demonstrated, the structure and bonding nature could be different from those of other GICs because the covalent bonding is considered more stable. Notably, the E_{form} for Sc, Y, Fr, and Ra is negative, although they have not been reported as GICs experimentally or computationally to date. According to the trends of other reported materials, these elements can also be intercalated into graphite to form new GICs.

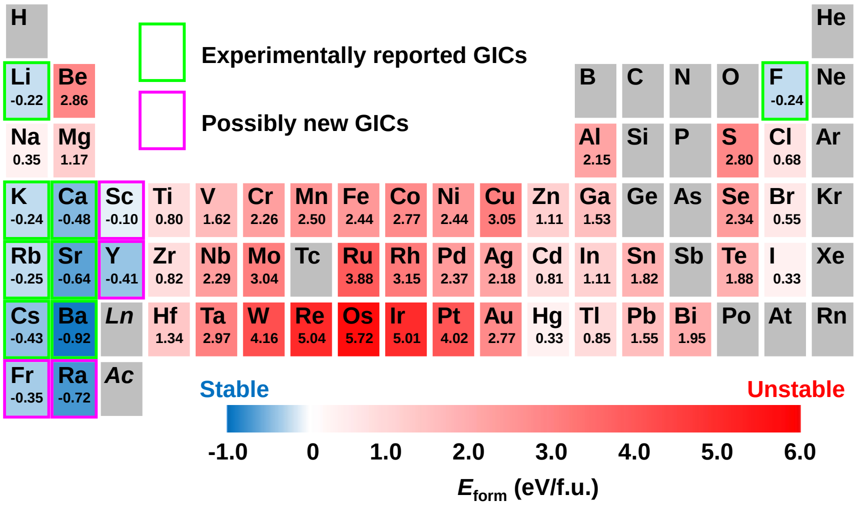

2. Research Achievements

2.1 Number of original journal papers: 10

2.2 International conference: 15 (including 5 invited presentations)

2.3 Domestic conference: 37 (including 15 invited presentation)

2.4 Number of patents: 0

3. List of awards

- 7 awards in domestic conferences, society, and university.

4. Research Grants

4.1 Total number of research grants: 3

4.2 Number of collaboration research with industries: 3

4.3 List of major research grants (serving as Principal Investigator)

- Grant-in-Aid for Scientific Research A from MEXT
- CREST
- NEDO

5. Education

5.1 Number of Ph.D. students (including current students): 3

5.2 Number of master students (including current students): 3

5.3 Number of other students: 0

6. Publication list

Journal Papers (selected)

1. "Lightweight and high-precision materials property prediction using pre-trained Graph Neural Networks and its application to small dataset", K. Nishio, K. Shibata, and T. Mizoguchi, Appl. Phys. Exp. 17 (2024) 037002-1-5.
2. "Combinatorial characterization of metastable luminous silver cations", H. Masai, M. Koshimizu, H. Kawamoto, S. Maruyama, Y. Matsumoto, C. Takahashi, H. Setoyama, and T. Mizoguchi, Scientific Reports, 14 (2024) 4638-1-8,
3. "Atomistic Probing of Defect-Engineered 2H-MoTe2 Monolayers", O. Okello, SY. Seo, J. Park, DH. Yang, D. Shin, YS. Chu, S. Yang, T. Mizoguchi, MH. Jo; SY. Choi, ACS Nano, 18 (2024) 6927-6935.
4. "Full automation of point defect detection in transition metal dichalcogenides through a dual mode deep learning algorithm", Dong-Hwan Yang, Yu-Seong Chu, Odongo Francis Ngome Okello, Seung-Young Seo, Gunho Moon, Kwang Ho Kim, Moon-Ho Jo, Dongwon Shin, Teruyasu Mizoguchi, Sejung Yang, Si-Young Choi, Mater. Horizon, 11 (2024), 747-757.
5. "A lithium superionic conductor for millimeter-thick battery electrode", Y. Lee, S. Song, H. Kim, K. Nomoto, H. Kim, X. Sun, S. Hori, K. Suzuki, N. Matsui, M. Hirayama, T. Mizoguchi, T. Saito, T. Kamiyama, and R. Kanno, Science, 381 (2023), 50-53
6. "Twist-induced interlayer charge buildup in a WS2 bilayer revealed by electron Compton scattering and density functional theory", A Talmantaite, Y Xie, A Cohen, PK Mohapatra, A Ismach, T Mizoguchi, SJ Clark, BG Mendis, Phys. Rev. B, 107 (2023) 235424-1-10
7. "Prediction of the Ground State Electronic Structure from Core-loss Spectra of Organic Molecules by Machine Learning", PY. Chen, K. Shibata, K. Hagita, T. Miyata, and T. Mizoguchi, J. Phys. Chem. Lett., 14 (2023) 4858-4865.
8. "Possible New Graphite Intercalation Compounds for Superconductors and Charge Density Wave Materials: Systematic Simulations with Various Intercalants Using a van der Waals Density Functional Method", N. Kawaguchi, K. Shibata, and T. Mizoguchi, J. Phys. Chem. C, 127 (2023) 9833-9843.
9. "Tensile strength of a transverse grain boundary in a single-walled carbon nanotube" , YS. Xie, K. Shibata, and T. Mizoguchi, J. Ceram. Soc. Jpn., 131 (2023), 621-627.
10. "A guideline for searching for stable grain boundary structure by utilizing crystallographic information: a method based on non-identical termination", Y. Hata, YS. Xie, K. Shibata, and T. Mizoguchi, J. Ceram. Soc. Jpn., 131 (2023), 738-745.

Conference Presentations (selected)

Teruyasu Mizoguchi
"Machine learning for functional core characterization" (Invited)
Materials Research Meeting (MRM) 2023, Kyoto, Dec. 12, 2023

Teruyasu Mizoguchi
"Artificial Intelligence for EELS/XAFS" (Invited)
PRICM 2023, Jeju, Korea, Nov. 21, 2023

Teruyasu Mizoguchi
"Unlocking the power of EELS via machine learning" (Invited)
ICAE 2023, Jeju, Korea, Nov. 3, 2023

Teruyasu Mizoguchi
"Application of Machine Learning for Nano-Characterization" (Invited)
NanoKorea 2023, KINTEX, Seoul, Republic of Korea, July 6, 2023

ACS NANO

www.acsnano.org

ARTICLE

Atomistic Probing of Defect-Engineered 2H-$MoTe_2$ Monolayers

Odongo Francis Ngome Okello,¶ Dong-Hwan Yang,¶ Seung-Young Seo, Jewook Park, Gunho Moon, Dongwon Shin, Yu-Seong Chu, Sejung Yang, Teruyasu Mizoguchi, Moon-Ho Jo,* and Si-Young Choi*

Cite This: *ACS Nano* 2024, 18, 6927−6935

Read Online

ACCESS | Metrics & More | Article Recommendations | Supporting Information

ABSTRACT: Point defects dictate various physical, chemical, and optoelectronic properties of two-dimensional (2D) materials, and therefore, a rudimentary understanding of the formation and spatial distribution of point defects is a key to advancement in 2D material-based nanotechnology. In this work, we performed the demonstration to directly probe the point defects in 2H-$MoTe_2$ monolayers that are tactically exposed to (i) 200 °C-vacuum-annealing and (ii) 532 nm-laser-illumination; and accordingly, we utilize a deep learning algorithm to classify and quantify the generated point defects. We discovered that tellurium-related defects are mainly generated in both 2H-$MoTe_2$ samples; but interestingly, 200 °C-vacuum-annealing and 532 nm-laser-illumination modulate a strong n-type and strong p-type 2H-$MoTe_2$, respectively. While 200 °C-vacuum-annealing generates tellurium vacancies or tellurium adatoms, 532 nm-laser-illumination prompts oxygen atoms to be adsorbed/chemisorbed at tellurium vacancies, giving rise to the p-type characteristic. This work significantly advances the current understanding of point defect engineering in 2H-$MoTe_2$ monolayers and other 2D materials, which is critical for developing nanoscale devices with desired functionality.

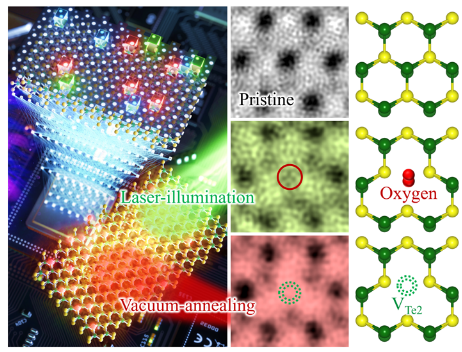

KEYWORDS: *2H-$MoTe_2$, point defect, vacuum-annealing, laser-illumination, scanning transmission electron microscopy, deep learning*

INTRODUCTION

As the channels in modern electronic devices become increasingly ultrathin with a target gate-length of less than 5 nm, the application of conventional Si-based transistors encounters certain bottlenecks, *e.g.*, the carrier mobility is compromised by surface-roughness-induced scattering and impeded by quantum-mechanical source−drain tunneling effect.[1−3] The discovery of atomically thin two-dimensional (2D) materials such as trigonal-prismatic-coordinated hexagonal molybdenum ditelluride (2H-$MoTe_2$) with distinctive tunable electric and optoelectronic properties presents an alternative solution to Si-based electronic devices.[4,5] Moreover, thickness controllability in 2H-$MoTe_2$ is ideal for highly scalable field-effect transistors (FETs) with significantly reduced short-channel effects while ensuring a high carrier mobility critical for exceptional performance at low-voltage device operations.[6−8] Recently, several studies have suggested that the optoelectronic properties of 2H-$MoTe_2$ and other 2D materials can be enhanced through meticulous control of atomic defects.[9,10] This possibility has been widely demonstrated by employing strategic engineering techniques, *e.g.*, laser-illumination,[11] vacuum-annealing, and chemical functionalization by oxygen.[12] Subsequent structural and electrical investigations indicate that such engineering technologies can manifest 2H-$MoTe_2$ with either n- or p-type electrical properties by generating a specific type of extrinsic structural defects.[13]

Despite such advancements in defect-engineering techniques, a comprehensive understanding of the correlation between defect structure−property modulation in 2H-$MoTe_2$ and other 2D materials remains insufficient. Atomically thin 2D materials are prone to structural degradation, which often result in a compromised optoelectronic property;[14−16] therefore, a continuous search for nondestructive and efficient defect-engineering technologies is still ongoing. Fifth-order spherical aberration-corrected scanning transmission electron microscopy (5^{th}-order C_s-corrected STEM) has been an indispensable tool to enable the visualization and study of defect dynamics with high-speed subpicometer resolution.[17,18] However, the large amount of data generated during atomic

Received: September 9, 2023
Revised: February 1, 2024
Accepted: February 5, 2024
Published: February 20, 2024

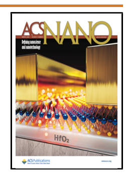

https://doi.org/10.1021/acsnano.3c08606
ACS Nano 2024, 18, 6927−6935

THE JOURNAL OF PHYSICAL CHEMISTRY C
A JOURNAL OF THE AMERICAN CHEMICAL SOCIETY

pubs.acs.org/JPCC

Article

Possible New Graphite Intercalation Compounds for Superconductors and Charge Density Wave Materials: Systematic Simulations with Various Intercalants Using a van der Waals Density Functional Method

Naoto Kawaguchi,* Kiyou Shibata, and Teruyasu Mizoguchi*

Cite This: J. Phys. Chem. C 2023, 127, 9833–9843

Read Online

ABSTRACT: Graphite intercalation compounds (GICs) are formed by inserting various atoms and molecules between the layers of graphite. Among these GICs, five structures have been reported wherein a single atom M was intercalated into graphite. Here, the formation energies of the GICs with these crystal structures and various M were investigated using a van der Waals density functional method. Consequently, we found the stable GICs for M = Sc, Y, Fr, and Ra, which are yet to be reported. Furthermore, we found that Ra-GICs have the possibility to exhibit a superconductivity of $T_c \sim 0.07$ K and that Sc- and Y-GICs have the possibility to exhibit the charge density wave, due to the strong interaction of the electron and lattice. This insight provides further understanding of how intercalants and graphite interact with each other in GICs that exhibit unique physical properties. The calculated formation energies of experimentally reported ones showed a good agreement with the experimentally reported stabilities, which provides insights into the synthesizing mechanism of GICs including the new ones.

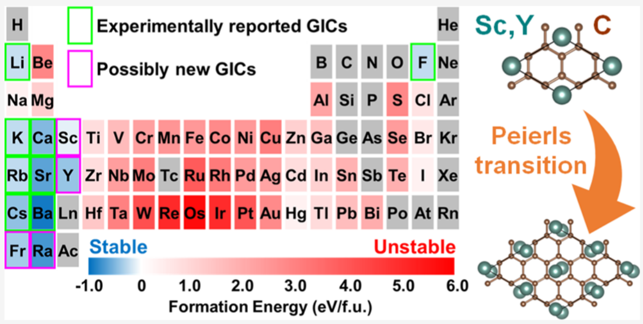

1. INTRODUCTION

Graphite intercalation compounds (GICs) have been extensively studied because of their unique physical properties. For example, LiC_6, which can be synthesized by a reversible reaction of graphite and Li ions, is widely used in Li-ion secondary batteries.[1,2] Moreover, superconductivity has been reported in several GICs with chemical formulae MC_6 (M = Ca,[3] Sr,[4] Ba,[5] and Yb[6]) and MC_8 (M = K, Rb, and Cs[7]). The GICs are typically characterized by their stacking order and compositions. Three types of stacking structures (Aα-, AαAβ-, and AαAβAγ-stacking) have been reported for the MC_6 composition, and the AαAβAγ-stacking and AαAβAγAδ-stacking have been reported for the MC_8, as shown in Figure 1.[8−14] Although several studies have suggested the synthesis of CF_x ($2 < x < 5$) as GICs,[15−18] their treatment in the same category as other GICs is controversial because their bonding is relatively covalent and their structure is different from that of others.[19,20]

In computational science, various correction methods that include long-range dispersive interaction, particularly van der Waals (vdW) interaction, have been proposed using the first-principles calculation based on density functional theory (DFT)[22,23] as vdW density functional methods.[24−29] Consequently, much research on vdW materials has been demonstrated, such as graphite and GICs, wherein considering the vdW interaction is essential. Thus, various investigations using the first-principles calculation have been performed on the phenomenon that alkali metals (AMs) and alkaline earth metals (AEs) can be inserted into graphite, except Na (among AMs), Be, and Mg (among AEs); various insights have also been provided.[30−35] For example, Okamoto reported that the high Na/Na^+ redox potential is responsible for the lack of Na insertion,[30] while Wang et al.[31] and Liu et al.[32] concluded the binding energy between graphite and the intercalant as the cause. In addition, Moriwake et al. found that Li is rather specific because it creates covalent bonding-like charge density.[33] Lenchuk et al. also reported the formation of stable Li-intercalated GIC (Li-GIC) due to the covalent bonding contribution and vdW interaction.[34] However, most of these studies have been limited to the discussion of the formation energies of GIC with AMs and AEs, and only a few systematic studies of other elements have been reported.[36]

Received: February 16, 2023
Revised: April 19, 2023
Published: May 10, 2023

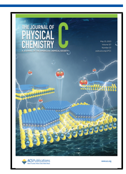

https://doi.org/10.1021/acs.jpcc.3c01073
J. Phys. Chem. C 2023, 127, 9833–9843

BATTERIES

A lithium superionic conductor for millimeter-thick battery electrode

Yuxiang Li[1]†, Subin Song[2], Hanseul Kim[2], Kuniharu Nomoto[1], Hanvin Kim[1]‡, Xueying Sun[2]§, Satoshi Hori[1], Kota Suzuki[1], Naoki Matsui[1], Masaaki Hirayama[1,2], Teruyasu Mizoguchi[3], Takashi Saito[4,5,6], Takashi Kamiyama[4,5]¶, Ryoji Kanno[1]*

No design rules have yet been established for producing solid electrolytes with a lithium-ion conductivity high enough to replace liquid electrolytes and expand the performance and battery configuration limits of current lithium ion batteries. Taking advantage of the properties of high-entropy materials, we have designed a highly ion-conductive solid electrolyte by increasing the compositional complexity of a known lithium superionic conductor to eliminate ion migration barriers while maintaining the structural framework for superionic conduction. The synthesized phase with a compositional complexity showed an improved ion conductivity. We showed that the highly conductive solid electrolyte enables charge and discharge of a thick lithium-ion battery cathode at room temperature and thus has potential to change conventional battery configurations.

All-solid-state lithium batteries (ASSLBs) have attracted research interest because the solid battery configuration—which uses lithium superionic conductors as the electrolyte instead of liquids in the current lithium batteries—has potential for improved safety and enhanced energy–power characteristics (*1*–*4*). After decades of research all-solid-state cells are capable of discharging at a high current density of >10 mA cm^{-2} (*5*). Although the cathode used in that study was only tens of micrometers thick, such fast discharge properties imply high energy and power densities for future ASSLBs, especially at elevated temperatures such as 100°C in which the operation of Li-ion batteries using organic liquid electrolytes (e.g., those containing $LiPF_6$ and ethylene carbonate) are currently restricted due to safety concerns (*4*, *6*, *7*). These results are attributed to solid electrolytes with Li^+ conductivities higher than 10 mS cm^{-1} at room temperature, which is comparable to that of traditional liquid electrolytes (*8*–*10*). These solid electrolytes include $Li_{10}GeP_2S_{12}$ (LGPS) (*8*) and Li-argyrodites represented by Li_6PS_5Cl (*11*). A conductivity of 25 mS cm^{-1} was reported for $Li_{9.54}Si_{1.74}P_{1.44}S_{11.7}Cl_{0.3}$ (LSiPSCl) (*5*) having the same kind of crystal structure as that of LGPS (LGPS-type structure), which is characterized by a *bcc*-like anion sublattice, a framework composed of tetrahedral [P/*Tt*]S_4 units (*Tt* = Si, Ge, Sn), and widely distributed Li sites (*12*, *13*).

Although the conductivities of these solid electrolytes are comparable to those of liquid electrolytes their stiff nature can be a disadvantage. As a result of the difficulty in wetting the surface of the cathode active material as a catholyte, solid electrolytes must be incorporated at the microstructural level into the electrode, resulting in void space inside it. This hinders the homogeneous supply of Li^+ to the active material, leading to a capacity loss (*14*) that makes the performance of ASSLBs inferior to that of Li-ion batteries despite the superior conductivity of the solid electrolytes relative to liquid ones. This problem presumably becomes more pronounced in millimeter-thick electrodes, where ohmic drop increases when the conductivity of solid electrolyte is low (*15*). In addition, the capacity decrease of the solid-state battery would be even more severe at low temperatures (below 0°C) in which the conductivity of the electrolyte drops sharply.

The history of the development of inorganic ionic conductors suggests that conductivity enhancement was achieved using the multiple substitution strategy. Ag^+ (*16*) and Cu^+ (*17*) conductors displayed high conductivities of >200 mS cm^{-1} at room temperature (*17*–*19*) through compositional changes from AgI to $RbAg_4I_5$ or CuI to $Rb_4Cu_{16}I_7Cl_{13}$. This approach corresponds to the "mixed (poly)-anion" (*20*, *21*) or "high-entropy" (*22*, *23*) design reported previously for the development of some Li^+ conductors, in which the aim was to flatten the potential barrier for Li^+ migration (*21*). The multisubstitution approach is attractive for realizing phases with higher ion conductivity, provided that the materials possess a specific crystal structure having superionic conduction pathways, such as LGPS-type crystal structures. However, there has been no practical principle to realize compositional complexity in the anions and cations or to avoid collapse of the target crystal structure. Consequently, this multi-element substitution strategy has not been used in designing superionic crystals with high conductivity nor have researchers explored the full potential of the crystal structure that enables superionic conduction.

We developed a solid with high Li^+ conductivity using a high-entropy material design while preserving the target crystal structure. The simple design rule, as shown in Fig. 1, is derived from the chemical composition trend of well-known argyrodite-type and LGPS-type superionic crystals (*8*, *11*). The diagram shows the plot for two composition parameters: the crystal structure indicator (t) and the compositional complexity metric (S_{mix}). The former is the ratio of sum of volumes for constituent anions ($V_{sum\text{-}anion}$) to that of cations including lithium ($V_{sum\text{-}cation}$) and can be calculated from

[1]Research Center for All-Solid-State Battery, Institute of Innovative Research, Tokyo Institute of Technology, 4259 Nagatsuta, Midori-ku, Yokohama 226-8502, Japan. [2]Department of Chemical Science and Engineering, School of Materials and Chemical Technology, Tokyo Institute of Technology, 4259 Nagatsuta, Midori-ku, Yokohama 226-8502, Japan. [3]Institute of Industrial Science, the University of Tokyo, Tokyo 153-8505, Japan. [4]Neutron Science Division (KENS), Institute of Materials Structure Science, High Energy Accelerator Research Organization (KEK), 203-1 Shirakata, Tokai, Ibaraki 319-1106, Japan. [5]Department of Materials Structure Science, School of High Energy Accelerator Science, The Graduate University for Advanced Studies, SOKENDAI, 203-1 Shirakata, Tokai, Ibaraki 319-1106, Japan. [6]Japan Proton Accelerator Research Complex (J-PARC) Center, Materials and Life Science Division, 203-1 Shirakata, Tokai, Ibaraki 319-1106, Japan.
*Corresponding author. Email: kanno@echem.titech.ac.jp
†Present address: Advanced Materials and Processing Laboratory, Research Division, Nissan Motor Co., Ltd., 1, Natsushima, Yokosuka, Kanagawa 237-8523, Japan.
‡Present address: Next Generation Battery R&D Center, SK On, 325, Expo-ro, Yuseong-gu, Daejeon, 34124, Republic of Korea.
§Present address: Research department for All-Solid-State Battery, Institute of battery Technology, Mache Power Technology Co., Ltd, 202 Zhendong Road, Huangpu, Guangzhou 510799, P.R. China.
¶Present address: China Spallation Neutron Source (CSNS), Institute of High Energy Physics (IHEP), Chinese Academy of Sciences (CAS) and Spallation Neutron Source Science Center (SNSSC), 1 Zhongziyuan Road, Dalang, Dongguan, Guangdong 523803, P.R. China.

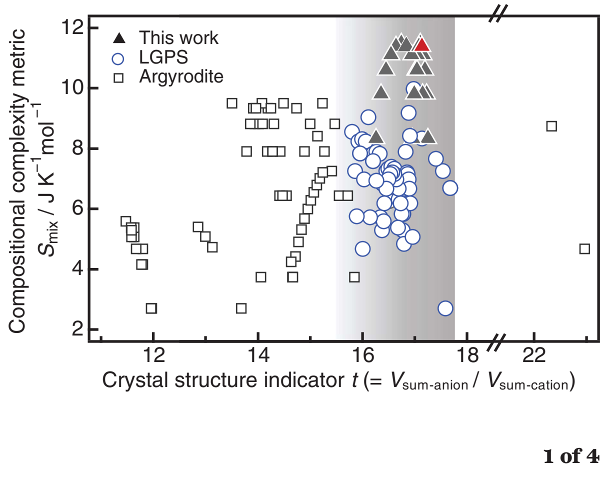

Fig. 1. Relationship between the crystal structure indicator (t, volume ratio of anions to that of cations) and compositional complexity metric (S_{mix}) for reported LGPS-type (open circles) and argyrodite-type (open squares) electrolytes. The newly explored phases in this work are indicated by filled triangles. Gray shading indicates the $V_{sum\text{-}anion}/V_{sum\text{-}cation}$ range for LGPS-type phases and the red filled triangle corresponds to the phase with the highest conductivity.

OPEN ACCESS
Applied Physics Express **17**, 037002 (2024)
https://doi.org/10.35848/1882-0786/ad2a06

LETTER

Lightweight and high-precision materials property prediction using pre-trained Graph Neural Networks and its application to a small dataset

Kento Nishio[1*], Kiyou Shibata[2], and Teruyasu Mizoguchi[2*]

[1]Graduate School of Engineering, The University of Tokyo, Tokyo 113-8656, Japan
[2]Institute of Industrial Science, The University of Tokyo, Tokyo 153-8505, Japan

*E-mail: knishio@iis.u-tokyo.ac.jp; teru@iis.u-tokyo.ac.jp

Received January 26, 2024; revised February 9, 2024; accepted February 15, 2024; published online March 6, 2024

Large data sets are essential for building deep learning models. However, generating large datasets with higher theoretical levels and larger computational models remains difficult due to the high cost of first-principles calculation. Here, we propose a lightweight and highly accurate machine learning approach using pre-trained Graph Neural Networks (GNNs) for industrially important but difficult to scale models. The proposed method was applied to a small dataset of graphene surface systems containing surface defects, and achieved comparable accuracy with six orders of magnitude and faster learning than when the GNN was trained from scratch. © 2024 The Author(s). Published on behalf of The Japan Society of Applied Physics by IOP Publishing Ltd

Supplementary material for this article is available online

Recent advances in machine learning have significantly accelerated the rate of scientific discovery, and the materials field is no exception.[1–3] The development of deep learning methods, such as Graph Neural Networks (GNNs), coupled with the increase in dataset size analyzed by a first-principles calculation, has led to faster and larger molecular dynamics simulations with high accuracy, facilitating the developments of novel materials and molecules.[4–7]

Open Catalyst 2020 (OC20),[8] which contains over two million of the first-principles calculations for catalytic materials, is a prime example of a large dataset that facilitates the materials discovery. The release of such huge datasets spurred the development of new GNNs, such as GemNet,[9] PaiNN,[10] and SCN.[11] On the other hand, the cost of the GNNs' training has been increasing as the datasets have grown and the GNN algorithms have become more complex. In addition, all deep learning methods, including GNNs, require millions to tens of millions of training parameters, so a large dataset is essential for their training.[6,11,12]

In materials research, however, the cost of the first-principles calculations to create the reference datasets remains high, making it difficult to create the large datasets for practically important materials that require large simulation models, such as structures containing defects.[13,14] Similarly, materials that require expensive approximation methods to simulate their accurate electronic states are also difficult to scale up. For example, one such material is the graphene surface system. The graphene and defected graphene have been utilized as a very good catalyst support due to its large specific surface area.[15,16] When dealing with van der Waals (vdW) materials such as graphene, in which dispersion forces make an important contribution to their properties, accurate simulations based on a vdW density functional[17,18] are essential, which is another factor that prevents the dataset from being scaled up. If a GNN is trained when the dataset is not large enough, the number of training parameters may be too large, resulting in overfitting and limited applicability (namely less generalization performance) of the trained GNN model.

When applying deep learning methods to such small datasets, a method called transfer learning is often used. Transfer learning is the method of fine-tuning a pre-trained deep learning model to solve problems in different subtasks, and is considered a province in various fields such as image recognition and natural language processing.[19,20] In the field of materials informatics, methods are also being considered that utilize parameters from models that have been pre-trained by the large datasets to make predictions on different datasets.[21–25]

This study proposes a machine learning method for constructing high-precision models with a low cost by utilizing pre-trained GNNs for a small material dataset that are important for practical use but difficult to scale up. Specifically, we devised a method to predict rotationally invariant material properties, such as formation energy by a linear regression using a pre-trained GNN on OC20 to obtain a material-specific embedded representation, using each dimension of the embedded representation as an explanatory variable. The proposed method adapts the models trained on the large dataset constructed under lower theoretical levels to the smaller dataset simulated by higher theoretical levels.

The proposed method was validated using monatomic adsorption structures on the graphene and defected graphene surfaces. We found that the proposed method achieves an accuracy equivalent to that of learning the GNN from scratch, but learning is six orders of magnitude faster. Furthermore, it was revealed that the higher accuracy could be achieved when the embedding was generated by simpler GNN algorithms.

The GNN architecture generally consists of three blocks: the embedding block, the interaction block, and the output block. Given the aforementioned GNN architecture, the embedding vectors obtained from the final interaction block can be considered descriptors that fully reflect the local environment of the system, representing the target variable of the GNN. Therefore, utilizing these embedding representations for each atom in a material from pre-trained GNN should be beneficial even for predicting properties of material in a domain different from one for pre-training.

THE JOURNAL OF PHYSICAL CHEMISTRY LETTERS
A JOURNAL OF THE AMERICAN CHEMICAL SOCIETY
pubs.acs.org/JPCL Letter

Prediction of the Ground-State Electronic Structure from Core-Loss Spectra of Organic Molecules by Machine Learning

Po-Yen Chen,* Kiyou Shibata,* Katsumi Hagita, Tomohiro Miyata, and Teruyasu Mizoguchi*

Cite This: *J. Phys. Chem. Lett.* 2023, 14, 4858−4865 Read Online

ACCESS | Metrics & More | Article Recommendations | Supporting Information

ABSTRACT: The core-loss spectrum reflects the partial density of states (PDOS) of the unoccupied states at the excited state and is a powerful analytical technique to investigate local atomic and electronic structures of materials. However, various molecular properties governed by the ground-state electronic structure of the occupied orbital cannot be directly obtained from the core-loss spectra. Here, we constructed a machine learning model to predict the ground-state carbon s- and p-orbital PDOS in both occupied and unoccupied states from the C K-edge spectra. We also attempted an extrapolation prediction of the PDOS of larger molecules using a model trained by smaller molecules and found that the extrapolation prediction performance can be improved by excluding tiny molecules. Besides, we found that using smoothing preprocess and training by specific noise data can improve the PDOS prediction for noise-contained spectra, which pave a way for the application of the prediction model to the experimental data.

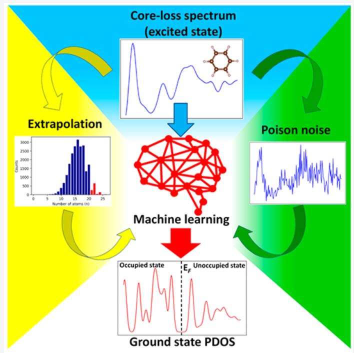

With the development of technology, various nanomaterials with specific properties are needed to deal with multifarious situations. In this case, local atomic and electronic structures play an important role as a result of their intimate correlation with the properties of nanomaterials. Thus, characterizing the local atomic and electronic structures becomes essential for investigating and designing the nanomaterials.[1,2] Among characterization methods for the nanomaterials, core-loss spectroscopy, namely, energy loss near-edge spectroscopy (ELNES) and X-ray absorption near-edge structure (XANES), has been widely used because it reflects the atomic and electronic structures of materials in high spatial resolution and sensitivity.[3,4] For example, the electronic states of catalysis can be probed through ELNES/XANES spectra to investigate the oxidation states of catalysis.[5] Besides, ELNES/XANES spectra are also useful to understand the mechanism and dynamics during chemical reactions.[6] Also, for carbon materials, Suenaga et al. used the carbon K-edge ELNES spectra to discriminate the local electronic and atomic structures for graphene.[7]

However, the molecular structure, chemical bonding, and various molecular properties, such as magnetic and mechanical properties, are mainly governed by the ground-state electronic structure of the occupied orbital, which cannot be directly obtained from the core-loss spectra.[8,9] Furthermore, the connection between the ground-state electronic structure and core-loss spectra is indirect because the spectra merely correspond to the excited state.[10] If the way to obtain the ground-state electronic structure of both occupied and unoccupied orbitals from the core-loss spectra would be paved, the acceleration of functional nanomaterial design will be achieved. Besides, investigating the s- and p-orbital density of states (DOS) has traditionally been a challenging task, with non-resonant inelastic X-ray scattering being the most common method, despite its seldom availability and inconvenience.[11] Therefore, finding a correlation between s- and p-orbital DOS and the widely used core-loss spectra would simplify the material characterization process.

Hence, we introduced the machine learning (ML) method to achieve these targets. ML is a technique that can find out the unclear relationship between variant events. Recently, it has been used in materials science for replacing time-consuming processes to reduce computation costs. Besides, ML enables scientists to discover the obscure relationship between material properties and spectroscopies to explore unknown applications for these spectroscopies.[12−15] Therefore, in this work, we aimed to use ML to obtain the full ground-state electronic structures, in particular s- and p-orbital partial density of states (PDOS), for organic molecules from carbon K-edge core-loss spectra.

The present study is schematically illustrated, as shown in Figure 1. We used a feedforward neural network (FNN) with two hidden layers as the ML model, and the carbon K-edge ELNES/XANES in the database and the ground-state PDOS of carbon s- and p-orbital were used as the input and output, respectively.[16] While ELNES/XANES spectra are commonly

Received: January 16, 2023
Accepted: April 18, 2023
Published: May 18, 2023

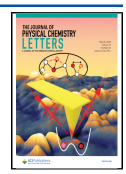

https://doi.org/10.1021/acs.jpclett.3c00142
J. Phys. Chem. Lett. 2023, 14, 4858−4865

NOMURA Laboratory

Current Research Activities 2023-2024

Nomura Laboratory

1. Research Topics

1.1 Hydrodynamic thermal phonon transport in graphite

Phonon hydrodynamics has been intensively reviewed owing to its peculiar phenomena, very similar to fluid dynamics. In graphite, the dominance of momentum-preserved normal scattering promoted the demonstration of second sound and phonon Poiseuille flow latterly. However, the impact of isotope scattering on the phonon hydrodynamic conduction in graphite remains vacant.

We experimentally demonstrate that phonon Poiseuille flow only exists in ^{13}C isotopically purified graphite ribbons. We investigate phonon Poiseuille flow (illustrated in Fig.1a) in suspended graphite ribbons (Fig. 1b) with both natural (1.1%) and enriched (0.02%) carbon isotope concentrations. Based on a steady-state μTDTR setup, we first study the suppression of thermal conductivity (κ) by isotope-phonon scattering, as shown with a significant reduction of κ in a natural graphite ribbon at the intermediate temperature range in Fig. 1c. Furthermore, we examine the observation of phonon Poiseuille flow under an explicit criterion ($\kappa/G_{ballistic}$) in Fig. 1d. As the temperature increases, κ is enhanced over the ballistic case from 30 to 60 K, attributed to the hydrodynamic transport of phonons in the isotopically enriched sample. Whereas $\kappa/G_{ballistic}$ solely decreases in the natural graphite sample, which indicates the absence of phonon Poiseuille flow resulted from the sufficient momentum-destroyed isotope scattering [1]. Supported by our theoretical calculation by solving the phonon Boltzmann transport equation, we demonstrate that the phonon Poiseuille flow can only be observed in isotopically purified graphite ribbon, thus orientating future progress for a deeper understanding of phonon hydrodynamics in solids [2].

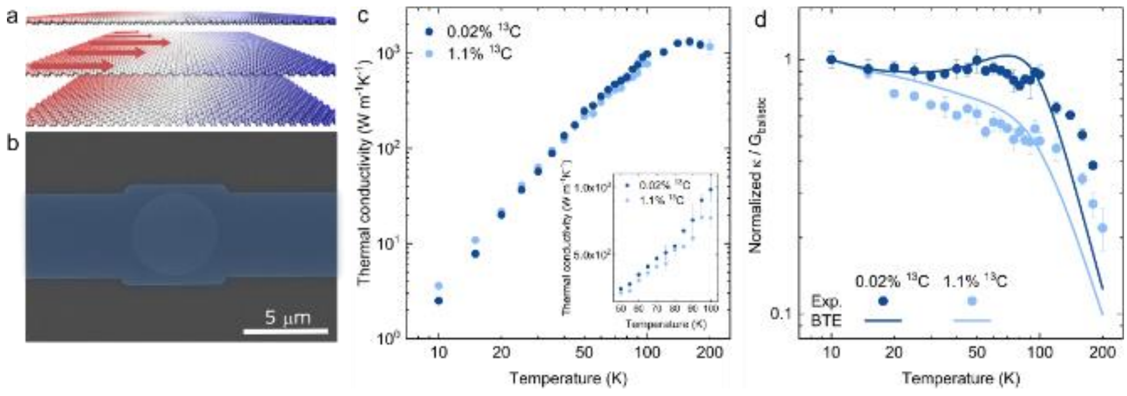

Figure 1: (a) Illustration of phonon Poiseuille flow in graphite. (b) SEM image of a 65-nm-thick suspended graphite ribbon (blue color). (c) Temperature-dependent thermal conductivity of isotopically enriched (dark blue) and natural (light blue) graphite ribbons. I (d) Normalized thermal conductivity over ballistic thermal conductance as a function of temperature.

References: [1] X. Huang, et al. Nat. Commun. 14, 2044 (2023). [2] Y. Guo, et al., Phys. Rev. B 104, 075450 (2021).

1.2 Suppressed thermal transport in mathematically inspired 2D heterosystems

The Golomb ruler, a mathematic concept, is a set of marks at integer positions along a ruler such that no two pairs of marks are the same distance apart. Applying this concept to physics may shed light on some entirely new phenomena, especially in some optimization problems.

In binary 2D heterosystems, the role played by heterointerfaces is significant and intriguing. In this work, we demonstrate efficient suppression of phonon thermal transport in the 2D heterosystems constituted of graphene (Gr) and h-BN based on the Golomb ruler sequences as shown in Fig. 1(a). By applying this concept to the heterosystem sequences, achieving stronger disordering with the fewer interfaces, and thereby achieving extremer suppression of thermal transport. In the superlattice structures (i.e., O2 and O4), thermal conductivity first decreases until reaching a minimum value and then increase with the interface density, as shown in Fig. 1(b). Such a significant non-monotonic trend of thermal conductivity clearly shows the transition of phonon transport regime from the incoherence to coherence. Importantly, in the Golomb ruler structures O5 ~ O8, the coherent transport characteristics of phonons almost disappear as indicated by the monotonous decreasing trend of thermal conductivity with the increase of interface density. Strikingly, compared with the quasi-periodic Gr/h-BN superlattice ribbons based on other sequences such as Fibonacci, Thue-Morse, and Double-period in Fig. 1(c), the Golomb ruler-based structures can achieve the maximized suppression effect on phonon thermal transport with the minimized interface density. Our extensive numerical calculations and analysis also reveal the Golomb ruler sequence can largely cancel the coherent phonon transport and effectively suppress thermal transport by phonon backscattering at the interfaces [1].

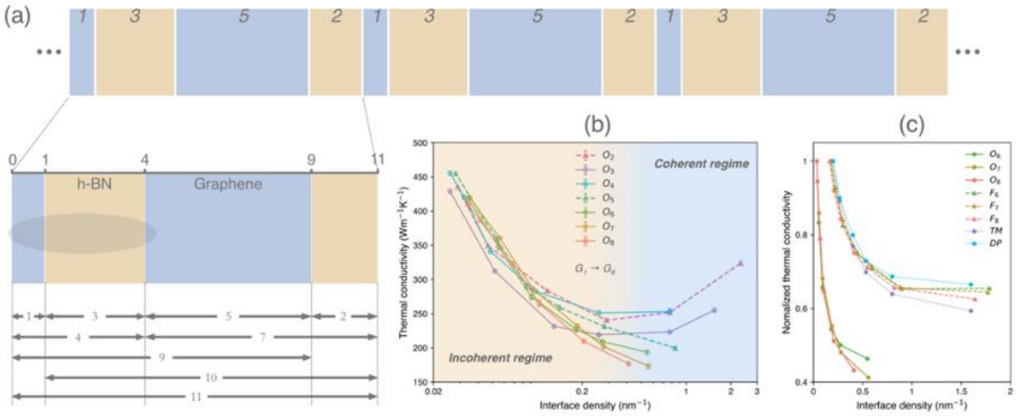

Fig. 1 (a) The illustration of graphene/h-BN in-plane heterostructures with the Golomb array. (b) Thermal conductivity of the heterostructures as a function of their interface density in six different orders of optimal Golomb array G3 ~ G8. Herein, the O2 and O4 are superlattices as the reference group. (c) The normalized thermal conductivity versus the interface density of graphene/h-BN in-plane heterostructures with sixth to eighth Golomb, Fibonacci (F6 ~ F8), Thue-Morse (TM), and double-period (DP) array.

References

[1] X. Wu, X. Huang, L. Yang, Z. Zhang, Y. Guo, S. Volz, Q. Han, and M. Nomura, "Suppressed thermal transport in mathematically inspired 2D heterosystems", Carbon 213, 118264 (2023).

2. Research Achievements

2.1 Number of original journal papers: 15

2.2 International conference: 36 (including 17 invited presentations),

2.3 Domestic conference: 29 (including 6 invited presentations)

2.4 Number of patents: 5

3. List of awards

1. M. Nomura, PCOS2023 Best Presentation Award, The 35th Symposium on Phase Change Oriented Science
2. R. Yanagisawa, Best Presentation Award, 20th Annual Conference of the Thermoelectrics Society of Japan
3. Dr. B. Kim, Best Presentation Award, 7th Phonon Engineering Workshop
4. Dr. X. Huang Best Presentation Award, 7th Phonon Engineering Workshop
5. Dr. Huang, The Japan Society of Applied Physics (JSAP) Incentive Award
6. Dr. R. Anufriev, Young Scientist Award in Science and Technology by the Minister of Education, Culture, Sports, Science and Technology

4. Research Grants

4.1 Total number of research grants: 21

4.2 Number of collaboration research with industries: 2

4.3 List of major research grants (serving as Principal Investigator)

- JST Moonshot, JST CREST, JST ALCA-Next, JST Mirai, JSPS (S, A)

5. Education

5.1 Number of Ph.D. students (including current students): 4

5.2 Number of master students (including current students): 2

5.3 Number of other students: 4

6. Publication list

Journal Paper (selected)

1. R. Anufriev, Y. Wu, S. Volz, and M. Nomura, “Quasi-ballistic thermal transport in silicon carbide nanowires,” Appl. Phys. Lett. 124, 022202 (2024).
2. B. Kim, H. Kurokawa, K. Sakai, K. Koshino, H. Kosaka, and M. Nomura,” Diamond optomechanical cavity with a color center for coherent microwave-to-optical quantum interfaces,” Phys. Rev. Appl. 20, 044037 (2023).
3. X. Wu, X. Huang, L. Yang, Z. Zhang, Y. Guo, S. Volz, Q. Han, and M. Nomura, “Suppressed thermal transport in mathematically inspired 2D heterosystems”, Carbon 213, 118264 (2023).

4. J. Ordonez-Miranda, L. Jalabert, Y. Wu, S. Volz, and M. Nomura, “Analytical integration of the heater and sensor 3ω signals of anisotropic bulk materials and thin films,” J. Appl. Phys. 133, 205104 (2023).
5. J. Ordonez-Miranda, Y. A. Kosevich, B. J. Lee, M. Nomura, and S. Volz, “Plasmon Thermal Conductance and Thermal Conductivity of Metallic Nanofilms”, Phys. Rev. Appl. 19, 044046 (2023).
6. X. Huang, Y. Guo, Y. Wu, S. Masubuchi, K. Watanabe, T. Taniguchi, Z. Zhang, S. Volz, T. Machida, and M. Nomura, “Observation of phonon Poiseuille flow in isotopically purified graphite ribbons”, Nat. Commun. 14, 2044 (2023).
7. J. Ordonez-Miranda, M. Coral, M. Nomura, and S. Volz, “Resonant thermal transport driven by surface phonon-polaritons in a cylindrical cavity”, Int. J. Thermophys. 44, 73 (2023).

International Conference (selected)

1. M. Nomura (Invited), and R. Yanagisawa, “Si-based Planar-type Thermoelectric Generators,” TMS2024 153rd Annual Meeting & Exhibition, Orlando, USA (2024).
2. M. Nomura (Keynote), R. Yanagisawa, T. Sujii, T. Mori, P. Ruther, and O. Paul, “Planar-type Si thermoelectric generator for 100 μW harvesting,” MRM2023 IUMRS-ICA2023, B1-O201-01, Kyoto, Japan (2023).
3. M. Nomura (Keynote), “Enhancement of Thermal Conductance in Isotopically Purified Graphite by Phonon Hydrodynamic Behavior,” 5th International Conference on Nanomaterials, Materials and Manufacturing Engineering (ICNMM), 2, Tokyo, Japan (2023).
4. J. Ordonez-Miranda,R. Anufriev, M. Nomura, S. Volz (Invited), “Conductive Heat Shuttling Driven by Thermal Waves in VO2,” Phonons 2023, MO4, Paris, France (2023).
5. R. Anufriev, D. Singh, and M. Nomura (Invited), “Ray phononics for thermal management in micro and nano-electronics,” IEEE-NANO 2023, MoGT6.2, Jeju, South Korea (2023).
6. M. Nomura (Invited), “Advances in Si-based Planar-type Thermoelectric Generators,” ICMAT2023, A-1263, Singapore (2023).
7. J. Ordonez-Miranda,R. Anufriev, M. Nomura, S. Volz (Invited), “Thermoelectric Shuttling Driven by Thermal Waves,” ICMAT2023, A-1295, Singapore (2023).
8. M. Nomura (Plenary), “Behavior of thermal phononis in contrast to photons,” Phononics2023, A3a-2, Manchester, UK (2023).
9. M. Nomura (Invited), “Photons help phonons: ultrafast thermal energy transport in SiN nanofilms,” International Conference on Nano-photonics and Nano-optoelectronics (ICNN2023), ICNN9-01, Yokohama, Japan (2023).

Applied Physics Letters ARTICLE pubs.aip.org/aip/apl

Quasi-ballistic thermal transport in silicon carbide nanowires

Cite as: Appl. Phys. Lett. **124**, 022202 (2024); doi: 10.1063/5.0180685
Submitted: 11 October 2023 · Accepted: 21 December 2023 ·
Published Online: 10 January 2024

Roman Anufriev,[1,2,a)] Yunhui Wu,[1] Sebastian Volz,[1,2] and Masahiro Nomura[1,2]

AFFILIATIONS

[1]Institute of Industrial Science, The University of Tokyo, Tokyo 153-8505, Japan
[2]LIMMS, CNRS-IIS UMI 2820, The University of Tokyo, Tokyo 153-8505, Japan

Note: This paper is part of the APL Special Collection on Advances in Thermal Phonon Engineering and Thermal Management.
[a)]**Author to whom correspondence should be addressed:** anufriev@iis.u-tokyo.ac.jp

ABSTRACT

Silicon carbide (SiC) is an important industrial material that enables the thermal stability of power electronics. However, the nanoscale phenomenon of ballistic thermal conduction, which may further improve the thermal performance, remains unexplored in SiC. Here, we reveal the length and temperature scales at which SiC exhibits quasi-ballistic thermal conduction. Our time-domain thermoreflectance measurements probe the thermal conductivity of SiC nanowires as a function of their length and temperature. The deviation of the thermal conductivity from the diffusive limit in nanowires shorter than a few micrometers indicates the transition into a quasi-ballistic thermal conduction regime. Naturally, the deviation is greater at lower temperatures, yet the effect persists even above room temperature. Our Monte Carlo simulations of phonon transport support our experimental results and show how phonons with long mean free paths carry a substantial amount of heat, causing quasi-ballistic conduction. These findings show that quasi-ballistic heat conduction can persist at the microscale at operating temperatures of power devices, and thus may help improve the thermal design in electronics based on SiC.

Heat in semiconductors is primarily conducted by phonons—the quantized vibrations of the crystal lattice. At the macro scale, heat conduction is seen as a diffusive process driven by random collisions between phonons. The average distance between phonon collisions is called mean free path (MFP). Remarkably, the phonon MFP can exceed hundreds of nanometers,[1,2] so that in nanostructures, phonons can travel across the structure with minimal scattering. Such heat conduction regime with reduced resistive scattering is no longer diffusive and is called ballistic. This improved thermal transport regime has implications for heat dissipation at the nanoscale. Therefore, understanding the length and temperature scales of ballistic heat conduction is crucial for improving the thermal performance of modern semiconductor electronics.

Among semiconductors, silicon carbide (SiC) has a special place in the industry as the leading material for power microelectronics. Transistors made of SiC power a wide range of devices, from electric cars to interplanetary spacecraft.[3] SiC is also used in nanoelectronics,[4] photonics,[5,6] MEMS,[7] and countless other applications.[8] Yet, despite the importance of this material, its ballistic thermal properties remain to be uncovered.

Observations of ballistic thermal transport are particularly convenient in nanowires.[9] The one-dimensional shape of nanowires enables measurements of their thermal conductivity as a function of their length, making them an ideal platform for studying ballistic thermal transport. Indeed, in the case of diffusive transport, the thermal resistance of a nanowire should be linearly proportional to its length $R \propto L$. Any degree of ballistic transport reduces the thermal resistance and breaks this relation. In this non-diffusive case, the thermal conductivity relates to the length as $\kappa \propto L^{\alpha}$, where α is the rate of divergence from the diffusive limit. Heat conduction regime that is neither diffusive ($\alpha = 0$) nor ballistic ($\alpha = 1$) is called quasi-ballistic ($0 < \alpha < 1$), which implies that only a portion of phonons traveled ballistically through only some portions of a nanowire.

Over the past decade, researchers have measured the length dependence of the thermal conductivity in various nanowires.[9] Some experiments showed purely ballistic conduction ($\alpha \approx 1$) in GaP, SiGe, and $Ta_2Pd_3Se_8$ nanowires.[10–12] By contrast, other experiments sensed only a weak presence of ballistic conduction ($\alpha \approx 1/3$) in Si, SiGe, and $NbSe_3$ nanowires.[13–16] Simulations tend to support this more modest estimation of ballistic contribution.[17–19] Moreover, some experiments detected no length dependence of the thermal conductivity,[13,19,20] at least at room temperature.

Here, we study ballistic thermal transport in SiC nanowires at different length scales and temperatures. By measuring the length

Carbon 213 (2023) 118264

Contents lists available at ScienceDirect

Carbon

journal homepage: www.elsevier.com/locate/carbon

Research paper

Suppressed thermal transport in mathematically inspired 2D heterosystems

Xin Wu [a,b,*], Xin Huang [a], Lei Yang [c], Zhongwei Zhang [d], Yangyu Guo [e], Sebastian Volz [a,f], Qiang Han [b,**], Masahiro Nomura [a,**]

[a] *Institute of Industrial Science, The University of Tokyo, Tokyo 153-8505, Japan*
[b] *Department of Engineering Mechanics, School of Civil Engineering and Transportation, South China University of Technology, Guangzhou, Guangdong Province 510640, People's Republic of China*
[c] *Key Laboratory of Thermal Science and Power Engineering of Ministry of Education, Department of Engineering Mechanics, Tsinghua University, Beijing 100084, People's Republic of China*
[d] *Center for Phononics and Thermal Energy Science, School of Physics Science and Engineering, Tongji University, 200092 Shanghai, People's Republic of China*
[e] *School of Energy Science and Engineering, Harbin Institute of Technology, Harbin 150001, People's Republic of China*
[f] *Laboratory for Integrated Micro and Mechatronic Systems, CNRS-IIS UMI 2820, The University of Tokyo, Tokyo 153-8505, Japan*

ARTICLE INFO

Keywords:
Phonon thermal transport
Golomb ruler
2D lateral heterosystem
Graphene/h-BN
Molecular dynamics

ABSTRACT

In two-dimensional (2D) heterosystems, the contribution of coherent phonon transport makes superlattices with high interface density exhibit unexpected high thermal conductivity. Herein, inspired by mathematics, we demonstrate efficient suppression of phonon thermal transport in a 2D heterosystem constituted of graphene and hexagonal boron nitride based on the Golomb ruler sequences. This design realizes extreme suppression of thermal conductivity with a minimal number of interfaces, and without any defects or dopants. Extensive numerical simulations combined with wave packet analysis show that the Golomb ruler sequence largely cancels the coherent phonon transport. This work, as the first attempt for realizing novel thermal physics using the mathematically inspired Golomb ruler design, provides a new and efficient solution for the suppression of thermal transport in 2D heterosystems.

1. Introduction

In the scientific process of nanotechnology promoting the miniaturization of functional devices and equipment, the investigation of thermal transport in micro/nano-scale materials and structures has attracted much attention. This interest is not only related to the solutions to many practical engineering and scientific problems, such as heat dissipation in electronic devices and thermoelectricity but also to many novel physical effects that macro-systems do not have [1–4]. Two-dimensional (2D) materials, triggered by graphene, are undoubtedly the most attractive platforms to investigate novel thermal properties [5–8], partly due to their highly flexible structural integrability and designability. Specifically, heterostructures based on different 2D materials perfectly illustrate this advantage, and gradually become a great carrier for structural design-driven performance modulation research [9–11].

A 2D superlattice, a special 2D lateral heterosystem, hosts many unique physical and chemical properties owing to its alternating periodic structure, but not limited to, the coherent phonon transport [12–15]. In addition, the hybrid structure of the heterosystem also shows great potential in performance optimization, such as energy conversion and storage in thermoelectric [16], photovoltaic [17], and other devices [10]. In thermoelectric materials, to optimize the thermoelectric figure of merit, it is often required to reduce their thermal conductivities. However, this is contrary to the effect brought about by the phonon coherent transport in 2D superlattice systems. In recent years, the enhancement of phonon scattering by adding interfaces, doping, and porosity has destroyed the coherence of phonons in 2D systems and their heterostructures, thereby reducing their thermal conductivities [18–21]. However, these methods adversely affected the integrity and stability of the system, and the suppression of thermal conductivity did not appear to be efficient. Actually, machine learning algorithms have also shown considerable potential for application in structure search for aperiodic superlattices with minimum thermal conductivity [22–24]. Unfortunately, current research is limited to quasi-one-dimensional and three-dimensional systems, and has not yet involved 2D systems that we are interested in.

Mathematics and physics have a long history of interdependence, with each discipline informing and inspiring the other in a continuous feedback loop. An elegant and solid mathematical language can not

* Corresponding author at: Institute of Industrial Science, The University of Tokyo, Tokyo 153-8505, Japan.
** Corresponding authors.
E-mail addresses: xinwu@iis.u-tokyo.ac.jp (X. Wu), emqhan@scut.edu.cn (Q. Han), nomura@iis.u-tokyo.ac.jp (M. Nomura).

https://doi.org/10.1016/j.carbon.2023.118264
Received 9 May 2023; Received in revised form 21 June 2023; Accepted 27 June 2023
Available online 3 July 2023

Diamond optomechanical cavity with a color center for coherent microwave-to-optical quantum interfaces

Byunggi Kim,[1,*] Hodaka Kurokawa,[2] Katsuta Sakai,[3,4] Kazuki Koshino,[2,3] Hideo Kosaka,[2,5] and Masahiro Nomura[1,†]

[1] *Institute of Industrial Science, The University of Tokyo, 4-6-1 Komaba, Meguro, Tokyo 153-8505, Japan*
[2] *Quantum Information Research Center, Institute of Advanced Sciences, Yokohama National University, 79-5 Tokiwadai, Hodogaya, Yokohama 240-8501, Japan*
[3] *College of Liberal Arts and Sciences, Tokyo Medical and Dental University, 2-8-30 Konodai, Ichikawa, Chiba 272-0827, Japan*
[4] *KEK Theory Center, Institute of Particle and Nuclear Studies, High Energy Accelerator Research Organization, 1-1 Oho, Tsukuba, Ibaraki 305-0801, Japan*
[5] *Department of Physics, Graduate School of Engineering Science, Yokohama National University, 79-5 Tokiwadai, Hodogaya, Yokohama 240-8501, Japan*

(Received 21 May 2023; revised 5 September 2023; accepted 26 September 2023; published 13 October 2023)

Quantum transduction between microwave and optical photons plays a key role in quantum communication among remote qubits. Although the quantum transduction schemes generating communication photons have been successfully demonstrated by using optomechanical interfaces, the low conversion efficiency remains an obstacle to the implementation of a quantum network consisting of multiple qubits. Here, we present an efficient quantum transduction scheme using a one-dimensional diamond optomechanical crystal cavity tuned at a color-center emission without optomechanical coupling. The optomechanical crystal cavity incorporates a thin aluminum nitride (AlN) pad piezoelectric coupler near the concentrator cavity region, while retaining ultrasmall mechanical and optical mode volumes of about $1.5 \times 10^{-4}(\Lambda_p)^3$ and $0.2(\lambda/n)^3$, respectively. The energy level of a coherent color-center electron is manipulated by a strong mechanical-mode–color-center electron-coupling rate up to 16.4 MHz. In our system, we theoretically predict that the population-conversion efficiency from a single microwave photon into an optical photon can reach 15% combined with current technologies. The coherent conversion efficiency is over 10% with a reasonably pure decay time of $T_2^* > 10$ ns. Our results imply that an atomic color center strongly coupled to the optomechanical crystal cavity will offer a highly efficient quantum transduction platform.

DOI: 10.1103/PhysRevApplied.20.044037

I. INTRODUCTION

Quantum transduction platforms for a single microwave-to-optical conversion are of paramount interest for quantum networks between microwave-controlled qubits. For this purpose, the use of the optomechanical interface [1–6] has emerged as an efficient way to convert between microwave and optical photons. The scheme using a one-dimensional (1D) optomechanical cavity typically integrates a piezoelectric coupler and phononic waveguide [1,2,7]. A microwave photon produces a phonon with the same frequency as that required to couple with an optical photon in optomechanical interfaces via photoelastic and moving-boundary effects [8–10]. The cavity-enhanced interaction between photon and phonon exerts frequency modulation of an optical photon, thereby enabling quantum transduction.

In the last decade, a quantum interface using a diamond color center has attracted enormous attention for the generation of remote entanglement between coherent spin qubits [11–14]. The photonic nanocavity with high cooperativity enables control of the spin and orbital states of the color-center electron [15,16], leading to the large-scale integration of multinode quantum processors [17]. In addition, spin memory-enhanced quantum interfaces have been implemented via the optomechanical system [18]. However, the low microwave-to-optical conversion efficiency remains a challenge for the implementation of the multinode quantum network. The optomechanical interface requires significant photonic cooperativity of the optomechanical cavity with a large number of pumping photons [19,20], which generates critical thermal noise in the subkelvin temperatures. To suppress thermal noise, we proposed quantum interfaces using diamond spin memory

*bkim@iis.u-tokyo.ac.jp
†nomura@iis.u-tokyo.ac.jp

Plasmon Thermal Conductance and Thermal Conductivity of Metallic Nanofilms

Jose Ordonez-Miranda,[1,2,*] Yuriy A. Kosevich,[2,3,4] Bong Jae Lee,[5,6] Masahiro Nomura,[1,2] and Sebastian Volz[1,2]

[1] *Laboratory for Integrated Micro Mechatronic Systems (LIMMS), CNRS-IIS UMI 2820, The University of Tokyo, Tokyo 153-8505, Japan*
[2] *Institute of Industrial Science, The University of Tokyo, Tokyo 153-8505, Japan*
[3] *N. N. Semenov Federal Research Center for Chemical Physics of Russian Academy of Sciences, 4 Kosygin Street, Moscow 119991, Russian Federation*
[4] *Plekhanov Russian University of Economics, 36 Stremyanny per., Moscow 117997, Russian Federation*
[5] *Department of Mechanical Engineering, Korea Advanced Institute of Science and Technology, Daejeon 34141, Republic of Korea*
[6] *Center for Extreme Thermal Physics and Manufacturing, Korea Advanced Institute of Science and Technology, Daejeon 34141, Republic of Korea*

(Received 28 November 2022; revised 7 February 2023; accepted 14 March 2023; published 17 April 2023)

The thermal conductance and thermal conductivity of surface plasmon polaritons propagating along a metallic nanofilm deposited on a substrate are quantified and analyzed, as functions of the film thickness, length, and temperature. This is done by analytically solving the dispersion relation of plasmons for their wave vectors and propagation length. It is shown that the plasmon energy transport along the film interfaces is driven by two modes characterized by symmetric and antisymmetric spatial distributions of the magnetic field. For a gold nanofilm deposited on a silicon substrate, both modes have comparable contributions of the plasmon thermal conductance, which takes higher values for hotter and/or longer nanofilms and saturates for films thicker than 50 nm. This saturation arises from the decoupling of the plasmon modes, the transition of which to a coupled state for thinner films maximizes the plasmon thermal conductivity. For a 1-cm-long gold nanofilm at 300 K, the maximum thermal conductivity appears for a thickness of 10 nm and takes the value of 15 W m^{-1} K^{-1}, which is about 25% of its electron counterpart. As a result of the huge propagation distance (> 1 cm) of plasmons, this plasmon thermal conductivity increases significantly with the film length and temperature and it could therefore be useful to improve the heat dissipation along metallic nanofilms.

DOI: 10.1103/PhysRevApplied.19.044046

I. INTRODUCTION

Heat dissipation from nanomaterials is one of the most important issues in the development of modern devices, due to the usual reduction of their thermal performance as their dimensions scale down to a few tens to hundreds of nanometers. In nanofilms, this reduction gets stronger for thinner films and is generated by the decrease of their thermal conductivity, which mainly results from the increasing boundary scattering of phonons or electrons propagating inside their volumes. However, as the surface-to-volume ratio ($\propto 1/\text{thickness}$) increases as the film thickness decreases, the predominant surface effects in nanofilms indicate that they could support the heat conduction not only inside their volumes but also along their interfaces. This interfacial heat transport can be driven by surface electromagnetic waves, such as the surface phonon polaritons (SPhPs) and surface plasmon polaritons (SPPs) that appear in polar and metallic nanofilms, respectively [1–7]. The in-plane propagation and cross-plane evanescent nature of these surface waves enable them to propagate over distances (> 1 mm) much greater than the typical mean free path of phonons and electrons [8–11], at speeds close to the speed of light in vacuum [1,2,12,13]. The fast and long-range surface waves can thus be powerful energy carriers, capable of enhancing the in-plane heat conduction in nanofilms.

The SPhPs are generated by the coupling of infrared photons with optical phonons at the interface of polar materials [7,14]. Previous theoretical [1,2,15] and experimental [16–18] works have reported that the SPhP contribution to the in-plane thermal conductivity of suspended polar nanofilms can actually be comparable to or higher than its phonon counterpart. These experimental works have shown that thinner [16], hotter [17], or longer [18] nanofilms exhibit a higher SPhP thermal conductivity, as

*jose.ordonez@cnrs.fr

nature communications

Article

https://doi.org/10.1038/s41467-023-37380-5

Observation of phonon Poiseuille flow in isotopically purified graphite ribbons

Received: 18 January 2022

Accepted: 10 March 2023

Published online: 19 April 2023

Check for updates

Xin Huang[1,6], Yangyu Guo[1,6], Yunhui Wu[1], Satoru Masubuchi[1], Kenji Watanabe[2], Takashi Taniguchi[1,3], Zhongwei Zhang[1], Sebastian Volz[1,4], Tomoki Machida[1] & Masahiro Nomura[1,5]

In recent times, the unique collective transport physics of phonon hydrodynamics motivates theoreticians and experimentalists to explore it in micro- and nanoscale and at elevated temperatures. Graphitic materials have been predicted to facilitate hydrodynamic heat transport with their intrinsically strong normal scattering. However, owing to the experimental difficulties and vague theoretical understanding, the observation of phonon Poiseuille flow in graphitic systems remains challenging. In this study, based on a microscale experimental platform and the pertinent occurrence criterion in anisotropic solids, we demonstrate the existence of the phonon Poiseuille flow in a 5.5 µm-wide, suspended and isotopically purified graphite ribbon up to a temperature of 90 K. Our observation is well supported by our theoretical model based on a kinetic theory with fully first-principles inputs. Thus, this study paves the way for deeper insight into phonon hydrodynamics and cutting-edge heat manipulating applications.

The classical Fourier's law well describes the diffusive phonon transport in macroscale materials at high temperatures, where the frequent Umklapp phonon-phonon scatterings damp the heat flux. Cooling or down-scaling of the systems invalidates the Fourier's law and gives rise to non-Fourier heat transport behaviors[1–4], such as coherent[5–8], ballistic[9–11], and hydrodynamic[12–16] transport. In contrast to ballistic or coherent phonon transport dictated by the boundary and interface, hydrodynamic transport is governed by intrinsically momentum-conserving normal phonon-phonon scattering. The frequent normal processes lead to exceptionally collective behaviors of phonons similar to those of fluids, including second sound in transient-state[14,15] and phonon Poiseuille flow in steady-state[16,17]. The theoretical prediction and experimental observation of phonon hydrodynamics in solids are of vital significance for both the fundamentals of lattice dynamics due to its unusual physics and the potential applications in thermal management due to its excellent transport properties.

The second sound, named analogously to the first sound (pressure wave), denotes the temperature wave propagating in solid-state materials[18,19]. The phonon Poiseuille flow is similar to that of viscous fluids under the pressure gradient in a pipe. The Poiseuille flow of phonons results from the interplay between normal scattering and diffuse boundary scattering events in the structure with a finite width. Phonon momenta are transferred along the gradient of drift velocity from the sample center to the sides by normal processes and destroyed at the boundaries[13,20,21], inducing a parabolic heat flux profile (Fig. 1a). The experimental detection of second sound in solids has a long history and has been widely reported owing to its direct wavy feature. The drifting second sound was first observed unambiguously in solid He^4 crystals[22], later in various other crystals[23–28] with heat-pulse and light-scattering methods at low temperatures, whereas the driftless counterpart has been detected very recently in Ge even at room temperature under a rapidly varying temperature field[19]. However, owing to the difficulty in observation and lack of direct evidence, there are limited experimental reports on the phonon Poiseuille flow[16,29,30]. Furthermore, this is also partially caused by the ambiguous criterion to confirm the evidence of phonon Poiseuille flow, as to be shown in the present study.

[1]Institute of Industrial Science, The University of Tokyo, Tokyo 153-8505, Japan. [2]Research Center for Functional Materials, National Institute for Materials Science, Tsukuba 305-0044, Japan. [3]International Center for Materials Nanoarchitectonics, National Institute for Materials Science, Tsukuba 305-0044, Japan. [4]LIMMS, CNRS-IIS IRL 2820, The University of Tokyo, Tokyo 153-8505, Japan. [5]Research Center for Advanced Science and Technology, The University of Tokyo, Tokyo 153-0041, Japan. [6]These authors contributed equally: Xin Huang, Yangyu Guo. e-mail: nomura@iis.u-tokyo.ac.jp

TIXIER-MITA Laboratory

Current Research Activities 2023-2024

Tixier-Mita Laboratory

1. Research Topics

1.1 Bio-mimetic stimulation electronic device to create a bio-hybrid brain-heart platform

In this research we propose to develop a bio-hybrid in-vitro brain-heart platform capable of reproducing the mechanisms involved in in-vivo. Heart disease investigation is often complex because it involves not only the heart but also other organs to which it is related, in the first place the nervous system managed by the brain. In particular, some diseases affect the generation of cardiac rhythm, like for instance arrhythmia. It alters the sinoatrial (SA) node, a cluster of pacemaker cells located in the right atrium of the heart, linked with the autonomic nervous system (ANS). The purpose of the pacemaker cells is to control the cardiac contraction rate through regular action potentials. The bio-hybrid platform purpose is to mimic the functioning of the couple “ANS – pacemakers”. It will be connected to an in-vitro neuron culture on one side, imitating brain neuron cells managing sensing information coming from heart, and an in-vitro cardiac muscle cell culture (cadiomyocytes), imitating the heart and which will contract in rhythm with the stimulation signals sent by the platform.

A Field Programmable Gate Array (FPGA) circuit has been chosen for the biomimetic platform to permit real-time calculation. Here only the pacemaker part of the platform is presented. A pacemaker model, capable of describing the electrical and biochemical behaviors of the sinoatrial node was chosen and implemented in the FPGA. It is based on the Maltsev-Lakatta model which behaves like an oscillator requiring no external stimulation. This model includes a calcium clock model and a membrane clock model, which describes in a quite realistic way the biological behavior of pacemaker cells. After implementation of the pacemaker cell model in the FPGA, the signal provided by the circuit is verified, then the circuit is connected to a cardiomyocyte cell culture then used as a stimulator. Cardiomyocyte cells, stimulated by the biomimetic pacemaker FPGA circuit, show contraction activity following the frequency of the signal. A threshold of 2V has to be applied to the cells to control the activity.

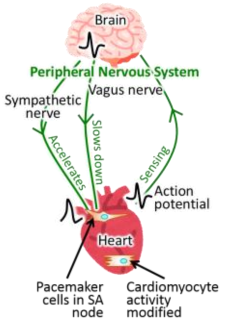

Brain-heart interaction in in-vivo.

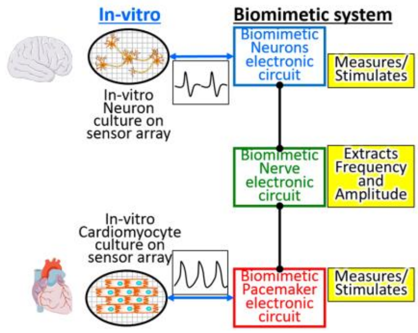

Biohybrid in-vitro brain-heart system in development.

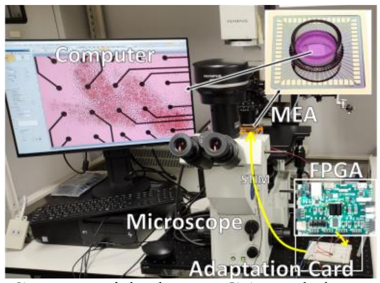

Set-up with the FPGA and the in-vitro cardiomyocyte culture.

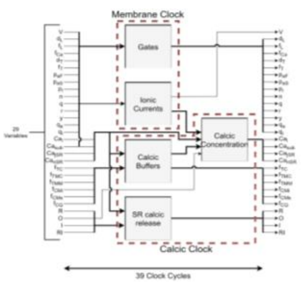

Architecture of the model on FPGA

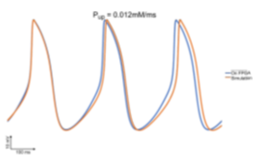

Output signal of the FPGA.

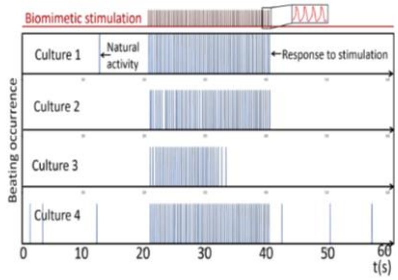

Contraction occurrence of the in-vitro cardiomyocytes recorded before, during and after biomimetic stimulation.

.

This work was performed in collaboration with the University of Bordeaux.

1.2 <u>2D Bioimpedance monitoring with a TFT bio-sensing platform</u>

Bioimpedance sensing is a dye-free technique used to characterize electrically cells. For instance, by measuring the spatial variation of impedance, it is possible to distinguish areas with no cells, dead cells, healthy cells and so on. In this project, a Thin-Film-Transistor platform is used to monitor cell culture on long term by realizing in real time 2D cartography of bioimpedance. The platform consists in a high spatial resolution sensor matrix. The sensor matrix is connected to a matrix of switch transistors for control and selection of individual sensors. The control of the switch transistors is performed by a control card previously developed, called JAPASTIM. The measurement of the impedance for each electrode is performed using Analog Discovery 2 with the impedance analyses module. Impedance spectrum (magnitude and phase) show clear difference with and without cell cultured on the device. The 2D impedance map shows the variation of the impedance magnitude and phase with and without cell.

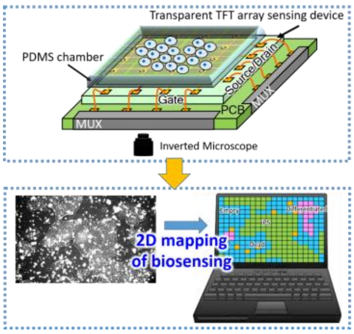

Target of the research。 .

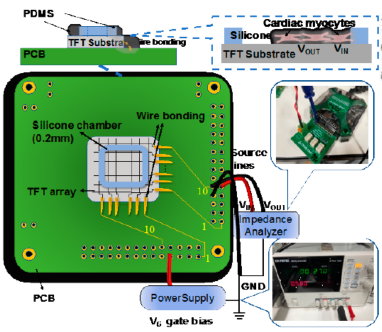

Experimental set-up for 2D bioimpedance mapping.

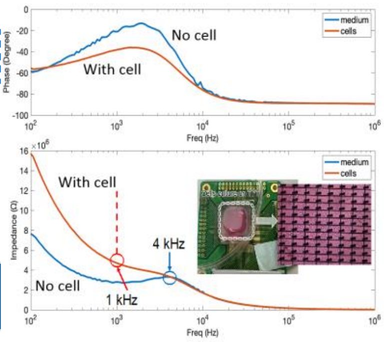

Impedance spectrum (magnitude and phase) with and without cell culture.

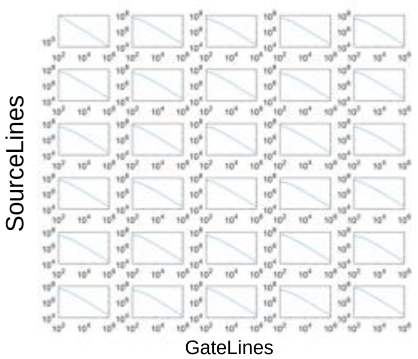

2D impedance magnitude spectrum on a 6x5 matrix of electrodes

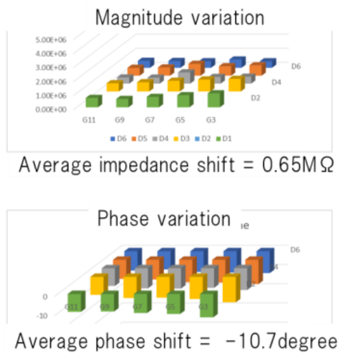

Variation of impedance magnitude and phase between cell culture and no cell culture on the device.

1.3 <u>Bimodal “Sensor chiplet” platform for albumin and pH multi-chemical sensing</u>

A new concept of agile and multimodal chemical sensing platform, named “Sensor Chiplet” is proposed and experimentally validated in this research. The concept is inspired by the recent trend in large scale integrated (LSI) circuits, to quickly realize high functionality by pieces of LSI “Chiplets”. As a proof of concept, pH and albumin sensing was demonstrated by a bimodal device composed of two planar “Sensor Chiplets” having microelectrode arrays (MEAs). Two 8×16 mm2 Si chiplets with thirteen gold (Au) and indium tin oxide (ITO) microelectrodes with maximum electrode size of 512 × 512 µm2 were fabricated, functionalized, integrated and tested using surface micromachining, deep-reactive ion etching (RIE) and subsequent chemical functionalization. Results obtained shows that the proposed concept enables the integration of modalities without sacrificing sensitivity.

Multimodal sensing purpose is to gather multiple information from an environment for fundamental understanding, for modeling or quantification of a series of parameters. For that purpose multiple sensors have to used, and if possible gathered on a same device for portability and miniaturization. However, gathering different sensors on a same device is sometimes tricky because of incompatibility in the fabrication among the different devices. So, the idea here is to create independent sensors called “sensor chiplet”, integrate them on a same PCB platform and use that device. Here we targeted a bi-modal sensor device, targeting albumin sensing and pH sensing. It could be used to investigate the activity of pancreatic β cells. The device has then be fabricated then tested on albumin and pH solutions.

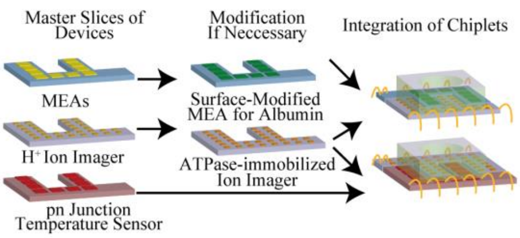

Principle of a bi-modal “sensor chiplet” platform.

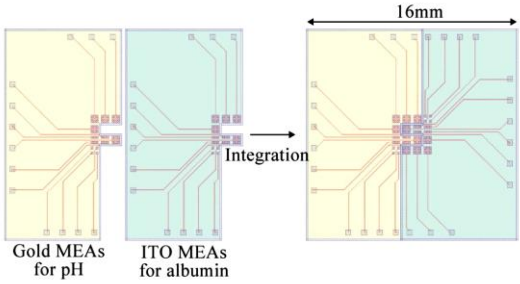

Design of the two “sensor chiplets” used here for albumin and pH sensing.

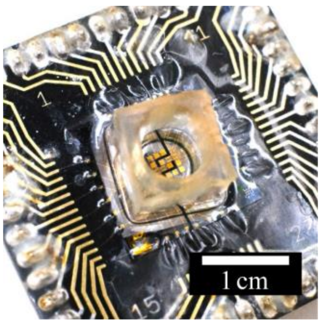

Integrated bimodal device.

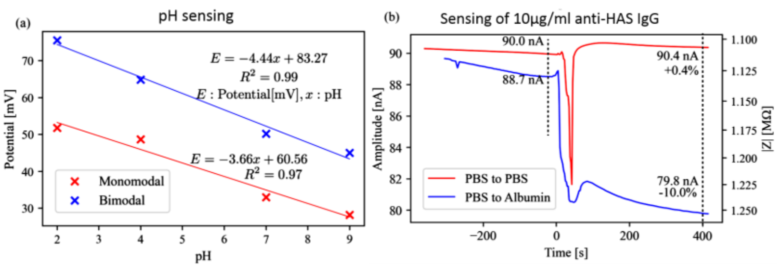

Results of pH sensing and albumin with the bimodal sensor chiplet device.

2. Research Achievements

2.1 Number of original journal papers: 0

2.2 International conference: 2

2.3 Domestic conference: 3 (including 0 invited presentations)

2.4 Number of patents: 0

3. List of awards

- /

4. Research Grants

4.1 Total number of research grants: 0

4.2 Number of collaboration research with industries: 1

4.3 List of major research grants (serving as Principal Investigator)

5. Education

5.1 Number of Ph.D. students (including current students): 1

5.2 Number of master students (including current students): 0

5.3 Number of other students: 4 (4 internship students)

6. Publication list

Conference Presentations (selected)

1. Pierre-Marie Faure, Agnès Tixier-Mita, and Timothée Lévi, “A digital hardware system for real-time biorealistic stimulation on in vitro cardiomyocytes”, 29th International Symposium on Artificial Life and Robotics, AROB-ISBC-SWARM2024, B-Con PLAZA, Beppu, Japan, January 24-26, 2024.
2. Thomas Wanchaï Menier, Bruno Mery, Hiroshi Toshiyoshi, Agnès Tixier-Mita, “OPEN-SOURCE LIVE-TRACKING SOFTWARE FOR CARDIOMYOCYTE CELLS ANALYSES”, 応用物理学会・第15回集積化MEMSシンポジウム, Kumamoto Hall, November 6-9 2023.
3. Xingzhuo Hu, Agnès Tixier-Mita, and Hiroshi Toshiyoshi, “High Resolution 2D Impedance Spectroscopy with a Thin-Film-Transistor device for Cell Culture Monitoring”, 応用物理学会・第15回集積化MEMSシンポジウム, Kumamoto Hall, November 6-9 2023.
4. Xingzhuo Hu, Hiroshi Toshiyoshi, and Agnès Tixier-Mita, “2D Impedance measurement with a TFT array device in the aim of cell culture characterization”, 2023年度電気学会E部門総合研究会（バイオ・マイクロシステム研究会）、豊田工業大学（愛知県名古屋市), June 30 - July 1 2023.
5. Ryugo Shimamura, Shun Yasunaga, Kei Misumi, Anne-Claire Eiler, Akio Higo, Gilgueng Hwang, Ayako Mizushima, Dongchen Zhu, Kikuo Komori, Yasuyuki Sakai, Hiroshi Toshiyoshi, Agnès Tixier-Mita, and Yoshio Mita, “A BIMODAL "SENSOR CHIPLET" PLATFORM APPLIED FOR ALBUMIN AND PH MULTI-CHEMICAL SENSING”, in Proc. 22nd International Conference on Solid-State Sensors, Actuators and Microsystems (Transducers 2023), June 25-29, 2023, Kyoto International Conference Center, Kyoto, Japan, pp. 2014-2017.

A real-time biorealistic stimulation system for *in vitro* cardiomyocytes

1st Pierre-Marie Faure
IMS Laboratory, CNRS UMR5218
University of Bordeaux
Talence, France
pierre-marie.faure@u-bordeaux.fr

2nd Agnès Tixier-Mita
Institute of Industrial Science (IIS)
The University of Tokyo
Tokyo, Japan
agnes@iis.u-tokyo.ac.jp

3rd Timothée Lévi
IMS Laboratory, CNRS UMR5218
University of Bordeaux
Talence, France
timothee.levi@u-bordeaux.fr

***Abstract*—Every year, cardiovascular disease causes millions of deaths worldwide. These diseases involve complex mechanisms that are difficult to study. To remedy this problem, we propose to develop a heart-brain platform capable of reproducing the mechanisms involved in generating the heartbeat. The platform will be designed to operate in real-time, with the most economical and integrated design possible. To achieve this, we are implementing highly biologically coherent cellular models on FPGA, which we interconnect with *in vitro* cell cultures. In our case, we are using the Maltsev-Lakatta cell model, which describes the behavior of the pacemaker cells responsible for the heart rhythm, to stimulate a cardiomyocyte culture.**

Index Terms*—Sinoatrial Node, real-time, FPGA, biomimetic, *in vitro

I. Introduction

According to WHO data, in 2019, 32% of deaths worldwide were caused by cardiovascular disease [1]. As populations age, this number will rise in the future years. Yet the mechanisms involved in these diseases remain poorly understood due to the interactions' complexity.

In reality, heart disease investigation is often complex because it involves not only the heart but also other organs, to which it is related, in the first place, the nervous system. This is the reason why it is essential to study the brain-heart system to obtain a realistic overview of the disease [2].

In this paper, we are focusing more specifically on diseases affecting the generation of cardiac rhythm (Fig. 1). This affects the sinoatrial (SA) node, a cluster of pacemaking cells located in the right atrium of the heart, linked with the autonomic nervous system.

The usual treatment for these diseases ranges from drugs to transplants and the implantation of assistive devices. Each of these treatments could induce difficulties, as they usually involve a loss of quality of life, with significant effects on lifestyle, as well as a substantial cost for society. These treatments target only the heart, while heart disease involves also other organs. If we can obtain a wider overview of all the relationships between these organs, especially in the case of heart disease, then it would be possible to propose more accurate treatment solutions.

We would like to thank Fondation Sasakawa and Nouvelle-Aquitaine region for their participation to fund this research.

For all these reasons, further research in this field is essential. However, research is focused mainly on the use of animal models, which have the advantage of being faithful to the system under study, but are also very costly, time-consuming and have ethical issues. *In vitro* neurocardiac coculture simplifies *in vivo* investigation but remains complex to be achieved and limited to the interaction between sympathetic neurons and cardiomyocytes [3]. In both cases, artificial control of the biological unit is complicated. On the other side, biorealistic models on computers have the advantage to reduce the time consumption and the cost to reproduce experiments but need to maintain heavy infrastructure and the specialized skills associated while being unable to process models in real-time [4].

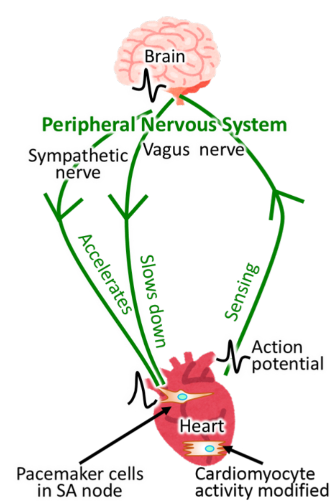

Fig. 1: Overview of the heart-brain interaction system

Here, we propose to develop a biohybrid platform that reproduces artificially the heart-brain system to overcome these limits (Fig. 2). It starts by recording the activity of *in vitro* neuron culture mimicking the measure of the blood flow. Then, this activity will be processed by a Spiking Neural Network (SNN) [5]–[7] that would speed up or slow down the sinoatrial node through parasympathetic and sympathetic stimulation. This output signal will be put on an *in vitro* cardiomyocyte culture to assess its efficiency, to prepare for a

A BIMODAL "SENSOR CHIPLET" PLATFORM APPLIED FOR ALBUMIN AND PH MULTI-CHEMICAL SENSING

PLEASE LEAVE THIS SPACE AVAILABLE TO LIST YOUR AUTHORS
PLEASE LEAVE THIS SPACE AVAILABLE TO LIST YOUR AUTHORS' AFFILIATIONS.
REMEMBER THAT NO NAMES OR INSTITUTIONS SHOULD APPEAR ON THIS ABSTRACT, AS IT IS PREPARED FOR DOUBLE-BLIND REVIEW

ABSTRACT

A new concept of agile and multimodal chemical sensing platform, named "Sensor Chiplet" is proposed and experimentally validated. The concept is inspired by the recent trend in large scale integrated (LSI) circuits, to quickly realize high functionality by pieces of LSI "Chiplets". As a proof of concept, pH and albumin sensing was demonstrated by a bimodal device composed of two planar "Sensor Chiplets" having microelectrode arrays (MEAs). Two 8 ×16 mm^2 Si chiplets with thirteen gold (Au) and indium tin oxide (ITO) microelectrodes with maximum electrode size of 512 × 512 µm^2 were fabricated, functionalized, integrated and tested using surface micromachining, deep-reactive ion etching (RIE) and subsequent chemical functionalization. Results obtained shows that the proposed concept enables the integration of modalities without sacrificing sensitivity.

KEYWORDS

Multimodality, Chemical Sensor, Sensor Chiplet, MEAs, MEMS

INTRODUCTION

Multimodal sensing for the gathering of multiple information from a single analyte, has been explored to increase its selectivity and sensitivity since its first introduction in the 1980s [1]. The applications of multimodal sensing include the detection of volatile organic compounds for gas monitoring, the quantification of minerals for agriculture and food industry or even the multicomponent analysis of significant ions for medical applications [2].

Although multimodality could open new possible applications, it is indispensable to miniaturize and integrate such multimodal sensors for their applications. Studies on the miniaturization and integration of multimodal sensors thus far can be categorized into two types. The first approach is to design and fabricate dedicated devices for target applications [3]. Such devices can support any modes of measurements if they are compatible with the production process. However, they could be limited in terms of flexibility in development as the cost of process optimization is large and it takes long from the initial research proposal to getting the sensor ready for usage. Another approach is to use a generic device such as an H^+ ion imager as a multimodal sensing platform with surface modifications of electrodes [4-7]. In this approach, sensing modality could easily be changed through chemical and lithography processes at the user's will. However, this method can only support modes which have a transduction scheme to whatever the platform measures (e.g., H^+ ions)

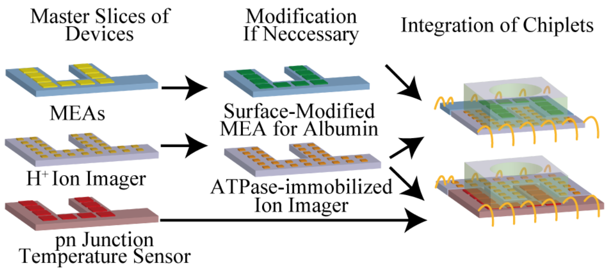

Figure 1: Planar "Sensor Chiplet": Bimodal Platform with side-by-side integrated Chiplets

and is limited in terms of comprehensiveness of modality. Therefore, multimodality supporting both flexibility and comprehensiveness has been wanted for a more agile development of miniaturized and integrated multimodal sensors. To achieve this, we propose the concept of "Sensor Chiplet" platform.

Since its introduction to large scale integrated (LSI) circuit packaging, chiplet technology has gained increasing attention for several advantages, such as the improvement of production yield rates and the combining of different technology nodes. Its application to the field of sensors will allow sensor packaging to benefit from two other features of chiplets: the ability to change chip configuration depending on the usage and the shortening of time needed to design and fabricate the chips [8]. In this research, chiplet technology is applied to the field of sensors for the first time and multimodality benefitting from the concept will be proposed and demonstrated.

The details of the "Sensor Chiplet" concept is shown in Fig. 1. As with LSI chiplets, there are "Sensor Chiplets" with varying functions such as microelectrode arrays (MEAs), H^+ ion imagers, or temperature sensors. These chips meet a design rule so that it can be later easily but seamlessly integrated. Users will choose chiplets according to their desired measurement modes, functionalize them using chemical processes if necessary and finally integrate the chiplets for usage. For example, a user in need of a bimodal sensor measuring acetylcholine (ACh) and temperature can choose to use a hydrogen ion imager and a p-n junction sensor without the need for considering their compatibilities. Users can then functionalize the ion imager with photocurable resin with ACh-ase in a day and integrate in another day. In a matter of days, users will have access to custom-made bimodal sensors which would have taken months if it were for the designing and production of conventional made-to-order sensors.

As a proof of concept for such bimodal sensor using the Planar "Sensor Chiplet" platform, we fabricated "Sensor Chiplets" of gold (Au) MEAs and indium tin oxide (ITO) MEAs, each dedicated to pH and human serum albumin

High Resolution 2D Impedance Spectroscopy with a Thin-Film-Transistor device for Cell Culture Monitoring

Xingzhuo Hu, Agnès Tixier-Mita, Hiroshi Toshiyoshi*
(Institute of Industrial Science, The University of Tokyo)

Abstract To conduct real-time analysis of cellular properties, numerous microelectrode array (MEA) configurations have been developed previously. In contrast to conventional MEAs, thin-film-transistor (TFT) active-matrix arrays offer several advantages, including a more substantial sensing area, optical transparency, and enhanced measurement precision. In this study, we present the first successful 2D impedance mapping of cardiomyocytes cultivated on a TFT array device. Additionally, we propose a corresponding circuit model for examination and simulation. These outcomes confirm the potential of this technology for characterizing cell cultures and measuring cellular activity in the future.

Keywords : microelectrode array, biosensor, impedance measurement, thin-film-transistor, cell characterization

1. Introduction

In recent years, significant improvements have been made in the field of micro-electrode array (MEA) technology, revolutionizing our ability to explore cellular activity with higher precision and efficiency. This advancement has been attractive with the help of non-invasive, label-free, and time-efficient approaches to study cellular behavior [1, 2].

Typically, MEAs offer two primary avenues for electrical characterization of cells: electrophysiology and impedance spectroscopy. Electrophysiology focuses on measuring the electrical activity of electrically active cells, while impedance spectroscopy provides valuable insights into the electrical characteristics of cells or cell culture conditions [3]. However, integrating both of these techniques into a single device has long been a challenge due to technological limitations.

Thin-film transistor (TFT) technology on a glass substrate has emerged as a promising solution to overcome these limitations. TFT technology is widely used in liquid display field, which brings a suite of advantages, including a spacious surface area, a high-density array of micro-electrodes, and optical transparency—essential for compatibility with simultaneous optical observations.

This technology comprising active matrices with transparent substrate comes on the heels of significant progress in MEA technology. Traditional MEAs consist of passive electrode arrays wired externally, which constrains their scalability and spatial resolution. To address these limitations, researchers have harnessed complementary metal-oxide-semiconductor (CMOS) processes, enabling the integration of measurement and processing electronics onto a single chip while reducing the pitch size [4-6]. While this approach enhances spatial-temporal resolution and response speed, it does have drawbacks, including higher fabrication costs and a lack of transparency—making CMOS-MEAs unsuitable for a traditional microscope system.

In the realm of cellular analysis, optical observation has long been a dominant technique. The simultaneous integration of electrical sensing alongside optical observation has become increasingly crucial. Electrical sensing not only complements optical analyses but also allows for the verification of information extracted from images.

In this background, the combination of TFT technology with MEAs emerges as a promising alternative for bio-measurement. With its expansive surface area, densely packed micro-electrodes, and optical transparency, TFT technology is poised to redefine our ability to study cellular activity. Previous studies from our group have demonstrated the effectiveness of this technology in monitoring and stimulating cell cultures [7]. We also had already achieved impedance sensing results on yeast cells and liver cells using 0D (two adjacent microelectrodes) and 1D (a single line of electrodes) configurations [8]. To expand upon these findings and extend our capabilities to 2D, we conducted impedance measurements on solutions containing gradient concentrations of micro particles made of polystyrene. These measurements allowed us to generate an impedance map of the transistor's matrices, confirming the device's potential for applications in bio-tissue measurements [9].

In this work, cardiac myocytes were cultured on the active area of the TFT array, and impedance measurements were performed on both the cell-cultured device and the device without cells. An equivalent circuit model was raised to better understand the mechanism of our measurement system and perform future simulation based on the impedance curves we acquired for discussion.

2. Impedance Measurement Set-up and Process

2.1 Bio-thin-film transistor (TFT) device

In the initial design of our experimental bio-TFT device, we incorporated a densely populated transparent electrodes array made of Indium Tin Oxide (ITO) on a glass substrate as shown in Fig. 1. The transistors on substrate represented in circuit diagram is indicated as well. What sets this device apart is its ability to apply individual control over each microelectrode via the integrated TFT switches.

In this design, the drain terminal of each TFT is directly linked to an ITO microelectrode deposited on glass substrate, while the gate terminals are interconnected in column and the source lines are connected in row. Activation of a specific gate column by applying a 12V DC potential turns on all the transistors associated with that particular column. At the intersection of a perpendicular source line,

TOCHIGI Laboratory

Current Research Activities 2023-2024

Tochigi Laboratory

1. Research Topics

1.1 In situ observations of mechanical behavior of interfaces

Practical materials are typically used in combination of different mater. Their interfaces are closely related to their properties. To meet the performance requirements of modern advanced materials, microstructure design of interfaces that takes into account atomic/electronic structures and functional additive elements is necessary. In addition, the interfaces are often structurally weaker due to inconsistent atomic arrangement, and fracture or delamination of interfaces can be a problem in practical use. However, much is unknown microstructural mechanical behavior of interfaces because of lack of experimental observations. Our research group investigates the microscopic mechanical behavior of interfaces based on in situ loading experiments.

In recent years, micromachining technology has made great progress, and small chips having precise loading machinery, the so-called MEMS, are being used. We have developed MEMS devices compatible with electron microscopes in order to perform in situ straining experiments of nanomaterials. Fig. 1 shows a custom-made instrument and a MEMS device for in situ testing in a scanning electron microscope (SEM). The MEMS device has two cantilevers driven by electrostatic actuators, and they are controlled by a source measure unit. A sample is typically prepared by focused ion beam system (FIB).

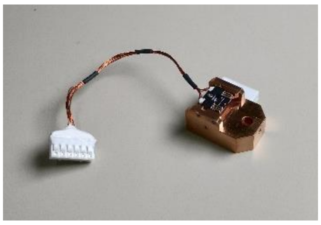

Fig. 1. MEMS device holder for in situ SEM mechanical testing.

Fig. 2 shows an example of sample preparation on the MEMS device. The sample is SiO_2-SiCN-SiO_2 layered material in amorphous phase, which is used as insulator film in integrated circuits. To evaluate the mechanical strength of the SiO_2-SiCN interface, a thin plate sample with a cross-sectional area approximately 500 nm × 200 nm was prepared by focused ion beam system (FIB). In situ straining experiment of the SiO_2-SiCN-SiO_2 layered sample was performed in SEM. As shown in Fig. 3, the sample was elongated with increasing applied load. The SiO_2-SiCN interface did not break even if the applied load reached 66.8 μN, which corresponds to the stress of 668 MPa. Instead, the SiO_2 layer fluidly deformed during loading. There are experimental reports that amorphous SiO_2 easily deforms with loading during observation by transmission electron microscopy (200 kV electron beam). In the present experiment was performed under 5 kV electron irradiation in SEM. The experimental results

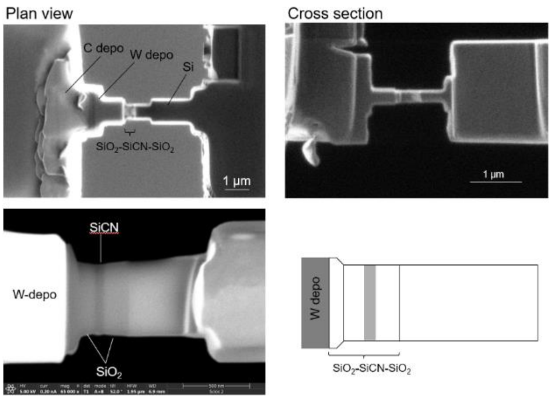

Fig. 2. Sample preparation of SiO_2-SiCN-SiO_2 material by FIB.

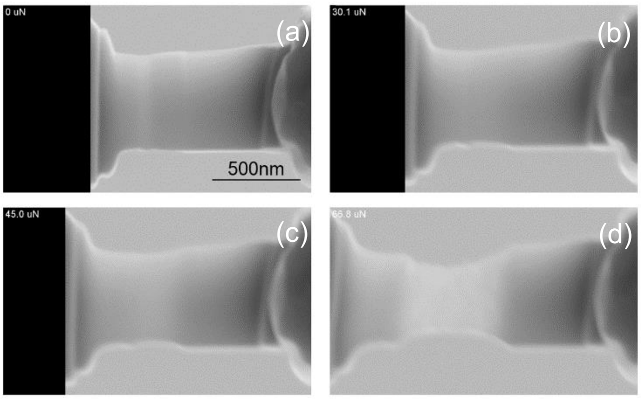

Fig. 3. In situ SEM tensile experiment. (a) 0 μN, (b) 30.1 μN, (c) 45.0 μN, (d) 66.8 μN.

demonstrate that such low energy electron irradiation still enhances the deformability of amorphous SiO_2. To evaluate the critical strength of the SiO_2-SiCN interface, the electron irradiation conditions must be optimized.

1.2 Microstructure analysis of stainless steel deformed at cryogenic temperatures

Hydrogen is attracting attention as a next-generation clean energy source. To spread the use of hydrogen, the development of large-scale tanks for liquid hydrogen having a boiling point of 20 K is crucial. Austenitic stainless steel is a candidate of the materials for liquid hydrogen tanks, because it has relatively good resistance to hydrogen and thermal embrittlement. However, the strain-induced martensite phase in austenitic stainless steel can spoil its mechanical properties. In this study, the microstructures of austenitic stainless steel deformed at 20K were examined by electron back scatter diffraction (EBSD) in SEM, and the distributions of the martensite phase were analyzed.

Fig. 4 shows inverse pole figure and phase maps of undeformed and 10%-deformed samples. The solidification mode of the present austenitic stainless steel is FA, and thus the sample contains precipitations with the delta phase (bcc) in addition to the bulk in the gamma phase (fcc) as shown in Fig. 4(b). The 10%-deformed sample contains many fine structures related to the strain-induced martensite phase, but they are identified to be delta phase because of almost the same lattice constants to the delta phase. Since the strain-induced martensite phases have relatively high strain, they can be distinguished from the delta phases by strain sensitive analysis such as kernel average misorientation (KAM). Using these microstructural analysis methods, we further investigate the formation mechanisms of the strain-induced martensite phase in austenite stainless steel at cryogenic temperatures.

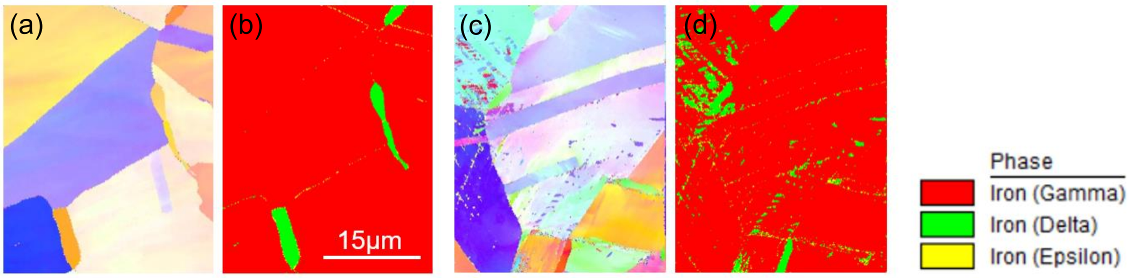

Fig. 4. EBSD mapping of austenitic stainless steel. (a) IPF mapping of undeformed sample, (b) Phase map of undeformed sample, (c) IPF map of 10%-deformed sample, (d) Phase mapping of 10%-deformed sample.

1.3 Development of in situ experimental systems

In recent years, the deformability of compound semiconductor materials is found to be drastically dependent on ambient light conditions. The origin of this phenomenon is considered to be due to the interaction between dislocations and electrons/holes induced by light irradiation. To reveal the mechanisms in detail, we characterized dislocation structures of compound semiconductors induced by deformation in darkness and light irradiation conditions. Fig. 5 shows a bright-field transmission electron microscopy (TEM) image of an indented region in a (0001) ZnO substrate formed by nanoindentation with a load of 300 μN in a darkness condition. It was found that dislocation structures associated with the pyramidal slip were formed to a depth of ~300nm from the sample surface, which was 30% deeper in the case of a sample indented under a light irradiation condition. These results indicate that light illumination suppresses the activity of pyramidal slip dislocations in ZnO.

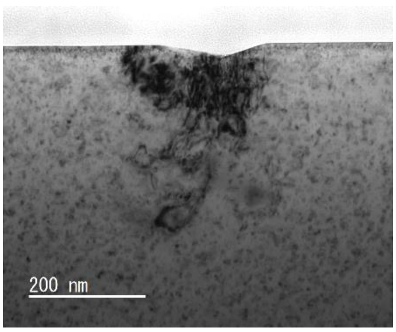

Fig. 5. TEM image showing a ZnO indented sample under completely darkness.

2. Research Achievements

2.1 Number of original journal paper: 6

2.2 International conferences: 4 (including 2 invited presentations)

2.3 Domestic conferences: 5

2.4 Number of patents: 0

3. List of awards

Not available

4. Research Grants

4.1 Total number of research grants: 7

4.2 Number of collaboration research with industries: 2

4.3 List of major research grants (serving as Principal Investigator)

- The University of Tokyo Excellent Young Researcher "*Investigation of atomistic structure and mechanical properties of crystalline defects*" from The University of Tokyo.

5. Education

5.1 Number of Ph.D. students (including current students): 0

5.2 Number of master students (including current students): 1

5.3 Number of other students: 0

6. Publication list

Journal Papers

1. Yan Li, Xufei Fang, Eita Tochigi, Yu Oshima, Sena Hoshino, Takazumi Tanaka, Hiroto Oguri, Shigenobu Ogata, Yuichi Ikuhara, Katsuyuki Matsunaga, Atsutomo Nakamura, "Shedding new light on the dislocation-mediated plasticity in wurtzite ZnO single crystals by photoindentation", Journal of Materials Science & Technology **156**, (2023) 206-216.
2. Yan Li, Hiroto Oguri, Ayaka Matsubara, Eita Tochigi, Xufei Fang, Yu Ogura, Katsuyuki. Matsunaga and Atsutomo Nakamura "Strain-rate insensitive photoindentation pop-in behavior in ZnS single crystals at room temperature", Journal of the Ceramic Society of Japan **131**, (2023) 685-689.
3. Bin Feng, Sena Hoshino, Bin Miao, Jiake Wei, Yu Ogura, Atsutomo Nakamura, Eita Tochigi, Katsuyuki Matsunaga, Yuichi Ikuhara and Naoya Shibata, "Direct observation of intrinsic core structure of a partial dislocation in ZnS", Journal of the Ceramic Society of Japan **131**, (2023) 659-664.
4. Yu Ogura, Atsutomo Nakamura, Tatsuya Kameyama, Yasuyoshi Kurokawa, Eita Tochigi, Naoya

Shibata, Tsukasa Torimoto, Sena Hoshino, Tatsuya Yokoi and Katsuyuki Matsunaga, "The effect of room-temperature plastic deformation in darkness on the photoluminescence properties of ZnS", Journal of the American Ceramic Society **107**, (2023) 2040-2047.

5. Hiroto Oguri, Yan Li, Eita Tochigi, Xufei Fang, Kenichi. Tanigaki, Yu Ogura, Katsuyuki Matsunaga and Atsutomo Nakamura, "Bringing the photoplastic effect in ZnO to light: A photoindentation study on pyramidal slip", Journal of the European Ceramic Society **44**, (2023) 1301-1305.
6. Takaaki Sato, Vivek Anand Menon, Hiroshi Toshiyoshi and Eita Tochigi, "Microfabricated double-tilt apparatus for transmission electron microscope imaging of atomic force microscope probe", Review of Scientific Instruments **95**, (2024) 23705.

International Conference Presentations

1. Eita Tochigi, "Atomic scale in situ observations of the mechanical response of lattice defects", The 11th Pacific Rim International Conference on Advanced Materials and Processing, Jeju, Korea, (2023) *Invited*.
2. Eita Tochigi, "In situ observations of local atomic behavior upon deformation and fracture phenomena in ceramic materials", Materials Science and Technology 2023, Columbus, USA, (2023) *Invited*.
3. Eita Tochigi, Takaaki Sato, Minjian Cao, Naoya Shibata and Yuichi Ikuhara, "Observations of local mechanical behavior of crystalline materials by in situ loading experiments in a scanning transmission electron microscope", MRM2023 Grand Meeting, Kyoto, Japan (2023).
4. Eita Tochigi, Takaaki Sato, Minjian Cao, Naoya Shibata and Yuichi Ikuhara, "Investigation of atomic behavior of crack tips in $SrTiO_3$ under loading by in situ STEM observations", The International Workshop on Advanced and In Situ Microscopies of Functional Nanomaterials and Devices (IAMNano), Matsue, Japan (2023).

Review of
Scientific Instruments

ARTICLE

pubs.aip.org/aip/rsi

Microfabricated double-tilt apparatus for transmission electron microscope imaging of atomic force microscope probe

Cite as: Rev. Sci. Instrum. 95, 023705 (2024); doi: 10.1063/5.0186983
Submitted: 10 November 2023 • Accepted: 6 February 2024 •
Published Online: 28 February 2024

View Online Export Citation CrossMark

Takaaki Sato,[a] Vivek Anand Menon, Hiroshi Toshiyoshi, and Eita Tochigi

AFFILIATIONS

Institute of Industrial Science, University of Tokyo, Tokyo, Japan

[a]**Author to whom correspondence should be addressed:** takaakis@iis.u-tokyo.ac.jp. **Telephone:** +81-3-5452-6112

ABSTRACT

Atomic force microscopy (AFM) uses a scanning stylus to directly measure the surface characteristics of a sample. Since AFM relies on nanoscale interaction between the probe and the sample, the resolution of AFM-based measurement is critically dependent on the geometry of the scanning probe tip. This geometry, therefore, can limit the development of related applications. However, AFM itself cannot be effectively used to characterize AFM probe geometry, leading researchers to rely on indirect estimates based on force measurement results. Previous reports have described sample jigs that enable the observation of AFM probe tips using Transmission Electron Microscopy (TEM). However, such setups are too tall to allow sample tilting within more modern high-resolution TEM systems, which can only tilt samples less than a few millimeters in thickness. This makes it impossible to observe atomic-scale crystallographic lattice fringes by aligning the imaging angle perfectly or to view a flat probe tip profile exactly from the side. We have developed an apparatus that can hold an AFM tip for TEM observation while remaining thin enough for tilting, thereby enabling atomic-scale tip characterization. Using this technique, we demonstrated consistent observation of AFM tip crystal structures using tilting in TEM and found that the radii of curvature of nominally identical probes taken from a single box varied widely from 1.4 nm for the sharpest to 50 nm for the most blunt.

INTRODUCTION

Atomic force microscopy (AFM) can mechanically profile nanoscale surfaces by scanning a stylus across a sample.[1] Similar to electron microscopy, it has become an indispensable measurement technique for the high-resolution characterization of surfaces.[2] In AFM, the interaction between the probe and the sample surface can be quantified by monitoring the displacement of the probe cantilever and, thereby, the force applied to the probe.[2,3] This force measurement can then be used to calculate physical parameters representing surface properties, such as surface roughness,[4,5] contact area,[6,7] mean pressure,[6–8] Tabor's parameter,[6,8–10] pull-off force,[6–8] work of adhesion,[11,12] and equilibrium separation distance.[11,12].

Since AFM measures the interaction between the probe and the surface, the resolution of AFM-based measurement is critically dependent on the geometry of the very end of the probe.[5,13] Therefore, the specific geometry of AFM-style nanoprobes is often a limiting factor in the development of other applications, including nanolithography,[14,15] tip-based nano-manufacturing,[16] nanoscale metrology for the semiconductor industry,[17] and probe-based data storage.[18] However, AFM itself cannot be practically used to directly observe probe geometry and only indirect estimates can be made from the force measurement results.

For these reasons, DeRose *et al.* developed a means to characterize the geometry of an AFM probe using transmission electron microscopy (TEM) with a customized specimen holder. Their unique holder featured an interchangeable tip into which a trench could be cut, thereby allowing an AFM chip to be slotted in and held in place from the side with a screw.[13,19] However, as TEM resolution has improved over the years, the physical space available for samples has become smaller and smaller, making such setups infeasible.[20] The distance between the sample and the magnetic lens of the TEM, known as the pole piece, continues to decrease, leaving a modern high-resolution TEM with only about 2–4 mm of vertical clearance to fit a sample in. The samples must be even thinner to allow tilting during observation, which is necessary to align the electron beam

Received: 23 June 2023 | Revised: 15 September 2023 | Accepted: 11 October 2023

DOI: 10.1111/jace.19564

Journal of the American Ceramic Society

RAPID COMMUNICATION

The effect of room-temperature plastic deformation in darkness on the photoluminescence properties of ZnS

Yu Ogura[1] | Atsutomo Nakamura[2] | Tatsuya Kameyama[3] | Yasuyoshi Kurokawa[4] | Eita Tochigi[5] | Naoya Shibata[6] | Tsukasa Torimoto[3] | Sena Hoshino[1] | Tatsuya Yokoi[1] | Katsuyuki Matsunaga[1,7]

[1]Department of Materials Physics, Nagoya University, Nagoya, Japan

[2]Department of Mechanical Science and Bioengineering, Osaka University, Toyonaka, Osaka, Japan

[3]Department of Materials Chemistry, Nagoya University, Nagoya, Japan

[4]Department of Materials Process Engineering, Nagoya University, Chikusa-ku, Nagoya, Japan

[5]Institute of Industrial Science, The University of Tokyo, Meguro-ku, Tokyo, Japan

[6]Institute of Engineering Innovation, The University of Tokyo, Bunkyo-ku, Tokyo, Japan

[7]Nanostructures Research Laboratory, Japan Fine Ceramics Center, Nagoya, Japan

Correspondence

Yu Ogura, Department of Materials Physics, Nagoya University, Furo-cho, Chikusa-ku, Nagoya 464-8603, Japan.
Email: ogura.yu.v8@f.mail.nagoya-u.ac.jp

Atsutomo Nakamura, Department of Mechanical Science and Bioengineering, Osaka University, 1-3 Machikaneyamacho, Toyonaka, Osaka 560-8531, Japan.
Email: a.nakamura.es@osaka-u.ac.jp

Funding information

Japan Society for the Promotion of Science, Grant/Award Numbers: JP19H05786, JP21H04618, JP21H04532, JP22K14500, JP22H04960, JP23KJ1059; Kyosyo Hatta Foundation; Nanotechnology Platform Program of MEXT, Grant/Award Numbers: JPMXP09A20NU0098, JPMXP09A21UT0257; JST FOREST Program, Grant/Award Number: JPMJFR223G

Abstract

Inorganic semiconductors have been considered to be brittle at room temperature generally, but recently zinc sulfide (ZnS), a II–VI compound semiconductor, was found to exhibit extraordinarily large plasticity even at room temperature if it was deformed in darkness. Room-temperature plastic deformation can achieve high density of glide dislocations in the crystal without significantly changing the point defect structure, and these dislocations themselves have a potential to provide unique functional properties different from those of the bulk. In this study, therefore, undoped ZnS crystals were plastically deformed at room temperature in darkness to generate only a large number of dislocations, and the changes in luminescence properties resulting from this process were investigated for the first time. As a result, we found that ZnS deformed in darkness exhibits characteristic photoluminescence and persistent luminescence emissions with a visible green color. SEM-CL analyses also identified the emissions from the dislocations. Theoretical calculations indicated that individual dislocations in ZnS have the ability to trap photo-excited carriers. Such changes in luminescence properties due to room temperature plastic deformation in darkness can be considered to originate from dislocations rather than point defects. In other words, the dislocations themselves serve as the significant recombination centers, realizing visible light emission.

KEYWORDS

compound semiconductors, dislocations, luminescence, plastic deformation

Journal of the European Ceramic Society 44 (2024) 1301–1305

Contents lists available at ScienceDirect

Journal of the European Ceramic Society

journal homepage: www.elsevier.com/locate/jeurceramsoc

Bringing the photoplastic effect in ZnO to light: A photoindentation study on pyramidal slip

Hiroto Oguri [a], Yan Li [a,*], Eita Tochigi [b], Xufei Fang [a,c,1], Kenichi Tanigaki [a,d], Yu Ogura [e], Katsuyuki Matsunaga [e], Atsutomo Nakamura [a,*]

[a] Department of Mechanical Science and Bioengineering, Osaka University, 1-3 Machikaneyama-cho, Toyonaka, Osaka 560-8531, Japan
[b] Institute of Industrial Science, The University of Tokyo, 4-6-1 Komaba, Meguro-ku, Tokyo 153-8505, Japan
[c] Department of Materials and Earth Sciences, Technical University of Darmstadt, Darmstadt 64287, Germany
[d] Department of Mechanical Engineering, Osaka Electro-Communication University, 18-8 Hatsu-cho, Neyagawa, Osaka 572-8530, Japan
[e] Department of Materials Physics, Nagoya University, Furo-cho, Chikusa-ku, Nagoya, Aichi 464-8603, Japan

ARTICLE INFO

Keywords:
Plasticity
Oxides
Compound semiconductors
Wurtzite
Dislocations

ABSTRACT

The external light environment has been reported to have a pronounced influence on the dislocation-based plasticity in various inorganic semiconductors. Herein, with a specific focus on the pyramidal slip in wurtzite structures, photoindentation tests were performed on the (0001) plane of ZnO crystal to activate the pyramidal slip and evaluate the effects of light on dislocation behaviors. Statistical analyses of the first pop-in events suggested that the corresponding maximum shear stresses in darkness were slightly smaller than those in 405 nm light, indicating a minor effect of light on dislocation nucleation event. Regarding nanoindentation creep tests, light illumination was found to suppress the indentation depth. Further transmission electron microscopy observations demonstrated that indentation-induced pyramidal dislocations were present deeper in darkness than in 405 nm light, revealing a suppressive effect of light illumination on the pyramidal slip in ZnO for the first time.

1. Introduction

The next-generation power electronics are required to operate at higher power levels, frequencies, and temperatures than today's leading silicon-based devices [1]. Wide band gap (WBG) semiconductors, including ZnO, GaN, and SiC, have emerged as potential candidates to meet such expectations and are referred to as third-generation semiconductors [2–4]. Numerous studies have focused on investigating the electrical, optoelectronic, photocatalytic, and optical properties of WBG semiconductors [5–9]. However, much less attention has been paid to their mechanical properties, which play a critical role in successfully processing and fabricating WBG-semiconductor-based functional devices.

Semiconducting materials have long been regarded as inherently brittle [10–12]. Recently, uniaxial bulk compression experiments on cubic ZnS crystals in darkness have proven that the material can exhibit large plasticity (up to ~45 % true strain) even at room temperature [13], making it a promising approach to improve the deformability and hence processability of materials by regulating the light environment. Based on thorough transmission electron microscope (TEM) analysis and density functional theory (DFT) calculations, such a dependence of plasticity on the light conditions in ZnS was thought to arise from the interactions between photo-excited carriers (electrons and holes) and dislocations [13–15]. The hexagonal symmetry in wurtzite WBG semiconductors is expected to make them behave differently from cubic semiconductors such as ZnS. Careful and systematic investigations are required to uncover how light affects the plasticity, also known as photoplastic effects (PPEs) [16,17], in wurtzite semiconductors. Although an increase in the flow stress of wurtzite ZnO upon illumination was discovered during uniaxial bulk compression as early as 1969 [18], an in-depth understanding of the illumination influence at the dislocation level concerning dislocation nucleation and motion is still lacking.

Recently, the combination of a modern nanoindentation testing system with a fully controlled light illumination system, coined as photoindentation [19], has enabled the direct investigation of the effects of light on the dislocation behavior in crystals. Most advanced semiconductors have been fabricated in the form of thin-film or one-dimensional nanostructures (e.g., nanowires and nanorods) [10],

* Corresponding authors.
E-mail addresses: li.yan.es@osaka-u.ac.jp (Y. Li), a.nakamura.es@osaka-u.ac.jp (A. Nakamura).
[1] Affiliated to Karlsruhe Institute of Technology part-time since 01.2023.

https://doi.org/10.1016/j.jeurceramsoc.2023.09.060
Received 28 August 2023; Accepted 23 September 2023
Available online 27 September 2023
0955-2219/

Journal of the Ceramic Society of Japan 131 [10] 685-689 2023
DOI https://doi.org/10.2109/jcersj2.23064

JCS-Japan

FULL PAPER

Strain-rate insensitive photoindentation pop-in behavior in ZnS single crystals at room temperature

Yan Li[1,†], Hiroto Oguri[1], Ayaka Matsubara[2], Eita Tochigi[3,4], Xufei Fang[1,5], Yu Ogura[2], Katsuyuki Matsunaga[2] and Atsutomo Nakamura[1,4,††]

[1]Department of Mechanical Science and Bioengineering, Osaka University, 1–3 Machikaneyama-cho, Toyonaka, Osaka 560–8531, Japan
[2]Department of Materials Physics, Nagoya University, Furo-cho, Chikusa-ku, Nagoya 464–8603, Japan
[3]Institute of Industrial Science, The University of Tokyo, 4–6–1 Komaba, Meguro-ku, Tokyo 153–8505, Japan
[4]PRESTO, Japan Science and Technology Agency (JST), 4–1–8 Honcho, Kawaguchi, Saitama 332–0012, Japan
[5]Department of Materials and Earth Sciences, Technical University of Darmstadt, 64287 Darmstadt, Germany

The structural and mechanical reliability of inorganic semiconductors for practical applications is determined by the rate at which they can deform and sustain externally applied strain. In this research, nanoindentation experiments under three strain rates and two light conditions were performed on single-crystal ZnS with an 80 nm radius Berkovich tip at a peak load of 60 μN. Significant pop-in events were observed in all indentation tests. The calculated maximum resolved shear stress at the first pop-in approximated the theoretical strength of ZnS, indicating a homogeneous dislocation nucleation process. The cumulative spreads of the maximum shear stress were found to be insensitive to the strain rate, and the distribution at a small strain rate was slightly broader than that of the other two strain rates because of thermal noise. Calculated activation energy ΔG required for the dislocation nucleation indicates that dislocation nucleation in ZnS could occur with external stress and without much assistance of thermal energy, leading to weak dependence of the first pop-in on the strain rate. At three strain rates, light consistently showed little influence on the pop-in behavior and dislocation nucleation process.

Key-words : Semiconductors, Ceramics, Rate-dependent materials, Nanoindentation pop-in, Dislocation, Plasticity

[Received March 31, 2023; Accepted May 5, 2023]

1. Introduction

Inorganic semiconductors have been widely used in various fields such as integrated circuits, optoelectronics, catalysis, and power electronics.[1)–4)] All these applications demand better mechanical integrity and structural reliability of the materials for long-term use in service. In conventional understanding, however, the majority of inorganic semiconductors are brittle at room temperature and prone to suffer from contact damage, which brings great challenges to expanding the applications of such materials.[5),6)] The lack of deformability and flexibility in inorganic semiconductors originates from the materials' intrinsic features of chemical bonding and defects, e.g., strong ionic or directional covalent bonds and poor mobility of dislocations.[7)] So far, bulk deformability at room temperature remains a long-sought aim for inorganic semiconductors, and intrinsic dislocation-based plasticity in these materials has been particularly poorly understood.

It is well known that the hardness and deformation stress of inorganic semiconductors are affected by the external light environment, which is termed photoplastic effect (PPE).[8),9)] Controlling external light conditions to tune plasticity has emerged as a promising approach to achieving deformable inorganic semiconductors.[10)–14)] ZnS, a representative II–VI inorganic compound semiconductor, has been found to be plastically deformed up to a compression strain of $\varepsilon = 45\,\%$ in complete darkness at room temperature[10)] although inorganic semiconductors have long been regarded as intrinsically brittle materials. Furthermore, light irradiation during creep tests on ZnS has been reported to cause an instant drop in the strain rate by several orders of magnitude, providing direct evidence for the light influence.[11)] Subsequent research on ZnS and ZnO using photoindentation technique has revealed that light irradiation affects dislocation motion more than dislocation nucleation.[12),14)] Most recently, density functional

† Corresponding author: Y. Li; E-mail: li.yan.es@osaka-u.ac.jp
†† Corresponding author: A. Nakamura; E-mail: a.nakamura.es@osaka-u.ac.jp
††† Preface for this article: DOI https://doi.org/10.2109/jcersj2.131.P10-1

Journal of the Ceramic Society of Japan 131 [10] 659-664 2023
DOI https://doi.org/10.2109/jcersj2.23065

JCS-Japan

FULL PAPER

Direct observation of intrinsic core structure of a partial dislocation in ZnS

Bin Feng[1,†], Sena Hoshino[2], Bin Miao[1,3], Jiake Wei[1,4], Yu Ogura[2], Atsutomo Nakamura[5,6], Eita Tochigi[6,7], Katsuyuki Matsunaga[2,8], Yuichi Ikuhara[1,8] and Naoya Shibata[1,8,††]

[1]Institute of Engineering Innovation, The University of Tokyo, Tokyo 113–8656, Japan
[2]Department of Materials Physics, Nagoya University, Nagoya 464–8603, Japan
[3]Tianjin Key Laboratory of Materials Laminating Fabrication and Interface Control Technology, School of Materials Science and Engineering, Hebei University of Technology, Tianjin 300401, China
[4]State Key Laboratory of Catalysis, Dalian Institute of Chemical Physics, Chinese Academy of Sciences, Dalian 116023, China
[5]Department of Mechanical Science and Bioengineering, Osaka University, Osaka 560–8531, Japan
[6]PRESTO, Japan Science and Technology Agency, Tokyo 102–0076, Japan
[7]Institute of Industrial Science, The University of Tokyo, Tokyo 153–8505, Japan
[8]Nanostructures Research Laboratory, Japan Fine Ceramics Center, Nagoya 456–8587, Japan

Mobility of dislocations in compound semiconductor materials can be changed by light illumination because the core structure of dislocations is supposed to be reconstructed by photoexcited carriers. However, the atomic structure of such dislocation cores has not been observed and is still poorly understood. In this study, we introduced dislocations in ZnS, one of the typical II–VI type compound semiconductors, by deformation under darkness, and investigated the atomic structure of the dislocation cores using scanning transmission electron microscopy (STEM) combined with theoretical calculations. Direct observation of the Zn core partial dislocation revealed that its atomic structure is in good agreement with the theoretically predicted dislocation core without electron trapping. Moreover, the dislocations were observed to move along a slip plane during the observation. These results indicate that the electron-trap-free dislocation is mobile and could be the origin of plasticity in the dark.

Key-words : ZnS, Dislocation, STEM

[Received March 31, 2023; Accepted April 26, 2023]

1. Introduction

Zinc sulfide (ZnS) is one of the most popular II–VI compound semiconductors, which has been widely used at diverse applications such as light-emitting diodes, optical devices, and sensors.[1] Like most of the ceramic materials, ZnS was considered to be brittle at low temperature. However, it has been recently reported that ZnS shows a surprising plastic deformation under the complete darkness by dislocation slip,[2] of which the plastic strain can reach up to 45 % at room temperature. Thus, the effect of light illumination on the mechanical properties of compound semiconductor has attracted much attention, and attempts were made to clarify the origin of such ductility under darkness.[3)–10)]

Oshima et al., investigated the room-temperature creep deformation behavior of ZnS under well-controlled light exposure conditions, and they found that the strain rates during the creep tests can be largely influenced by the light illumination with certain wavelengths.[4] These results suggest that ZnS should be intrinsically ductile, and its brittle feature results from the illumination of light with certain wavelengths. From a microstructural point of view, it was reported that dislocation glide accounts for the plasticity in darkness, while the mobility of dislocation is drastically decreased under light illumination.[7] These results indicate that the core structure and the mobility of intrinsic dislocations might be strongly affected by the light illumination. Furthermore, theoretical calculations show that the dislocation core structure of ZnS can be reconstructed by trapping the electrons or holes excited by light illumination.[3] Accordingly, it was proposed that the intrinsic dislocation core under darkness is mobile, while the carrier trapped one is immobile, which leads to the brittleness of ZnS[3] under light illumination. All these results strongly indicate that the dislocation core structure and their mobility are the key for the extraordinary plasticity of ZnS

† Corresponding author: B. Feng; E-mail: feng@sigma.t.u-tokyo.ac.jp
†† Corresponding author: N. Shibata; E-mail: shibata@sigma.t.u-tokyo.ac.jp
††† Preface for this article: DOI https://doi.org/10.2109/jcersj2.131.P10-1

MATSUHISA Laboratory

Current Research Activities 2023-2024

Matsuhisa Laboratory

1. Research Topics

Our group aims to develop electronic devices that harmonize with human lives. One of the approaches is to make electronic devices soft. We have developed soft, stretchable electronic materials using polymers, carbon nanotubes, and nanomaterials with low dimensions. These materials allow us to develop soft and stretchable electronic sensors and displays. The followings are the recent examples.

1.1 <u>Stretchable polymer conductors for wearable sensor arrays</u>

We have enabled stretchable polymer conductors with high conductivity, high-resolution patternability, and optical transparency (Figure a). In the previous design of stretchable conducting polymers, it was difficult to design materials that simultaneously maintained these properties. Our conducting polymer was realized by decoupling the engineering of the materials properties. High conductivity was achieved using a rationally designed additive (LiBETI). High stretchability was achieved by matching the mechanical properties with those of the substrate. The developed conducting polymer was patterned at a resolution of less than 10 μm using nanosecond UV laser ablation.

Moreover, we explore the applications of our polymer conductors. The first example is a stretchable transparent touch sensor matrix that can be easily implemented on arbitrary surfaces, including soft robotic skins (Figure b and c). The second example is a high-resolution strain sensor that can map pulse-wave signals. In addition, we developed skin-conformable piezoelectric sensors using this polymer conductor.

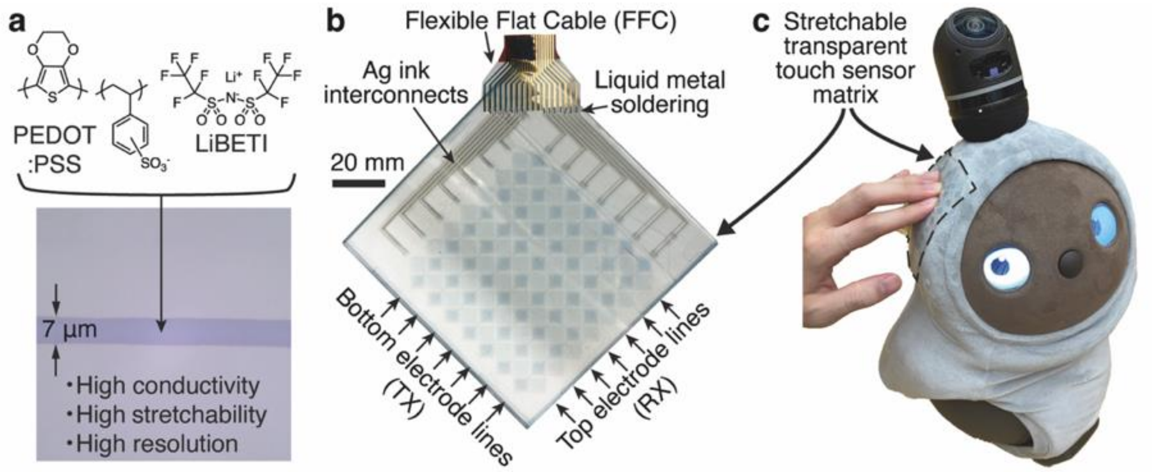

1.2 <u>A stretchable electrochromic display with exceptional skin conformability</u>

Skin-like stretchable electronic devices are expected to lead to the next generation of advanced healthcare and health monitoring. Unlike conventional rigid devices, the development of soft devices with high skin-conformability is required. Displays that adhere to the skin can show a variety of information as the next-generation wearable devices. Among the stretchable displays, electrochromic displays (ECDs) can be driven by low voltage and are highly stable in air. However, ECDs reported so far are thick (about 50 μm),1 which are difficult to show high skin-conformability (Figure Left). Stretchable displays that adhere to the skin and operate stably in air are required. In this study, we demonstrate an ultrathin (<10 μm) stretchable ECD with high skin-conformability. Our ultrathin and stretchable ECDs worked stably even under 50% tensile strain, which is sufficient to allow ECDs to adhere to the skin and operate. Furthermore, our ECDs worked with a line width and spacing of 50 µm. High-resolution displays were realized. In the future, it is expected that the biological signals information read by the sensor can be displayed directly on the skin by a skin display. Furtheremore, our ECD succeeded in producing pulse wave signals for prosthetic hands (Figure Right).

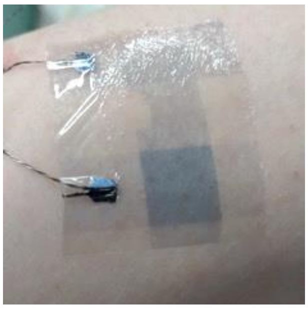

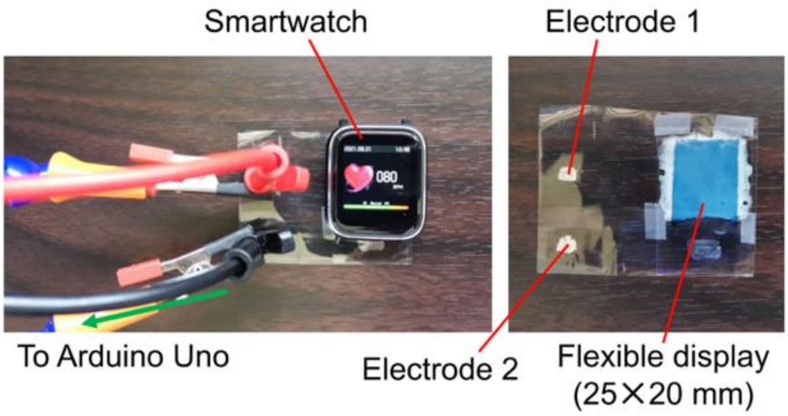

1.3 Stretchable semiconductor devices

Although conventional semiconducting materials like silicon is very stiff and brittle, some novel semiconducting materials are soft and stretchable. Prominent examples are carbon nanotubes and modified conjugated polymers.

Carbon nanotubes show high mobility and low parasitic capacitance, which is highly suitable for high-speed operation. We realized carbon nanotube-based transistors with a mobility of 20 cm^2/Vs, stretchability of 100%, and the ability of large-scale integration. The carbon nanotube transistor comprises various stretchable electronic materials including liquid metal, polymer conductors, and high-k dielectric polymer. Figure in right shows the carbon nanotubes-based stretchable ring oscillators which consist of 31 inverters. The ring oscillator worked at frequency higher than 100 kHz.

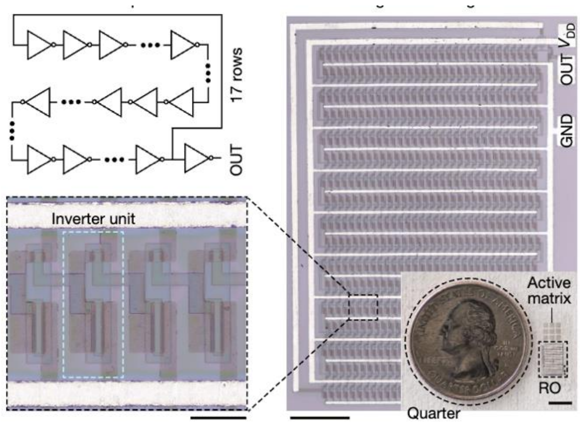

One of the unique properties of conjugated polymers is the high tunability from the molecular design freedom. Although the mobility is usually lower than that of carbon nanotubes, conjugated polymers can realize optoelectronic devices with various wavelengths from ultraviolet to near-infrared. For example, we recently fabricated highly-efficient (~14.2%) stretchable solar cells. Figure in right shows the structure which comprises from various polymer-based electronic materials.

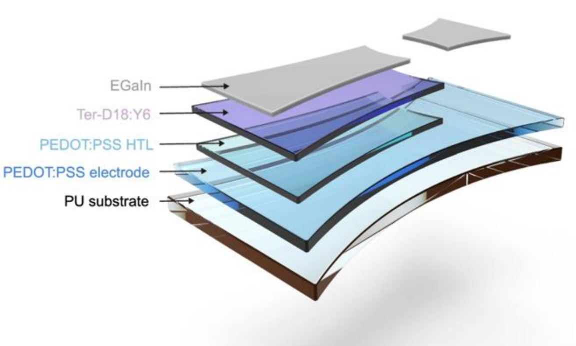

2. Research Achievements

2.1 Number of original journal papers: 5

2.2 International conference: 22 (including 19 invited presentations)

2.3 Domestic conference: 26

2.4 Number of patents: 2

3. List of awards

- PMI Future 50, September 20th 2023, Project Management Institute (N. Matsuhisa)
- PRESM2023 Young Researcher Award, July 20th 2023, Precision Engineering and Sustainable Manufacturing (PRESM2023) (N. Matsuhisa)

4. Research Grants

4.1 Total number of research grants: 4

4.2 Number of collaboration research with industries: 3

4.3 List of major research grants (serving as Principal Investigator)

- ASPIRE “A Comprehensive Study on Flexible and Stretchable Electronics” from JST
- PRESTO “Ultraflexible diodes using stretchable conductors and semiconductors” from JST

5. Education

5.1 Number of Ph.D. students (including current students): 3

5.2 Number of master students (including current students): 4

5.3 Number of other students: 4

6. Publication list

Journal Papers

1. (†Same contribution) D. Zhong†, C. Wu†, Y. Jiang†, Y. Yuan, M. Kim, Y. Nishio, C.-C. Shih, W. Wang, J.-C. Lai, X. Ji, T. Z. Gao, Y.-X. Wang, C. Xu, Y. Zheng, Z. Yu, H. Gong, N. Matsuhisa, C. Zhao, Y. Lei, D. Liu, S. Zhang, Y. Ochiai, S. Liu, S. Wei, J. B.-H. Tok, Z. Bao* "High-speed and large-scale intrinsically stretchable integrated circuits" *Nature* **627,** 313-320 (2024).
2. (†Same contribution) H.-C. Wu†, S. Nikzad†, C. Zhu, H. Yan, Y. Li, W. Niu, J. R Matthews, J. Xu, N. Matsuhisa, P. K. Arunachala, R. Rastak, C. Linder, Y.-Q. Zheng, M. F Toney, M. He*, Z. Bao* "Highly stretchable polymer semiconductor thin films with multi-modal energy dissipation and high relative stretchability" *Nature Communications* **14,** 8382 (2023).
3. T.-W. Chang, Y.-C. Weng, Y.-T. Tsai, Y. Jiang, N. Matsuhisa, C.-C. Shih* "Chain-Kinked Design: Improving Stretchability of Polymer Semiconductors through Nonlinear Conjugated Linkers" *ACS Applied Materials & Interfaces* **15,** 51507-51517 (2023).
4. N. Matsuhisa* "Spoiler alert of foods by your phone" *Nature Food* **4,** 362–363 (2023). (News&Views)

5. T. Shimura, S. Sato, T. Tominaga, S. Abe, K. Yamashita, M. Ashizawa, T. Kato, H. Ishikuro, N. Matsuhisa* "A High‐Resolution, Transparent, and Stretchable Polymer Conductor for Wearable Sensor Arrays" *Advanced Materials Technologies* **8,** 2201992 (2023).

Conference Presentations (selected)

[6] Naoji Matsuhisa, "Soft Electronic Sensors and Displays by Stretchable Electronic Materials" The 16th IEEE International Conference on Nano/Molecular Medicine and Engineering, Tokyo, Japan 2023/12/6.
[7] Naoji Matsuhisa, "Skin-conformable sensors and displays by soft and stretchable electronic materials" World Laureate Forum, Shanghai, China 2023/11/7.
[8] Naoji Matsuhisa, "Skin-conformable sensors and displays using soft and stretchable electronic materials" International Electron Devices and Materials Symposium (IEDMS2023), Kaohsiung, Taiwan 2023/10/20.
[9] Naoji Matsuhisa, "Soft transducers using stretchable electronic materials" 19th Annual International Symposium on Electrets (ISE19), Linz, Austria 2023/9/22.
[10] Naoji Matsuhisa, "Soft skin-integrated sensors and displays" The 23rd International Meeting on Information Display (IMID 2023), Busan, Korea 2023/8/23.

Article

High-speed and large-scale intrinsically stretchable integrated circuits

https://doi.org/10.1038/s41586-024-07096-7

Received: 27 September 2022

Accepted: 22 January 2024

Published online: 13 March 2024

Check for updates

Donglai Zhong[1,9], Can Wu[1,9], Yuanwen Jiang[1,9], Yujia Yuan[2], Min-gu Kim[1,6], Yuya Nishio[2], Chien-Chung Shih[1,7], Weichen Wang[3], Jian-Cheng Lai[1], Xiaozhou Ji[1], Theodore Z. Gao[3], Yi-Xuan Wang[1,4], Chengyi Xu[1], Yu Zheng[5], Zhiao Yu[5], Huaxin Gong[1], Naoji Matsuhisa[1,8], Chuanzhen Zhao[1], Yusheng Lei[1], Deyu Liu[1], Song Zhang[1], Yuto Ochiai[1], Shuhan Liu[2], Shiyuan Wei[1], Jeffrey B.-H. Tok[1] & Zhenan Bao[1]✉

Intrinsically stretchable electronics with skin-like mechanical properties have been identified as a promising platform for emerging applications ranging from continuous physiological monitoring to real-time analysis of health conditions, to closed-loop delivery of autonomous medical treatment[1–7]. However, current technologies could only reach electrical performance at amorphous-silicon level (that is, charge-carrier mobility of about 1 $cm^2 V^{-1} s^{-1}$), low integration scale (for example, 54 transistors per circuit) and limited functionalities[8–11]. Here we report high-density, intrinsically stretchable transistors and integrated circuits with high driving ability, high operation speed and large-scale integration. They were enabled by a combination of innovations in materials, fabrication process design, device engineering and circuit design. Our intrinsically stretchable transistors exhibit an average field-effect mobility of more than 20 $cm^2 V^{-1} s^{-1}$ under 100% strain, a device density of 100,000 transistors per cm^2, including interconnects and a high drive current of around 2 $\mu A\ \mu m^{-1}$ at a supply voltage of 5 V. Notably, these achieved parameters are on par with state-of-the-art flexible transistors based on metal-oxide, carbon nanotube and polycrystalline silicon materials on plastic substrates[12–14]. Furthermore, we realize a large-scale integrated circuit with more than 1,000 transistors and a stage-switching frequency greater than 1 MHz, for the first time, to our knowledge, in intrinsically stretchable electronics. Moreover, we demonstrate a high-throughput braille recognition system that surpasses human skin sensing ability, enabled by an active-matrix tactile sensor array with a record-high density of 2,500 units per cm^2, and a light-emitting diode display with a high refreshing speed of 60 Hz and excellent mechanical robustness. The above advancements in device performance have substantially enhanced the abilities of skin-like electronics.

Skin-like electronics that seamlessly integrate with the human body will enable comfortable, large-scale and high-fidelity physiological monitoring[1,2,15], real-time analysis of health conditions[3,16], localized treatment[17], sensorimotor function reconstruction for prosthetics[18] and augmented reality[19]. To realize device conformability and stretchability, three distinct approaches have been investigated: (1) structural engineering, such as buckled[20], wrinkled[21] or kirigami[22] structures; (2) stiffness engineering of active components interconnected with stretchable conductors[23–26]; and (3) intrinsically stretchable electronics[8–11,27]. Among them, intrinsically stretchable electronics have the unique advantage of intimate tissue contact even with movement and size changes, hence making it the ideal platform for human–machine interface, wearable and implantable[5–7].

To realize the desired sensing, processing and driving functionalities for advanced skin-like electronics, both high-performance intrinsically stretchable transistors and large-scale integrated circuits are needed (Fig. 1a). Towards this aim, substantial efforts have been made to develop stretchable electronics through both material innovation and device engineering[8–11,27–34]. Challenges remain in realizing both high spatial resolution and electrical performance. Although recent attempts in material design resulted in directly photopatternable conductors, semiconductors and dielectric layers, together with improved device density, the electrical performance of stretchable devices is still orders of magnitude lower than those of most flexible thin film devices, particularly at short channel lengths (for example, transconductance normalized by channel width <0.5 $nS\ \mu m^{-1}$) because of low

[1]Department of Chemical Engineering, Stanford University, Stanford, CA, USA. [2]Department of Electrical Engineering, Stanford University, Stanford, CA, USA. [3]Department of Materials Science and Engineering, Stanford University, Stanford, CA, USA. [4]Tianjin Key Laboratory of Molecular Optoelectronic Sciences, Department of Chemistry, School of Science, Tianjin University, Tianjin, China. [5]Department of Chemistry, Stanford University, Stanford, CA, USA. [6]Present address: Department of Medical Engineering, Yonsei University College of Medicine, Seoul, Republic of Korea. [7]Present address: Department of Chemical Engineering and Materials Engineering, National Yunlin University of Science and Technology, Yunlin, Taiwan. [8]Present address: Institute of Industrial Science, The University of Tokyo, Tokyo, Japan. [9]These authors contributed equally: Donglai Zhong, Can Wu, Yuanwen Jiang. ✉e-mail: zbao@stanford.edu

nature communications

Article

https://doi.org/10.1038/s41467-023-44099-w

Highly stretchable polymer semiconductor thin films with multi-modal energy dissipation and high relative stretchability

Received: 23 December 2022

Accepted: 30 November 2023

Published online: 16 December 2023

Check for updates

Hung-Chin Wu[1], Shayla Nikzad[1], Chenxin Zhu[2], Hongping Yan[1,3], Yang Li[4], Weijun Niu[4], James R. Matthews[4], Jie Xu[1,6], Naoji Matsuhisa[1,7], Prajwal Kammardi Arunachala[5], Reza Rastak[5], Christian Linder[5], Yu-Qing Zheng[1], Michael F. Toney[3,8], Mingqian He[4] & Zhenan Bao[1]

Stretchable polymer semiconductors (PSCs) have seen great advancements alongside the development of soft electronics. But it remains a challenge to simultaneously achieve high charge carrier mobility and stretchability. Herein, we report the finding that stretchable PSC thin films (<100-nm-thick) with high stretchability tend to exhibit multi-modal energy dissipation mechanisms and have a large relative stretchability (*rS*) defined by the ratio of the entropic energy dissipation to the enthalpic energy dissipation under strain. They effectively recovered the original molecular ordering, as well as electrical performance, after strain was released. The highest *rS* value with a model polymer (P4) exhibited an average charge carrier mobility of 0.2 $cm^2V^{-1}s^{-1}$ under 100% biaxial strain, while PSCs with low *rS* values showed irreversible morphology changes and rapid degradation of electrical performance under strain. These results suggest *rS* can be used as a parameter to compare the reliability and reversibility of stretchable PSC thin films.

Polymer semiconductors (PSCs) have been developed for use in next-generation soft electronics (e.g., flexible, bendable, or stretchable devices)[1,2]. Both chemical design strategies and fabrication methods have been explored to enhance their electrical and mechanical performance. PSC thin films can now realize comparable and even superior electronic performance to that of amorphous silicon[3]. However, to truly harness the advantages of flexibility and stretchability of polymers, it is necessary to develop PSC thin films with good stretchability that maintain electrical performance under repeated cycles of strain. Such semiconducting thin films are essential in order to create mechanically robust electronics[4–13].

Chemical and physical approaches, such as tuning rigidity of the polymer backbone[14–19], inter-chain crosslinking[20,21], incorporating energy dissipating dynamic crosslinking[22], adding molecular additives[23–25], polymer blending[26–29], nanoconfinement[30,31], side-chain modification[18,20,32], block-copolymerization with flexible polymers[33,34], and tailoring polymer molecular weights[35–37] are reported as approaches for producing good mechanical properties under external strains. However, few of these approaches have achieved both high stretchability and good electrical properties under strain. In general, PSC thin films, typically less than 100 nm in thickness for field-effect transistors (FETs), possess various levels of conformational freedom from

[1]Department of Chemical Engineering, Stanford University, Stanford, CA 94305, US. [2]Department of Electrical Engineering, Stanford University, Stanford, CA 94305, US. [3]Stanford Synchrotron Radiation Lightsource, SLAC National Accelerator Laboratory, Menlo Park, CA 94025, US. [4]Corning Incorporated, Corning, NY 14831, US. [5]Department of Civil and Environmental Engineering, Stanford University, Stanford, CA 94305, US. [6]Present address: Nanoscience and Technology Division, Argonne National Laboratory, Lemont, IL 60439, US. [7]Present address: Institute of Industrial Science, The University of Tokyo, Meguro, Tokyo 153-8505, Japan. [8]Present address: Department of Chemical and Biological Engineering and Renewable and Sustainable Energy Institute (RASEI), University of Colorado Boulder, Boulder, CO 80309, US. e-mail: hem@corning.com; zbao@stanford.edu

ACS APPLIED MATERIALS & INTERFACES

www.acsami.org

Research Article

Chain-Kinked Design: Improving Stretchability of Polymer Semiconductors through Nonlinear Conjugated Linkers

Ting-Wei Chang, Yu-Ching Weng, Yi-Ting Tsai, Yuanwen Jiang, Naoji Matsuhisa, and Chien-Chung Shih*

Cite This: *ACS Appl. Mater. Interfaces* 2023, 15, 51507−51517

Read Online

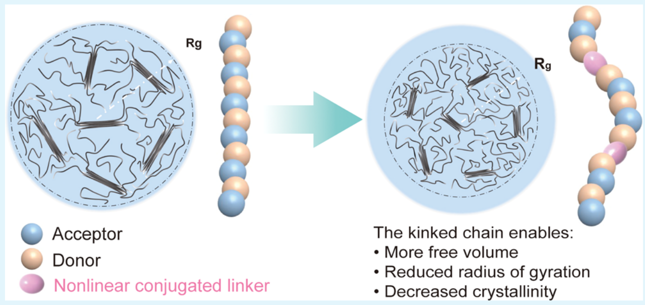

ABSTRACT: The manipulation of the polymer backbone structure has a profound influence on the crystalline behavior and charge transport characteristics of polymers. These strategies are commonly employed to optimize the performance of stretchable polymer semiconductors. However, a universal method that can be applied to conjugated polymers with different donor−acceptor combinations is still lacking. In this study, we propose a universal strategy to boost the stretchability of polymers by incorporating the nonlinear conjugated linker (NCL) into the main chain. Specifically, we incorporate meta-dibromobenzene (MB), characterized by its asymmetric linkage sites, as the NCL into the backbone of diketopyrrolopyrrole-thiophene-based (DPP-based) polymers. Our research demonstrates that the introduction of MB prompts chain-kinking, thereby disrupting the linearity and central symmetry of the DPP conjugated backbone. This modification reshapes the polymer conformation, decreasing the radius of gyration and broadening the free volume, which consequently adjusts the level of crystallinity, leading to a considerable increase in the stretchability of the polymer. Importantly, this method increases stretchability without compromising mobility and exhibits broad applicability across a wide range of donor−acceptor pair polymers. Leveraging this strategy, fully stretchable transistors were fabricated using a DPP polymer that incorporates 10 mol % of MB. These transistors display a mobility of approximately 0.5 cm^2 V^{-1} s^{-1} and prove remarkably durable, maintaining 90% of this mobility even after enduring 1000 cycles at 25% strain. Overall, we propose a method to systematically control the main-chain conformation, thereby enhancing the stretchability of conjugated polymers in a widely applicable manner.

KEYWORDS: *conjugated polymer, semiconductor, nonlinear, conformation, stretchable transistor*

■ INTRODUCTION

Conjugated polymers have garnered significant interest for their potential in fabricating lightweight, flexible, and adaptable electronic devices.[1−15] Traditional design approaches for these polymers emphasize well-ordered crystalline morphology to minimize structural and energetic disorder and maximize π-orbital overlap between backbones.[16−22] However, designing stretchable polymer semiconductors calls for a more relaxed chain structure, increasing amorphous regions to dissipate strain energy. This necessity does not fully align with the traditional principles of polymer design.[23−29] To tackle these challenges, several techniques have been explored to adjust the structure of polymer semiconductors and enhance their stretchability. The strategy of polymer blending adopted in the early stages requires tight control of phase separation, which makes it highly sensitive to the process. In contrast, developing intrinsically stretchable polymer semiconductors simplifies fabrication, offering promise for advancing flexible electronics and integrated devices. Previous efforts primarily focused on incorporating flexible nonconjugated segments into side chains[30,31] or backbones[24,32,33] to improve ductility. While this approach lowered the modulus, it often led to decreased mobility. More recent efforts have been aimed at preserving main-chain conjugation while reducing overall crystallinity in solid-state films. Approaches such as ultrahigh molecular weight[34,35] and near-amorphous polymers with highly planar conformation[3,35,36] have shown promise, yet they are held back by complex synthesis procedures. On the other hand, terpolymers with structural irregularities exhibit potential,[37,38] but their applicability is limited to specific systems. Consequently, there is a need for a versatile and practical strategy that enhances stretchability in conjugated polymers without compromising charge carrier mobility and can be achieved through simple and cost-effective synthesis.

Received: July 10, 2023
Revised: October 14, 2023
Accepted: October 16, 2023
Published: October 28, 2023

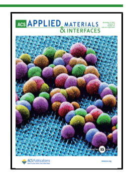

Food technology

https://doi.org/10.1038/s43016-023-00756-3

Spoiler alert of foods by your phone

Naoji Matsuhisa

A wireless miniaturized sensor can report a 'spoiler alert' via a mobile phone by detecting volatile biogenic amines that are produced by spoiled protein-rich foods, providing a feasible solution to identify and prevent food spoilage and promote food safety.

Fig. 1 | Developed sensors can be incorporated into food packages. By simply holding their smartphones close to the sensors, customers or individuals within the supply chain can accurately assess spoilage levels in protein-rich foods.

The world wastes 1.3 billion metric tons of edible food annually[1]. This waste, including spoiled food, contributes to global greenhouse-gas emissions, freshwater consumption and global agricultural land use. Moreover, the consumption of spoiled food results in outbreaks of food-borne diseases, causing enormous economic burdens due to loss of productivity and increased medical expenses. Inadequate cold storage conditions make best-before dates unreliable. Ideally, persons in the supply chain or end customers should receive a 'spoiler alert' based on an objective evaluation of the spoilage of the food. Such an alert will enable sustainable food production management, prevent food-borne diseases and eliminate food waste. This is particularly important for protein-rich foods such as meat, chicken and fish products as, each year, approximately 240 million tons goes to waste across the globe[2]. The spoilage of protein-rich foods releases biogenic amines that are produced by microbial activity and are important biomarkers for monitoring spoilage. High-accuracy and low-cost sensors of these amines are therefore needed for on-demand spoilage analysis.

In this issue of *Nature Food*, Emin Istif, Levent Beker and colleagues report a miniaturized wireless sensor to detect the spoilage of protein-rich foods that is also compatible with a mobile-phone readout[3]. The sensor is 2×2 cm^2 in size, and can be easily installed in food packages (Fig. 1). The structure of the sensor is simple and made using the amine-responsive polymer poly(styrene-co-maleic anhydride) (PSMA), an interdigitated electrode (IDE), an antenna and a low-cost (<US$1) near-field communication (NFC) chip. All materials are compatible with mass production and have the potential for scale-up in the farm-to-fork chain of protein-rich foods. Volatile biogenic amine produced by spoiled foods reacts with PSMA. Once the chemical structure of PSMA is altered, the electrical properties (capacitance and resistance) of the circuit formed with the IDE are influenced. The spoilage is detected once an NFC-compatible mobile phone is placed close to the sensor placed together with spoiled food. The wireless food sensors achieved high-sensitivity detection of volatile amines and low-cost fabrication when tested, which has been difficult in previous studies that have used colorimetric approaches or resistive sensors.

The capacitive sensor formed by the PSMA and IDE is highly sensitive to amines. The toxicity level of common volatile biogenic amines – for example, putrescine, cadaverine and spermidine – is equivalent to more than hundreds of parts per million (ppm). In this study, merely 20 ppm of ammonia increased the capacitance of the sensors by almost 20 times. PSMA acts as an insulator before reacting with amines but changes into ionic materials, which can form a large-capacitance electrical double layer at the interface between PSMA and the IDE. Even in a wireless readout using a mobile phone, 10 ppm of ammonia was detectable. Moreover, the PSMA did not respond to other potential gases from food, such as acetone, alcohols or moisture, and showed high selectivity to volatile biogenic amines. The feasibility of the sensor was confirmed across three days of periodic monitoring of beef and chicken stored with the sensors at −18 °C (freezer), 4 °C (refrigerator) and 20 °C (room temperature). Chicken and beef stored at 20 °C showed an abrupt increase of volatile amines on the second day. On the other hand, those stored at 4 °C showed a slight increase of volatile amines on the third day, and those stored at −18 °C showed no change. These results demonstrated the applicability of their sensors in real life.

The wireless sensor developed by Istif, Beker and colleagues provides a feasible solution to detect and prevent food spoilage, which has a substantial impact on the environment, human health and economics. Although the current sensing target is limited to protein-rich foods, spoilage of other food types can be enabled by developing different sensing layers that are specialized for other byproducts. Future development of this technology could be advanced by flexible and/or stretchable electronic sensors that are developed for wearable healthcare devices and electronic skin used for robots[4]. Materials developed for chemical sensors in healthcare monitoring may be able to increase the variety of detectable chemicals. The fabrication cost can be further reduced by a roll-to-roll printing process. Although NFC chips are not printable, proper system design might allow elimination of the relatively expensive NFC chips[5]. The sensor could be made as soft as food[4], which can prevent food spoilage caused by the mechanical contact between food and sensor during delivery. Some may think the sensor could be another plastic waste, but the materials can be replaced with biodegradable electronic materials[6,7]. In the future, spoiler alerts